~~NASA SUPPORTED~~

~~AIAA~~

PSU-IRL-SCI-436

Classification Numbers 1.4.2, 1.5.3, 1.6.1,
1.9.4, 3.2.2

THE PENNSYLVANIA
STATE UNIVERSITY

IONOSPHERIC RESEARCH

Scientific Report 436

GLOBAL EXOSPHERIC TEMPERATURES AND DENSITIES UNDER ACTIVE SOLAR CONDITIONS

by

Bernard J. Wydra

October 3, 1975

The research reported in this document has been supported by The Office of Naval Research under Contract Grant No. N00014-67-A-0385-0017 and the National Aeronautics and Space Administration under Contract Grant No. NGL 39-009-003.

IONOSPHERE RESEARCH LABORATORY

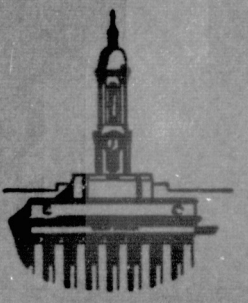

University Park, Pennsylvania

Security Classification

DOCUMENT CONTROL DATA - R & D

(Security classification of title, body of abstract and indexing annotation must be entered when the overall report is classified)

1. ORIGINATING ACTIVITY (Corporate author)

The Ionosphere Research Laboratory

2a. REPORT SECURITY CLASSIFICATION

2b. GROUP

3. REPORT TITLE

Global Exospheric Temperatures and Densities Under Active Solar Conditions

4. DESCRIPTIVE NOTES (Type of report and, inclusive dates)

Scientific Report

5. AUTHOR(S) (First name, middle initial, last name)

Bernard J. Wydra

6. REPORT DATE	7a. TOTAL NO. OF PAGES	7b. NO. OF REFS
October 3, 1975	96	

8a. CONTRACT OR GRANT NO.	9a. ORIGINATOR'S REPORT NUMBER(S)
NASA NGL 39-009-003 ONR N00014-67-A-0385-0017 b. PROJECT NO.	PSU-IRL-SCI-436
c.	9b. OTHER REPORT NO(S) (Any other numbers that may be assigned this report)
d.	

10. DISTRIBUTION STATEMENT

Supporting Agencies

11. SUPPLEMENTARY NOTES	12. SPONSORING MILITARY ACTIVITY
	The National Aeronautics and Space Administration The Office of Naval Research

13. ABSTRACT

Temperatures measured by the OGO-6 satellite using the 6300 A airglow spectrum are compared with temperatures derived from total densities and N_2 densities. It is shown that while the variation of the total densities with latitude and magnetic activity agree well with values used for CIRA (1972), the temperature behavior is very different. While the temperatures derived from the N_2 density were in much better agreement there were several important differences which radically affect the pressure gradients. The variation of temperature with magnetic activity indicated a seasonal and local time effect and also a latitude and delay time variation different from previous density derived temperatures. A new magnetic index is proposed that is better correlated with the observed temperatures. The temperature variations at high latitudes were examined for three levels of magnetic activity for both solstices and equinox conditions. A temperature maximum in the pre-midnight sector and a minimum in the noon sector were noted and seasonal and geomagnetic time and latitude effects discussed. Neutral temperature, density, pressure and boundary oxygen variations for the great storm of March 8, 1970 are presented.

PSU-IRL-SCI-436
Classification Numbers 1.4.2, 1.5.3, 1.6.1,
1.9.4, 3.2.2

Scientific Report 436

Global Exospheric Temperatures and Densities Under Active Solar Conditions

by

Bernard J. Wydra

October 3, 1975

The research reported in this document has been supported by The Office of Naval Research under Contract Grant No. N00014-67-A-0385-0017 and the National Aeronautics and Space Administration under Contract Grant No. NGL 39-009-003.

Submitted by:

L. A. Carpenter, Assistant
Professor of Electrical Engineering

Approved by:

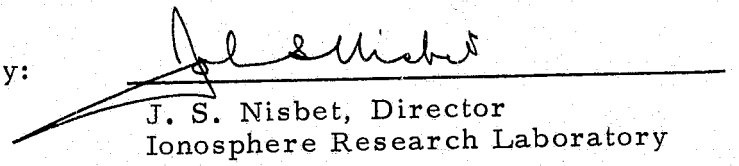

J. S. Nisbet, Director
Ionosphere Research Laboratory

Ionosphere Research Laboratory

The Pennsylvania State University

University Park, Pennsylvania 16802

ACKNOWLEDGEMENTS

The author wishes to express his appreciation to Drs. J. S. Nisbet and L. A. Carpenter for their advice and guidance during the course of this work and to Dr. J. R. Mentzer for serving on his committee. Also he wishes to extend his gratitude to Drs. C. A. Reber and A. E. Hedin of the Goddard Space Flight Center for their assistance in using the OGO-6 density data, Dr. J. E. Blamont of C.N.R.S. in France, for providing the OGO-6 temperature data, Bob Divany, Beatrice Romaniec, and Beverly Beiswenger for their assistance in the computer programming, and to Susan, Kristin, Ann and Ursula Wydra for their support and tolerance.

This work was supported by the Office of Naval Research under Grant No. N00014-67-A-0385-0017 and the National Aeronautics and Space Administration under Grant No. NGL 39-009-003.

TABLE OF CONTENTS

Page

LIST OF TABLES

LIST OF FIGURES

ABSTRACT

Temperatures measured by the OGO-6 satellite using the 6300A airglow spectrum are compared with temperatures derived from total densities and N_2 densities. It is shown that while the variation of the total densities with latitude and magnetic activity agree well with values used for CIRA (1972), the temperature behavior is very different. While the temperatures derived from the N_2 density were in much better agreement there were several important differences which radically affect the pressure gradients. The variation of temperature with magnetic activity indicated a seasonal and local time effect and also a latitude and delay time variation different from previous density derived temperatures. A new magnetic index is proposed that is better correlated with the observed temperatures. The temperature variations at high latitudes were examined for three levels of magnetic activity for both solstices and equinox conditions. A temperature maximum in the pre-midnight sector and a minimum in the noon sector were noted and seasonal and geomagnetic time and latitude effects discussed. Neutral temperature, density, pressure and boundary oxygen variations for the great storm of March 8, 1970 are presented.

CHAPTER I

INTRODUCTION

1.1 General Statement of the Problem

Satellite measurements of total density date from 1957 when the orbital decay of Sputnik I was used to calculate atmospheric densities. The total density varies greatly with altitude decreasing by a factor of 10 in 100 km so that some method of unifying the data had to be found. The solution to the problem was provided by the work of Nicolet (1961) who developed a family of atmospheric models based on the temperature profile assumed by the atmosphere when allowed to cool from a high temperature. By using constant boundary conditions these models enabled a unique relation to be established between the density at any altitude and the exospheric temperature for the appropriate model. Stein and Walker (1965) showed that depending on the boundary conditions for densities, temperatures, and temperature gradients a wide variation in models could be used to fit the experimental data.

The models of Jacchia (1964, 1965, 1970, 1971) used the total density measured by satellite drag to derive the exospheric temperature. Hedin, et al., (1972) used the molecular nitrogen density measured by a quadrupole mass spectrometer on the OGO-6 satellite to construct a model of the thermosphere, and to derive the exospheric temperature. Blamont and Luton (1972) used a Fabry-Perot 6300 A interferometer on the OGO-6 satellite to measure the thermospheric temperature at 250 to 350 km.

Now, using both the neutral temperature and density data from the OGO-6 satellite it is possible to compare the different methods of

obtaining the exospheric temperatures with thermospheric temperatures measured at approximately the same time and place. The combined data sets also makes it possible to compare the variations of temperature as a function of magnetic activity for each of the different methods of deriving the exospheric temperature, to relate them to previous measurements, and to explain the differences between them.

1.2 Development of Thermospheric Models

Nicolet (1961) examined satellite drag results and initiated a model of the thermosphere based on the theoretical calculations in which the atmosphere was allowed to cool. When this was done it was found that consistent temperature and density profiles were obtained which were almost independent of the initial conditions assumed.

Jacchia (1965, 1970, 1971) used satellite drag total density to construct a static diffusion model of the atmosphere above 110 km. The CIRA model incorporates the Jacchia (1971) model and also presents a review by Roemer of the new data which agrees and disagrees with the model. Jacchia (CIRA 1972) proposed that the model will show poorer results for comparatively short term variations - such as diurnal variation or geomagnetic storms - than long term variations. As discussed by Bauer (1967), Nisbet (1967), Swartz and Nisbet (1971) and Bauer, Waldtuefal and Alcayde (1970), incoherent scatter radar neutral temperature measurements indicate a phase difference of about two hours between the Jacchia (1971) model and measured data.

An empirical model based on OGO-6 mass spectrometer data has been constructed by Hedin, et al., (1974) for geomagnetically quiet conditions. This model unlike CIRA (1972) includes the morning maximum for helium, the high latitude of the diurnal temperature for solstice conditions while the oxygen maximum remains at low latitudes and the helium maximizes in the winter hemisphere, a winter maximum in the O to N_2 density ratio at 120 km with a 400°K summer to winter temperature difference, and the 1600 hour maximum for N_2 with an extended bulge in latitude. However, Hedin, et al., (1974) suggested cautious use of the model results for conditions which are beyond the data base used in generating the model.

Chandra and Herman (1969) solved the equations of continuity and heat conduction simultaneously for electrons, ions and neutral constituents. The model predicts a decrease of atomic oxygen in the lower thermosphere which results in a decrease of the peak F2 electron density and an increase in the neutral temperature and density. At higher altitudes the O density increases which causes the electron density to increase. This means that the slab thickness of the F-region increases, though the peak electron density and total electron content decrease as has been reported by Evans (1970). The N_2 and O_2 at higher altitudes should also increase as a result of the higher neutral temperature.

Perturbation theory formed the basis for a three-dimensional model by Volland and Mayr (1971) which was used to analyze a night-time source of heat input in the auroral zone. The results indicated that the effect of the disturbance depended on storm time, local time, and individual longitude of each event. The calculated delay time

varied from 2 to 8 hours from high to low latitudes.

The thermospheric wind circulation was investigated by Mayr and Volland (1972) using Joule heating as the energy source. The results indicated that the molecular nitrogen expansion in the auroral zone generates meridional winds towards the equator. The atomic oxygen density variation at 300 km with increasing magnetic activity is negligible while at 400 km it increased slightly. The molecular nitrogen density at high latitudes is ten times the concentration at low latitudes for Ap = 200. The model was used to reproduce and explain OGO-6 mass spectrometer data. Mayr and Volland (1973) used another three-dimensional two constituent model to describe the effects of geomagnetic activity. The model exhibits steep temperature enhancement at high latitudes, the depletion of helium and atomic oxygen, the negligible latitude variation of atomic oxygen at the same time that molecular nitrogen exhibits a gradual but significant increase towards the auroral zone, and the change of delay time from 2 to 8 hours from high to low latitudes. The results compared favorably with OGO-6 mass spectrometer data. Mayr and Volland (1974) proposed that adiabatic heating by thermospheric wind circulation would increase the neutral temperature at low latitudes. Calculations showed that the winds generated in the auroral region would peak in less than two hours at midlatitudes after the peak of the heat input. Mayr and Volland (1974) concluded that OGO-6 observations can be explained by diffusive mass transport associated with the thermospheric circulation.

Reber, Hedin and Chandra (1973) further analyzed the OGO-6 data and concluded that dynamics play a significant role in the upper

atmosphere. Specifically, the mass spectrometer data indicates that during geomagnetic disturbances circulation cells are formed which decrease the atomic oxygen at low altitudes where the lower boundary of the static diffusion models have been established. The phenomena observed by OGO-6 substantiates the need for dynamic processes to be included in the thermospheric models if the models are to reproduce the variations of density and neutral temperature during geomagnetic distrubances.

1.3 OGO-6 Satellite Neutral Temperatures and Densities

A Fabry-Perot interferometer experiment to measure the neutral temperature at altitude around 250 to 320 km is described by Blamont and Luton (1972). The OGO-6 satellite was launched into an 82^{o} inclination polar orbit so that the local time observed by the satellite changed slowly. The 6300 A airglow measurements enabled Blamont, Luton and Nisbet (1974) to determine the global temperature distribution for geomagnetically quiet conditions and each of the equinoxes and solstices. The conclusions of the quiet condition study are that the maximum temperature occurs near the summer pole at the solstices and that the effect of the day length at high latitudes is very pronounced.

A quadrupole mass spectrometer on the satellite provided an in situ measurement of atomic oxygen, molecular nitrogen and helium densities. Hedin, et al., (1974) used the undisturbed condition data to form a global model of the atmosphere at 450 km and 120 km. The model agreed well with both static diffusion models and incoherent scatter radar results. Reber and Hedin (1974) used the density data to propose a persistent heat source in the high and middle

latitudes during magnetically quiet periods. The heat source appeared to be co-rotating with the magnetic poles, exhibiting a maximum around 900 and 2100 hours universal time. The effect is present throughout the year and is stronger at the equinoxes than in the summer, and may have a maximum during the winter solstice.

Three studies of thermospheric response to geomagnetic disturbances using OGO-6 satellite data were reported. Reber, Hedin and Chandra (1973) deduced exospheric temperatures from the molecular nitrogen densities to demonstrate that the temperature at middle latitudes increased more than 1000^{o}K while the low latitude temperature increased by only 50^{o} to 150^{o}K during the great storm of 8 March 1970. The authors also suggest that the energy is deposited in the high latitudes during the storm, and thereby raises the temperature of the thermosphere and exosphere and generates a large scale circulation cell in the lower thermosphere.

Blamont and Luton (1972) used the 6300 A airglow related neutral temperatures to describe the storm period between September 25 and October 5, 1969. The results substantiate the dependence of the geomagnetic perturbation on latitude, but unexpected maximums of temperature occurred at the polar regions during quiet times. The observations showed that the principal effect of the geomagnetic activity occurs in polar regions and appears to depend on local time. The zone where this strong effect occurs is at lower latitudes at night. Very high temperatures are reached in this zone compared to the day and this may result in strong temperature gradients in the meridional direction which induce neutral winds with velocity above 500 m/sec.

The features of the storm temperatures demonstrate that the high latitudes are quickly affected by geomagnetic activity with a delay of less than 3 hours and the equatorial region has a more gradual temperature variation with a smaller magnitude.

Taeusch, Carignan and Reber (1971a, 1971b) also investigated the period between September 27 and October 3, 1969. The observations confirm many of the features reported by Blamont and Luton (1972). The density above 400 km reacted very quickly (less than an hour) to the geomagnetic activity at high latitudes, but was relatively unaffected in the equatorial region. The O/N_2 ratio variations suggested dynamic processes which result in a circulation that is upward at the poles, then towards the equator where the process subsided. Taeusch, et al., (1971a, 1971b) concluded that the major effect of the geomagnetic storms during the observation period was in the high latitudes (above 50° magnetic latitude) and that the data is better correlated with magnetic latitude than geographic latitude.

Anderson (1973) used a microphone total density gauge on the OGO-6 satellite and also investigated the storm period of September 25 to October 3, 1969 for magnetic latitudes between the magnetic equator and 40°N. A correlation study of the densities and magnetic indices indicated that the low latitude density response lagged the Dst index very little, while the density response lagged the Ap index by about 3 hours. The magnitude of the increase in total density was different from that suggested by Taeusch, et al., (1971a, 1971b). Anderson reported that the total density was over twice as large for Kp = 8 as for Kp = 0.

Many investigations have used various indices to try to quantify the variations of temperature and density with respect to the intensity of geomagnetic storms. An excellent review of the derivations of the Kp, Ap, AE, and Dst indices has been written by Rostoker (1972) in which he also discusses the strengths and weaknesses of each index. The main general weakness of all the indices is the non-uniform distribution of stations used to obtain the global indices. Small spatial variations with small time durations may be entirely missed by the measuring stations and therefore invalid conclusions drawn from the reported indices.

1.4 Density Variations During Geomagnetic Storms

Jacchia (1959a, 1959b) analyzed the speed and attitude changes of spherical satellites and deduced the total density necessary to produce the observed effects. The analysis of satellite drag was a major breakthrough in the development of the global picture of density variations. Diurnal, seasonal, latitudinal and longitudinal changes were able to be uniformly described on a global scale. Jacchia (1965, 1970, 1971) formulated a model based on the satellite drag density measurements which he has periodically reviewed and revised to include new data (Jacchia, 1974).

Much of the new density data analyzed has been used to attempt a description of the effects of geomagnetic activity on the global density structure. Lew (1969) used low altitude satellite drag data to demonstrate that the time delay between the maximum magnetic activity and the maximum variation of the densities below 200 km was between 2.4 and 11.52 hours, depending on the intensity of the storm.

Lew (1969) used the planetary Kp as the magnetic activity indicator, and analyzed the data from two different satellites. However, he was not able to determine the latitude dependence of the delay time.

Roemer (1971a, 1971b) reviewed the observational results up to 1971 and presented satellite drag measurements from six satellites to reach several conclusions. The temperature inferred from the density varied from the quiet condition as a function of latitude given by

$$\Delta T\ (\phi) = [(21.4 \pm 8.3) \sin |\phi| + 17.9]\ \overline{Kp} + 0.03 \exp (\overline{Kp}) \quad (1)$$

where ϕ is the latitude and $\overline{Kp}$ is the 0.4 day mean of the planetary index Kp. The mean time lag of the densities below 200 km is about 12 hours whereas the time lag above 250 km is approximately 5.5 ± 0.3 hours after a geomagnetic disturbance. There was a dependence of time lag on the length of the storm which is given by

$$\Delta t = (0.13 \pm 0.01)\ \Delta \tau + 0.01 \quad (2)$$

where τ is the storm length and time lag is given in days. The time lag above 250 km was not found to depend on altitude, local time or latitude. However, Reomer reported that the specific heating dependence is 30 % higher at night which led him to believe that the heat source was either stronger or the thermosphere more sensitive at night. Roemer and Lay (1972) used the same six satellites, orbiting from 1961 to 1966, to reiterate the time delay independence of latitude, and that the magnitude of the variations did depend on latitude and longitude.

A technique similar to satellite drag analysis has been used by May and Miller (1971) in which the spin rate of satellites equipped with solar cell paddles was observed. The Ariel 2 spin rate derived density showed a better correlation of low latitude variations with Dst than with Ap, but this may be due to the fact that Dst is measured at equatorial stations, whereas Ap is measured at high and mid-latitudes. In any case, the densities exhibited a time lag of about 2 hours with the Dst and an increase of 1 gamma in Dst was equivalent to a 1.25 percent increase in density. The data also displayed a slow recovery of the density after the storm, to values measured before the storm.

Various methods of measuring density have been used since the early studies done with satellite drag. Reviews and comparisons have benn written by Champion (1969, 1972), Von Zahn (1970) and Roemer (in the Cospar International Reference Atmosphere, 1972).

Newton (1970) used data from the Explorer 32 satellite density gauges to describe a strong positive density gradient above 40^{o} latitude which indicates a permanent source of heating above that latitude. He also observed that the heating may be influenced by increased geomagnetic activity. Anderson (1973) used a microphone density gauge on the OGO-6 satellite to measure total density, and his results exhibited a lag of about 3 hours near the auroral zone. The data showed that the density for Kp = 8 was twice the density for Kp = 0 at about 20 degrees latitude.

A low g accelerometer calibration system (LOGACS) was used by DeVries (1972a, 1972b) to measure total densitites during a period of high geomagnetic activity in May 1967. The time lag of the density variations in the polar regions was 90 minutes or less and gradually

increased to 4.5 to 6 hours at the equator. This led him to conclude that most of the energy associated with geomagnetic activity is deposited in the auroral zones, and then transported toward the equator by atmospheric waves and convective circulation. The density values before the disturbance were larger in the high latitudes, but after the storm, the values of density at about 150 km in the sunlit auroral region were only 70% of those before the storm. At the same time the densities at around 15° latitude were double the values before the storm, so that the 150 km densities were higher at low latitudes after the storm. However, the density variation at 170 km did not exhibit the depletion phenomena, but remained higher at the high latitudes.

The same data was further analyzed by Allen and Cook (1974) who concluded that there were three heating zones, near the equator, in the particle precipitation zones, and over the polar caps. They also suggested that particle precipitation and not Joule heating was the major source of heating. It was noted that the equatorial variation which was observed corresponded very well with the results of May and Miller (1971), and the heating in this region was probably due to the decay of the ring current.

An accelerometer was used on the OV1-15 (Spades) satellite provided data which led Forbes and Marcos (1973) to conclude that enhanced density variations at high latitudes are associated with auroral electrojet activity as indicated by the AE indices. They support the Joule heating mechanism as the source of heating and also note wavelike structures in the density profiles which may indicate gravity waves generated in the auroral zone. Forbes and Marcos also suggest that anyone attempting to model the high latitudes

should incorporate electric fields, Joule heating and dynamics into the model. Truttse (1969), using 6300 A emission measurements to deduce densities also noted a linear relation between density variation and the ten hour sum of the AE indices.

A radio frequency monopole mass spectrometer on the Cosmos 274 satellite enabled Romanovsky and Katyushina (1974) to demonstrate a morning-evening asymetry.. The morning density changes were significantly larger than the evening variations which led them to conclude that the effect is produced by precipitation of 10 to 40 Kev electrons, which has been shown to have a maximum in the morning hours. Prolss and Von Zahn (1974a, 1974b) used a similar gas analyzer on the ESRO-4 satellite to observe that the densities of molecular nitrogen can increase by 150% and atomic oxygen can increase by 50% in the mid and low latitudes during geomagnetic storms. They also proposed that the neutral upper atmospheric storms and ionospheric storms are coupled and complimentary effects of geomagnetic storms, and that the data concerning these phenomena could be used to supplement each other. Philbrick (1974) used data obtained from mass spectrometers on OV3-6 and OV1-15 satellites to demonstrate that molecular nitrogen has a large variability in the auroral zone, presumably due to energy sources located there. He also notes that the measurements exhibit significantly larger variations than presently allowed by static diffusion models and that these models may be inadequate to describe the atmosphere during severe geomagnetic storms.

1.5 Temperature Variations During Geomagnetic Storms

A method of determining neutral temperatures from parameters measured by incoherent scatter radar was first developed by Nisbet (1967) using the atomic oxygen thermal energy balance equation and data taken at the Arecibo radar site. The results show a significant difference in the phase of the diurnal variation of the temperature and the diurnal variation of the satellite drag densities. Therefore, there is a discrepancy between the incoherent scatter radar temperature measurements and the Jacchia (1965, 1970, 1971) model temperatures derived from satellite drag densities (Swartz and Nisbet, 1971).

Bauer, Waldteufel and Alcayde (1970) used (St. Santin-Nancay) radar measurements of electron density, ion and electron temperature to determine oxygen concentration and exospheric temperature. The results exhibited a similar phase difference between density and temperature to that reported by Nisbet (1967), and also found that the temperature shape parameter displayed higher values in the day than at night.

Analytic Green's functions enabled Thomas and Ching (1969) to solve the heat conduction equations and to calculate the response of the thermosphere to time dependent heat sources. Their results showed that the time lags of temperature and density were distinctly different and that there was no simple relationship between them. The authors stated that the possible reason for this was that the density lag depended on pressure and the entire temperature profile, whereas the temperature lag depended only on the local temperature.

Magnetic storm effects on thermospheric temperatures were studied by Waldteufel and Cogger (1971) using data from the incoherent scatter radar at Arecibo. They proposed that storm effects could not be described by a simple relation of the magnitude of the planetary Kp index, and that the characteristics as well as the time delay of the observed effects vary for different storms.

Truttse and Yurchenko (1971) used a Fabry-Perot interferometer at the Zvenigorod Observatory in the Soviet Union to measure the width of the Doppler contour of the atomic oxygen red line (6300 A) emission. The method to calculate the temperature from the measurement was similar to that of Blamont and Luton (1972) and the results showed higher temperature variations than predicted by static diffusion models based on satellite drag density measurements (Jacchia, 1965, 1970, 1971), and that the temperature increased towards the north which would be in agreement with the OGO-6 results (Blamont and Luton, 1972, and Taeusch, Carignan and Reber, 1971a, 1971b).

Rees (1971) used fluorescent emission measurements made during rocket flights in the morning and evening twilight to demonstrate that the heating associated with geomagnetic activity was enhanced by a factor of 2 compared to the global mean Kp variation derived temperatures using the formula of Roemer (1970). Rees (1971) also suggested that the time required for the neutral atmosphere to relax to the undisturbed condition was about 12 to 24 hours after the end of the magnetic activity.

Watkins and Banks (1974) applied a method similar to Nisbet (1967) to determine neutral temperatures at the Chatanika incoherent

scatter radar site using electron density and temperature, ion temperature and velocity measurements. The preliminary results indicate that during one storm in the summer of 1972, the neutral temperature exhibited no substantial increase from the undisturbed day or the mildly disturbed day. But the authors pointed out that the Joule heating or the most disturbed day was less than 5 ergs/cm^2 sec.

Solar EUV attenuation was measured by Knight, Uribe and Woodgate (1973) at sunrise and sunset from the OSO-6 satellite to determine the neutral temperature. Their results show that the geomagnetic storm effects are about twice as large at dawn as at dusk, using the Kp index as an indicator of geomagnetic activity. The operational time period of OSO-6 overlapped the operational period of OGO-6 although the OSO-6 satellite was in an equatorial orbit. The local time effect is similar to that which Blamont and Luton (1972) reported. Knight, Uribe and Woodgate also suggested that the Kp index was not a good indicator of short term geomagnetic activity.

1.6 Geomagnetic Storm Effects on Thermospheric Wind Systems

Johnson and Gottlieb (1973) described a wind system by using the latitudinal variation of oxygen and calculating the circulation system that would be necessary to correspond to the variations. It is a system constructed for low magnetic activity. The atomic oxygen is produced at the subsolar point by photodissociation of molecular oxygen, and then transported by the wind system toward the poles at equinox and the winter pole at solstice. Blum and Harris (1972) calculated a quiet condition wind system using the Navier-Stokes equation combined with an atmospheric model of Jacchia (1965) and an

ionospheric model of Nisbet (1971), the Penn State Mk I model. The blum and Harris model also predicts that the winds travel from subsolar point to antisolar point. Kohl and King (1967) used Jacchia's (1965) model and an assumed function of ion density to produce similar results.

Burge, et al., (1973) used the temperature latitudinal dependence on Kp derived by Roemer (1971a, 1971b) to determine a wind system at storm times. The results showed radical alterations of the quiet wind system. The preferential heating of the high latitudes during geomagnetic disturbance is sufficient to reverse the normal poleward daytime wind during equinox and winter conditions. Johnson (1974) combined available data from various sources concerning density variations and concluded that although during undisturbed periods the winds are towards the poles, when geomagnetic storms occur, the heat input at the auroral region may be equal to or greater than the solar heating at low latitudes so that there will be large scale winds away from the auroral region.

Cole (1971) calculated that Joule heating could result in winds of around 500 m/sec equatorwards from the auroral region. Chang, et al., (1974) used magnetohydrodynamic equations to calculate winds resulting from Joule heating. Winds of the order of 1000 m/sec were obtained, but the model neglected viscosity which would significantly reduce the winds (Zimmerman and Rosenberg, 1972).

A theoretical study of the thermosphere using Joule heating and particle precipitation as the energy sources was completed by Hays, et al., (1973). They calculated vertical winds in the auroral zone of a few m/sec which would in turn drive horizontal winds of a

larger scale in a cellular motion. The authors also suggested that the downward movement at lower latitudes would cause compressional heating and a decrease in the mean molecular weight.

From the O/N_2 ratio variations measured by the mass spectrometer on OGO-6, Taeusch, Carignan and Reber (1971a) indicated the observance of a reversal in the quiet time winter hemisphere wind pattern during a geomagnetic storm in 1969. DeVries (1972b) indicated that the LOGACS data also exhibited large density gradients which would correspond to considerable winds directed away from the auroral zone, contrary to the undisturbed circulation.

A ground based Fabry-Perot interferometer measuring the Doppler shift of the 6300 A emission of oxygen was used by Hays and Roble (1971) to obtain wind measurement data during geomagnetic storms. The data taken in the auroral oval at 42° north latitude indicated wind speeds of 250 to 300 m/sec and 350 to 400 m/sec in two storm events during the night at an altitude of about 400 km.

Vasseur (1969) used St. Santin-Nancay incoherent scatter radar measurements of ion drift velocity to infer quiet condition neutral winds during winter 1966 and summer 1967. The results were compared to theoretical models and showed some agreement and some discrepancies. Amayenc and Vasseur (1972) concluded that electric fields must be considered in the calculation of the neutral winds from the ion drift velocities. Results from February and July 1969 were used to show the better agreement with theoretical models. Salah and Holt (1974) presented similar results using Millstone Hill incoherent scatter radar measurements.

Evans (1973) inferred neutral winds for quiet and disturbed conditions in October 1968 using the incoherent scatter radar at Millstone Hill Observatory. The quiet condition neutral winds showed good agreement with theoretical models, but the magnetically disturbed conditions showed the neutral wind direction at midday to be toward the equator, which would be a reversal of the undisturbed wind pattern. Carpenter and Kirchhoff (1974) used Millstone Hill radar measurements to infer neutral winds for several periods, quiet and disturbed. One disturbed period in May 1972 exhibited a neutral wind daytime reversal from quiet condition patterns similar to Evans (1973). Carpenter and Kirchhoff (1974) included the effect of electric fields in the periods measured.

Brekke, Doupnik and Banks (1973) used the incoherent scatter at Chatanika to measure ion drift velocities and derive neutral velocities. The results agreed fairly well with theoretical model patterns, but the authors suggested that there may be distortions to the calculated patterns due to the drag of the high speed ion flows in the higher latitudes. Brekke, Doupnik and Banks (1974) stated that the position of the radar with respect to the auroral oval during the measurement is very important in the neutral wind and electric field calculations. The results of measurements taken during a geomagnetically disturbed period, August 3-9, 1972, showed that the wind pattern was altered from quiet conditions as a result of local pressure gradients due to a heat source in the auroral oval. The equatorward motion at night was enhanced and the poleward motion in the afternoon was diminished.

CHAPTER II

METHODS OF DATA ACQUISITION

2.1 OGO-6 Satellite Measurements

The OGO-6 satellite was launched 5 June 1969 into an 82^{o} inclination polar orbit with a perigee of about 398 km and an apogee of about 1100 km. The orbit was such that the local time at the equator decreased by eight minutes each universal time day. The change in longitude was -25^{o} for two consecutive orbits and the time required for each orbit was about 100 minutes.

The 6300 A oxygen emission line profile was determined by using a spherical Fabry-Perot interferometer aimed towards the horizon. Blamont and Luton (1972) discuss the instrument, procedure of operation, raw data handling, and determination of the neutral temperatures of the experiment in detail. The accuracy of the measurement of the neutral temperatures determined by the profile of the 6300 A line was calculated to be $\pm 65^{o}$K for an individual measurement. The spatial resolution of the measurement was approximately 1^{o} longitude, 6^{o} latitude, and 30 km in altitude at the equator. Only the reduced data for the daylight period has been used because of the sensitivity of the measurement. The magnetically quiet period neutral temperatures have been examined and presented by Blamont, Luton and Nisbet (1974).

The quadrupole mass spectrometer used in situ to measure the concentrations of O, He and N_2 is described by Carignan and Pinkus (1968) and Hedin, et al., (1972, 1973, 1974). The accuracies of the measurements which these authors have determined vary with

constituent and altitude. Systematic uncertainties in the measurements of O and N_2 increase with altitude and are usually less than 10% to 15% near perigee. No data was used where the estimated uncertainty was greater than 25% for N_2 and O and 50% for He. There is also a laboratory calibration uncertainty of about 10% to 15%. The spatial resolution of the measurement is less than $1/2^{o}$ latitude and longitude and less than 5 km in altitude. Magnetically quiet condition data have been analyzed and presented by Hedin, et al., (1972, 1973, 1974) and Reber and Hedin (1974). Also Taeusch, Carignan and Reber (1971a, 1971b) presented the densities observed during the magnetically disturbed period near the end of September and beginning of October of 1969, which was the same period examined by Blamont and Luton (1972) using the 6300 A derived neutral temperature data.

CHAPTER III

DISCUSSION OF ANALYSIS

3.1 Comparison of the Temperatures Measured from the 6300 A Line Width with Model Temperatures Derived from Molecular Nitrogen and Total Mass Density

The use of 6300 A emission spectrum to determine the thermospheric temperature is a relatively direct method of kinetic temperature measurement. The basic assumption is that the radiating oxygen atoms are in equilibrium with the ambient neutral atmosphere. The altitude scanned by the interferometer varied from 250 km to 350 km with an average value of about 285 km. Temperatures in this altitude range are normally within 100 K of the exospheric temperature. A correction was applied to convert the temperatures to exospheric temperature using the Bates (1959) formula to facilitate comparison with other data

$$T(Z) = T_\infty - (T_\infty - T_o) \exp(-S(Z - Z_o)) \qquad (3)$$

where $T(Z)$ is the measured temperature at altitude Z and $Z_o = 120$ km, $T_o = 355$ K and $S = 0.016$ km^{-1}.

To convert neutral densities to exospheric temperatures requires assumptions about the lower boundary conditions, the shape of the temperature profile and diffusive equilibrium of the atmospheric constituents. In this work it was intended to compare our values with the values of temperature derived from techniques adopted previously by others, and procedures similar to those that had been employed were adopted.

The CIRA (1972) reference atmosphere and the model due to Jacchia (1971) were based on satellite orbital drag data. In the present work total density derived temperatures were taken to be the exospheric temperature of the appropriate CIRA (1972) model atmosphere that would give the measured total density at the altitude of the measurement.

The Goddard Space Flight Center OGO-6 model of the quiet thermosphere (Hedin, et al., 1972) based its temperatures on molecular nitrogen densities. Molecular nitrogen is the major constituent in the region where eddy diffusion effects predominate and the effects of diffusive equilibrium assumptions are small. Boundary densities and the temperature profile still have to be assumed. The technique employed in this work was to match the observed N_2 density to the appropriate CIRA (1972) model. Temperatures derived in this manner are referred to as "N_2 density derived temperatures."

Figure 1 shows the magnetic latitude variations of the 6300 A temperature measurements and the total density and N_2 density derived temperatures during 11 March 1970 where the Kp magnetic index had an average value of 0.58 and a maximum value of 1.3. It is apparent that the total density and N_2 density derived temperatures are in excellent agreement at all latitudes, but that the 6300 A temperatures are systematically lower by 100°K to 150°K at lower latitudes. These observations are in agreement with Hedin, et al., (1972) who showed that the temperature estimated from their model was about 100°K larger than those observed by incoherent scatter techniques at Millstone Hill Observatory at 42.6°N by Salah and Evans (1972).

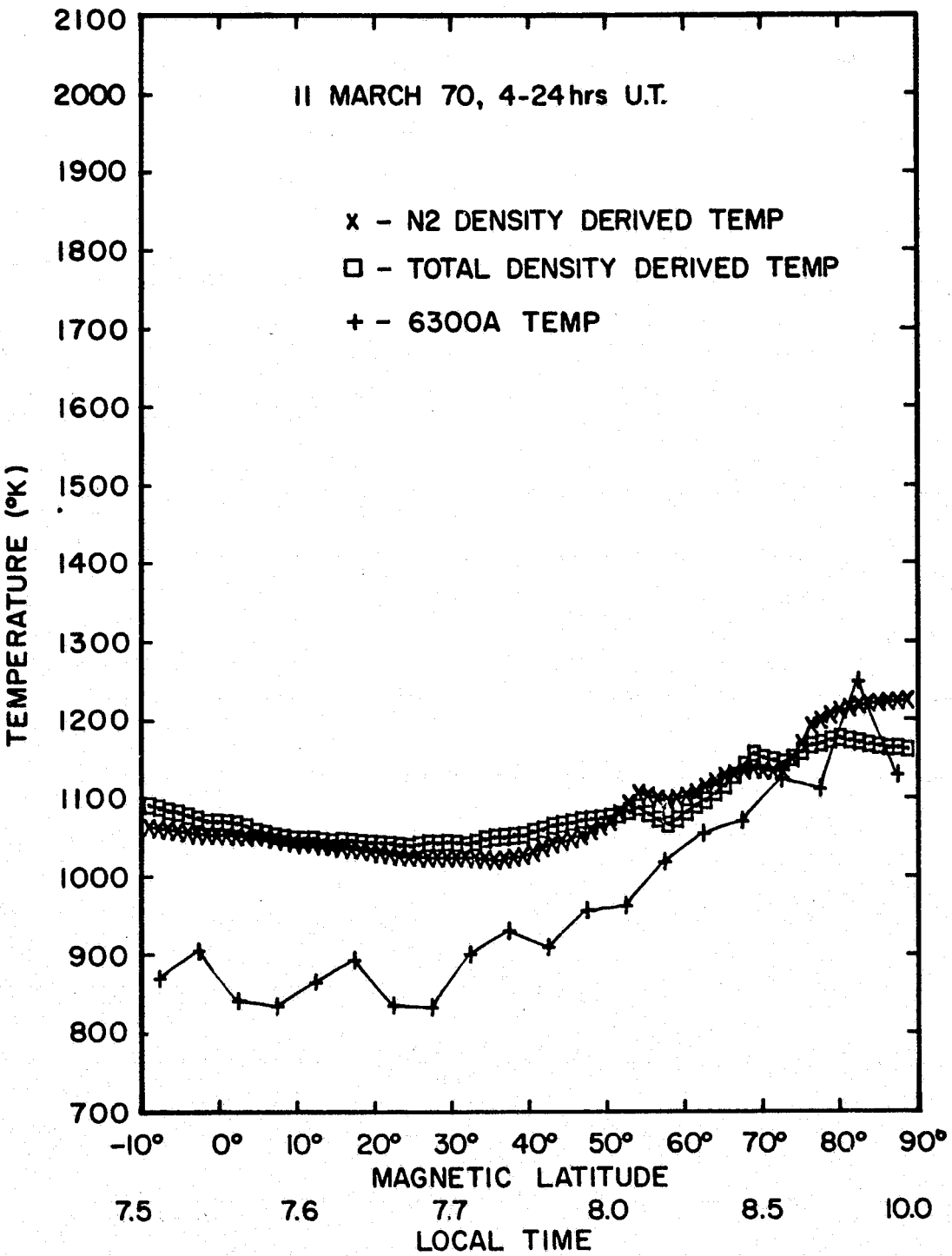

Figure 1 Comparison of 6300 A temperatures with N_2 and total density derived temperatures for an undisturbed period

The latitudinal temperature difference from the 6300 A airglow between equator and pole under these quiet conditions is observed to be about 300°K compared to the 150°K indicated by the temperatures derived from the densities.

Figure 2 shows the magnetic latitude variation of the 6300 A temperature measurements and the N_2 and total density derived temperatures for 6 and 7 March 1970 when the average value of the Kp magnetic index was 4.04 and the maximum value was 5.7. Below 35° magnetic latitude the 6300 A temperature is still about 150°K lower than the total density and N_2 density derived temperatures, and all the temperatures have increased about 120°K from the undisturbed condition in this region. Above that latitude the 6300 A temperature and the N_2 density derived temperature increase at the rate of about 8°K per degree magnetic latitude. The total density derived temperature for higher latitudes has a slight increase at the rate of about 2°K per degree magnetic latitude. The increase in temperature over the undisturbed magnetic doncition at 70° magnetic latitude is about 350°K for the 6300 A temperatures and the N_2 density derived temperature, and only a few degrees for the total density derived temperature. The explanation for the total density derived temperature will be made evident when the variations of N_2 and O densities are discussed in Section 3.6. The 6300 A temperature and the N_2 density derived temperature disagree above 75° magnetic latitude where the 6300 A temperature continues to increase, whereas the N_2 density derived temperature decreases.

Figure 3 shows the magnetic latitude variation of the 6300 A temperature measurements and the N_2 and total density derived temperatures during the large disturbance caused by the great storm

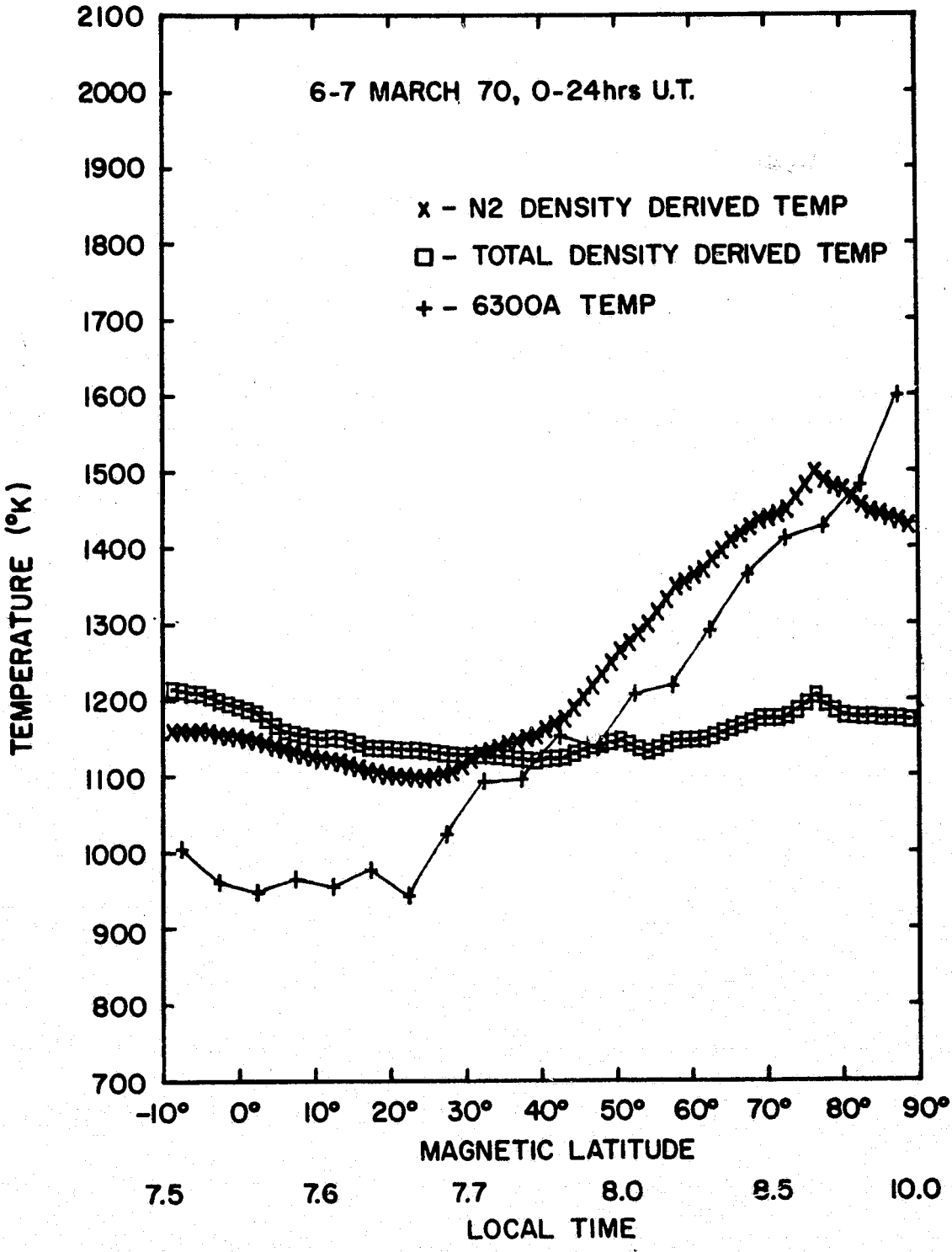

Figure 2 Comparison of 6300 A temperatures with N_2 and total density derived temperatures for a moderately disturbed period

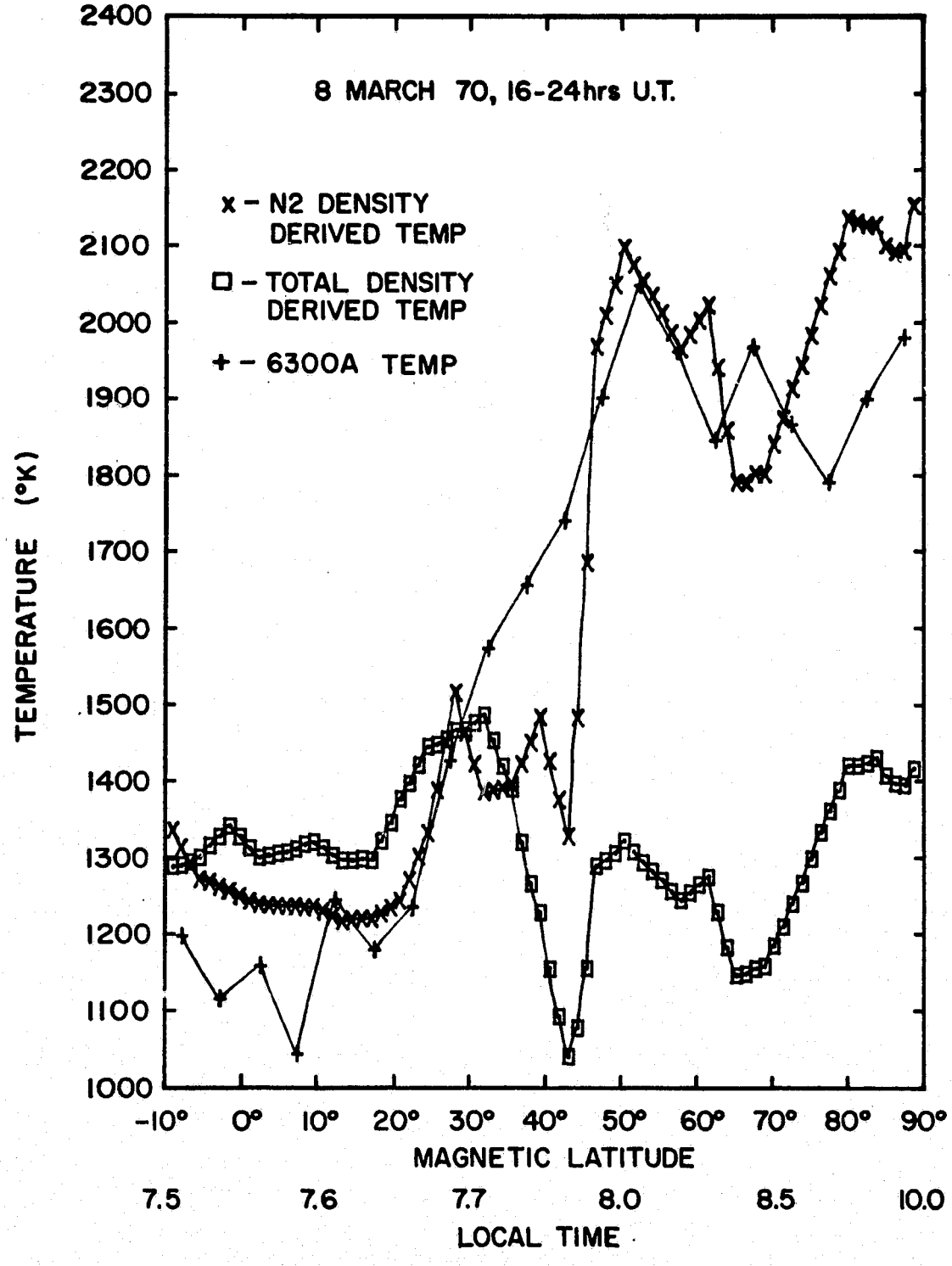

Figure 3 Comparison of 6300 A temperatures with N_2 and total density derived temperatures for a greatly disturbed period

of 8 March 1970 when the average value of Kp was 8.15 and the maximum value was 9.0. The 6300 A temperatures and the N_2 density derived temperature exhibit close agreement except from 25° to 40° magnetic latitude where the N_2 density derived temperature decreases slightly and then increases sharply at about 170°K per degree magnetic latitude while the 6300 A temperature increases at a relatively constant rate of about 26°K per degree magnetic latitude, and below 10° magnetic latitude where the difference is about the same as for the undisturbed condition.

At this very high level of magnetic activity, it is apparent that the temperatures derived from total density fail to show the 700°K increase between the equator and the pole. The total density derived temperatures also show a large negative gradient in the 30° to 45° magnetic latitude region which is opposite to the variation shown by the 6300 A temperatures.

3.2 Variations of Temperatures as a Function of Magnetic Index Kp

Figure 4 shows the rate of change of temperature with Kp for the 6300 A temperatures and the temperatures derived from the N_2 and total densities. They were obtained using 11 days, June 14 to 24, 1970. During this period the average value of Kp was 2.2 and the maximum value was 5.3. The $\Delta T/\Delta Kp$ values were obtained by least square fitting the data to the equation

$$T = A + B S_{10.7} + (\Delta T/\Delta Kp) Kp \qquad (4)$$

where $S_{10.7}$ is the 10.7 cm solar flux index.

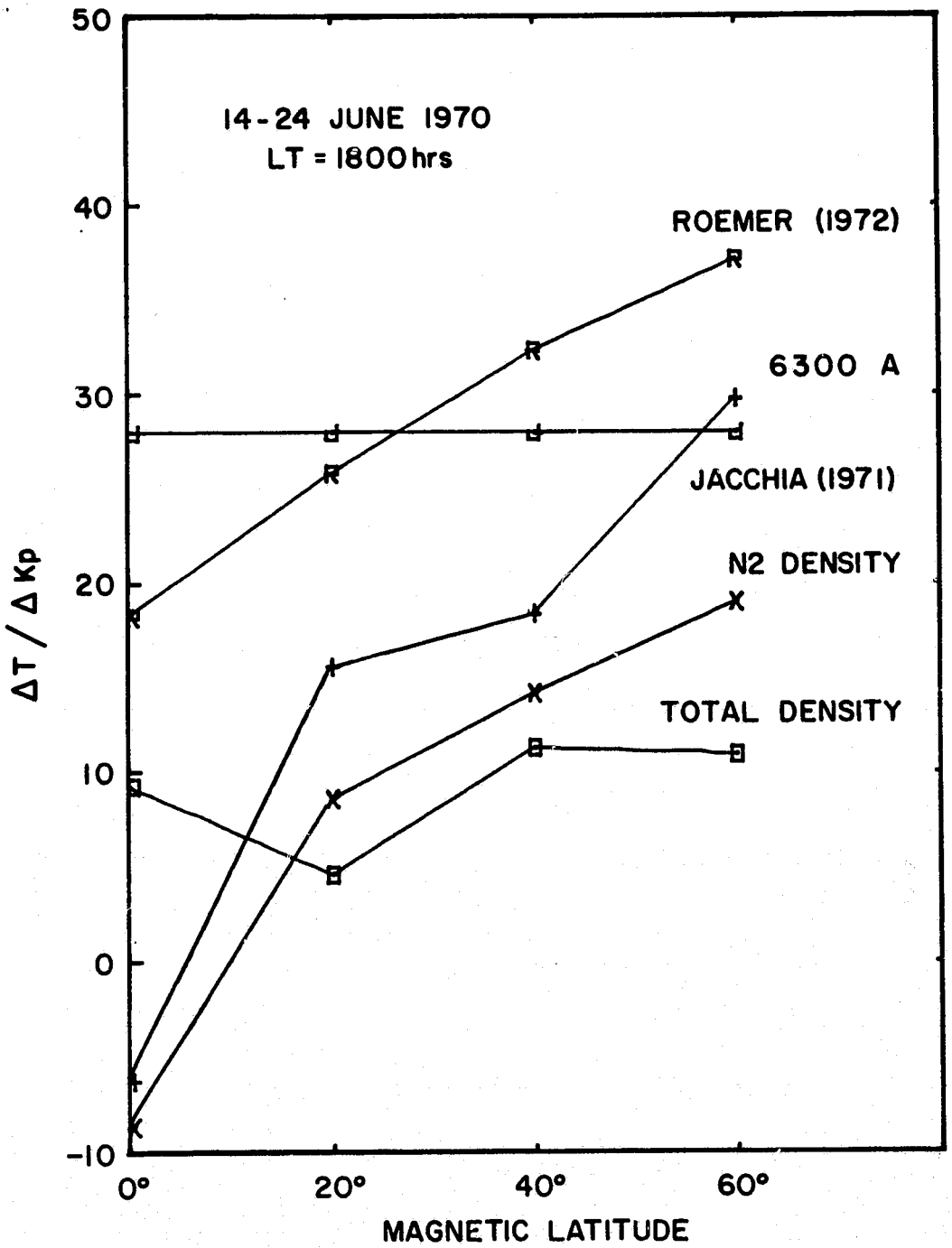

Figure 4 $\Delta T/\Delta Kp$ versus magnetic latitude derived from 6300 A temperatures, N_2 and total density derived temperatures, Jacchia (1971) and Roemer (1972), for summer PM local time

The coefficients of the least squares fits to the equation

$$\Delta T / \Delta Kp = K_o + K_1 \sin \theta \qquad (5)$$

where θ is the magnetic latitude,

are given in Table 1 for comparison with the Roemer (1972) and Jacchia (1971) coefficients. It is apparent that the 6300 A temperature coefficient K_1 is much larger than that given by Roemer (1972) or Jacchia (1971). The total density temperature coefficient K_1 is an order of magnitude smaller than that for the 6300 A and N_2 derived temperature coefficients and in better agreement with the Jacchia (1971) than the coefficients from Roemer (1972).

Table 1: $\Delta T / \Delta Kp$ Coefficients for Summer 1970 Afternoon

	K_0	K_1
6300 A	-3.5	38.6
N_2	-6.2	31.2
Total Density	7.3	3.8
Roemer (1972)	17.9	21.4
Jacchia (1971)	28.0	0.0

Figure 5 shows the rate of change of temperature with Kp versus magnetic latitude in the same manner as Figure 4. These were obtained using data from 11 days, March 1 to 10, 1970, when the average value of Kp was 3.0 and the maximum value was 9.0. The local time was around 800 hours. Table 2 gives the K_0 and K_1 coefficients for this period obtained in the same manner as Table 1. The $\Delta T / \Delta Kp$ for the 6300 A and the N_2 derived temperatures are

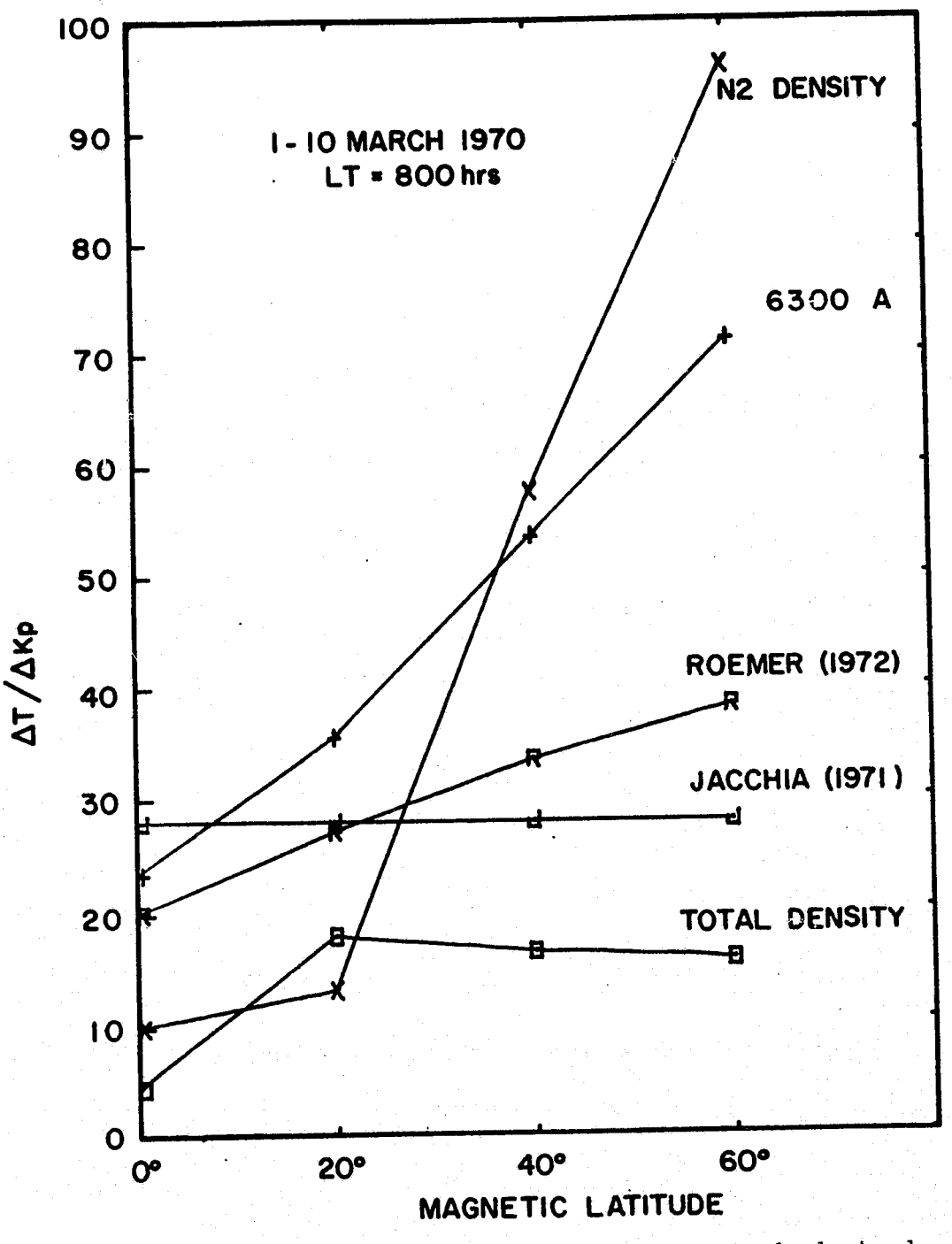

Figure 5 $\Delta T/\Delta Kp$ versus magnetic latitude derived from 6300 A temperatures, N_2 and total density derived temperatures, Jacchia (1971) and Roemer (1972), for 1970 March AM local time

considerably larger than the total density derived temperature cases of Roemer (1972) and Jacchia (1971). The total density $\Delta T/\Delta Kp$ is again closer to Jacchia (1971) than Roemer (1972). While the agreement between the 6300 A and N_2 density derived temperature is an order of magnitude better than for the total density derived temperature $\Delta T/\Delta Kp$,

Table 2: $\Delta T/\Delta Kp$ Coefficients for March 1970 Morning

	K_0	K_1
6300 A	20.45	54.95
N_2	-3.03	101.95
Total Density	8.01	11.18
Roemer (1972)	17.9	21.4
Jacchia (1971)	28.0	0.0

it appears that in this period the N_2 density derived temperature overestimates the effect of magnetic activity at high magnetic latitude and underestimates it at low magnetic latitude.

The March morning coefficients K_0 and K_1 are larger than the June afternoon coefficients. To examine the various factors influencing these coefficients, other periods were analyzed using the 6300 A temperatures and the results are shown in Figure 6 and the coefficients listed in Table 3. A suggestion by Blamont and Luton (1972) that the effect of magnetic activity is stronger in the morning than in the afternoon is confirmed by both the K_0 and K_1 coefficients for the Fall 69 and the Summer 70 cases. A small seasonal variation can be detected in the K_0 coefficient but it is not apparent in the K_1

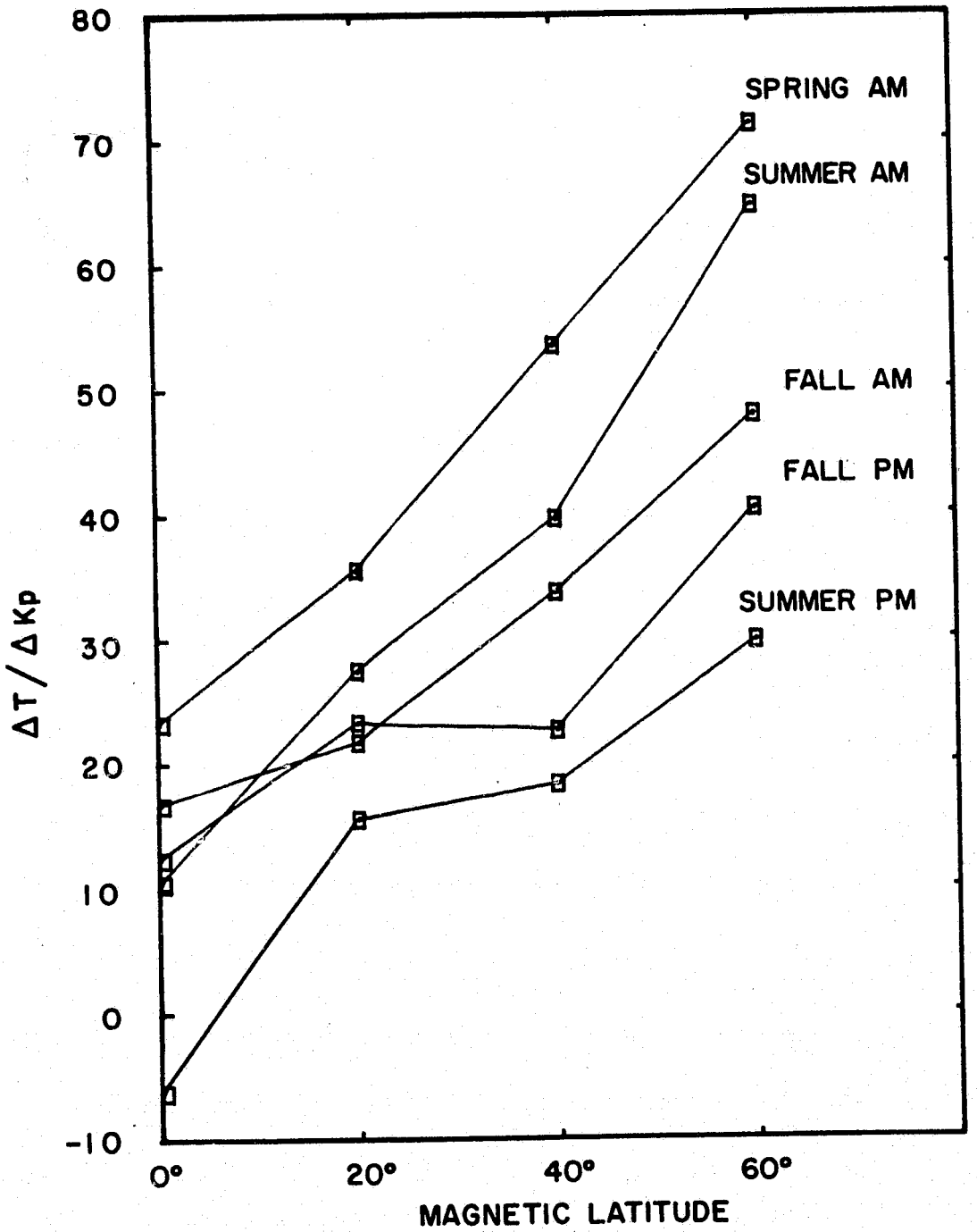

Figure 6 $\Delta T/\Delta Kp$ versus magnetic latitude calculated from 6300 A temperatures for Fall 69, Spring 70 and Summer 70 with AM and PM local times

coefficients which would indicate that the global effect may be weaker in the summer but that the latitudinal variation is not changing with the seasons. Although the local time variation is clear, the seasonal results are not decisive and much more data should be investigated for other periods before hard conclusions can be drawn.

Table 3: $\Delta T / \Delta Kp$ Coefficients for Fall 69, Spring 70 and Summer 70 with AM and PM Local Times

	K_0	K_1
Fall 69 AM	13.6	35.41
Fall 69 PM	11.76	27.88
Spring 70 AM	20.45	54.95
Summer 70 AM	8.17	59.13
Summer 70 PM	- 3.5	38.57

3.3 Fourier Analysis of Quiet Day Latitude Variation at Solstice and Equinox

The OGO-6 satellite 6300 A temperature measurements were made during 3 solstices and 2 equinoxes. The orbit was such that a global distribution of morning and evening temperatures were obtained on each occasion. Thus it is possible to observe a global latitude temperature variations for each solstice and equinox, and to determine the coefficients of a third order fourier series which best fit the global temperatures.

The temperature data were sorted and averaged in 20° latitude ranges which overlapped each other by 10° latitude, and a third order fourier series centered on the north pole was fitted to the averages. The results of the analysis are presented along with the averaged data

points in Figures 7, 8, 9, 10 and 11, and the fourier coefficients in Table 4. Due to a smaller number of data points, the Summer 69 and Winter 69 periods required several days to obtain a global distribution of temperatures.

The fourier series analysis will allow others to compare 6300 A undisturbed global temperature variations with model temperatures and other experimentally measured temperatures.

3.4 Anomalous Temperature Behavior in the Southern Hemisphere

Figures 12, 13, 14 and 15 show the longitude variation of the 6300 A morning temperature for 10° magnetic latitude ranges in the southern hemisphere for the interval 14-22 March 70 when the average value of Kp was 1.07 and the maximum value of Kp was 2.7. The figures indicate an area from -20° to -40° magnetic latitude and 10° to 60° west longitude which is consistently 300°K to 900°K hotter than the rest of the data for the period. This area of enhanced temperatures corresponds to the South Atlantic magnetic field anomally. Further study into other periods of low magnetic activity showed that the same area exhibited significantly higher temperatures only in the morning hours, usually before 1000 hours local time.

The N_2 densities and O densities were then investigated to find out if there was an N_2 enhancement and O depletion corresponding to the same magnetic latitude and longitude. The results showed no significant variation of either the N_2 or O densities at that location. It would seem that such large temperature gradients could not be maintained for long without producing a wind system which would largely equalize the pressure. It must be tenatively concluded that

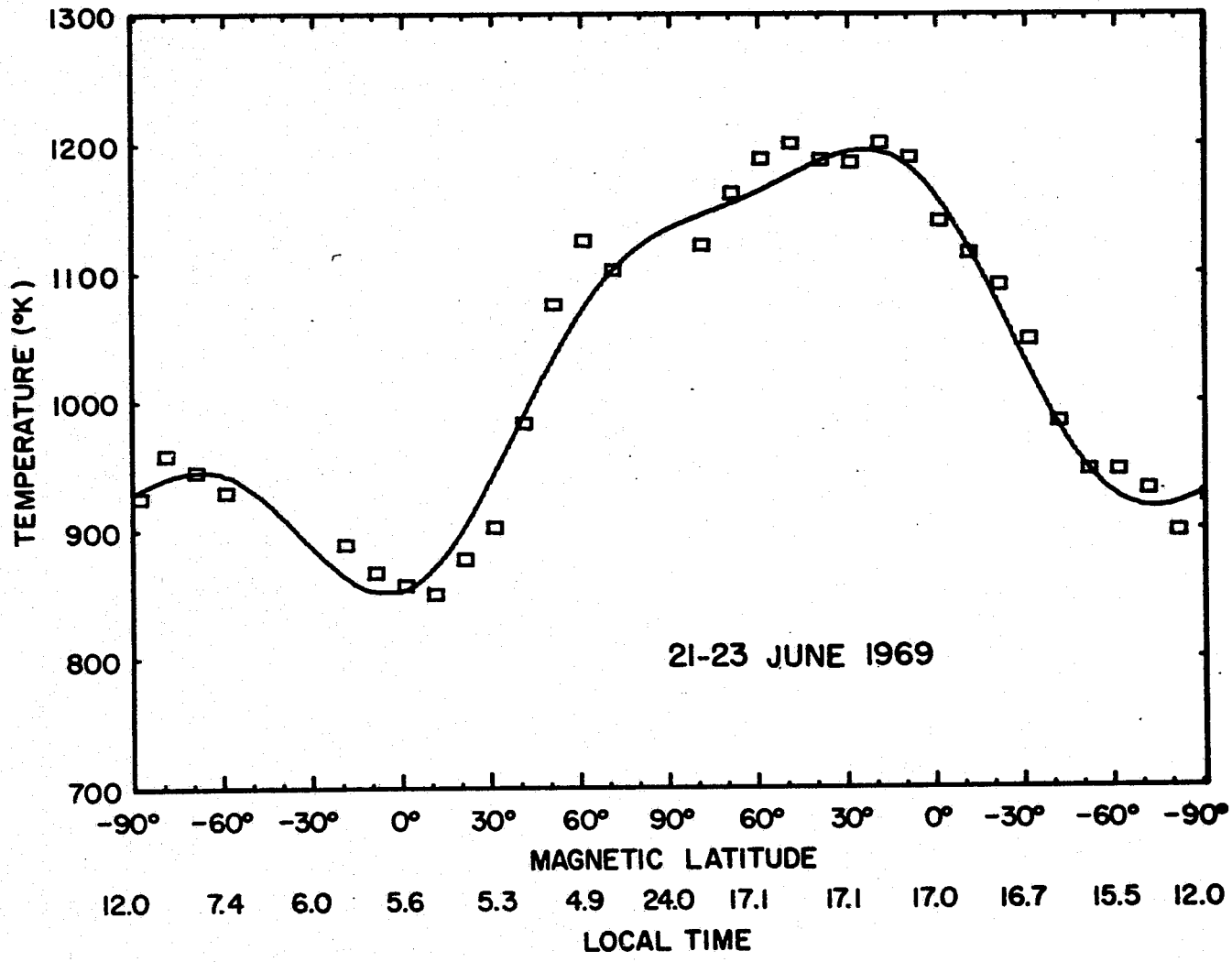

Figure 7 Orbital 6300 A temperature distribution with fourier series fit for June 69 solstice

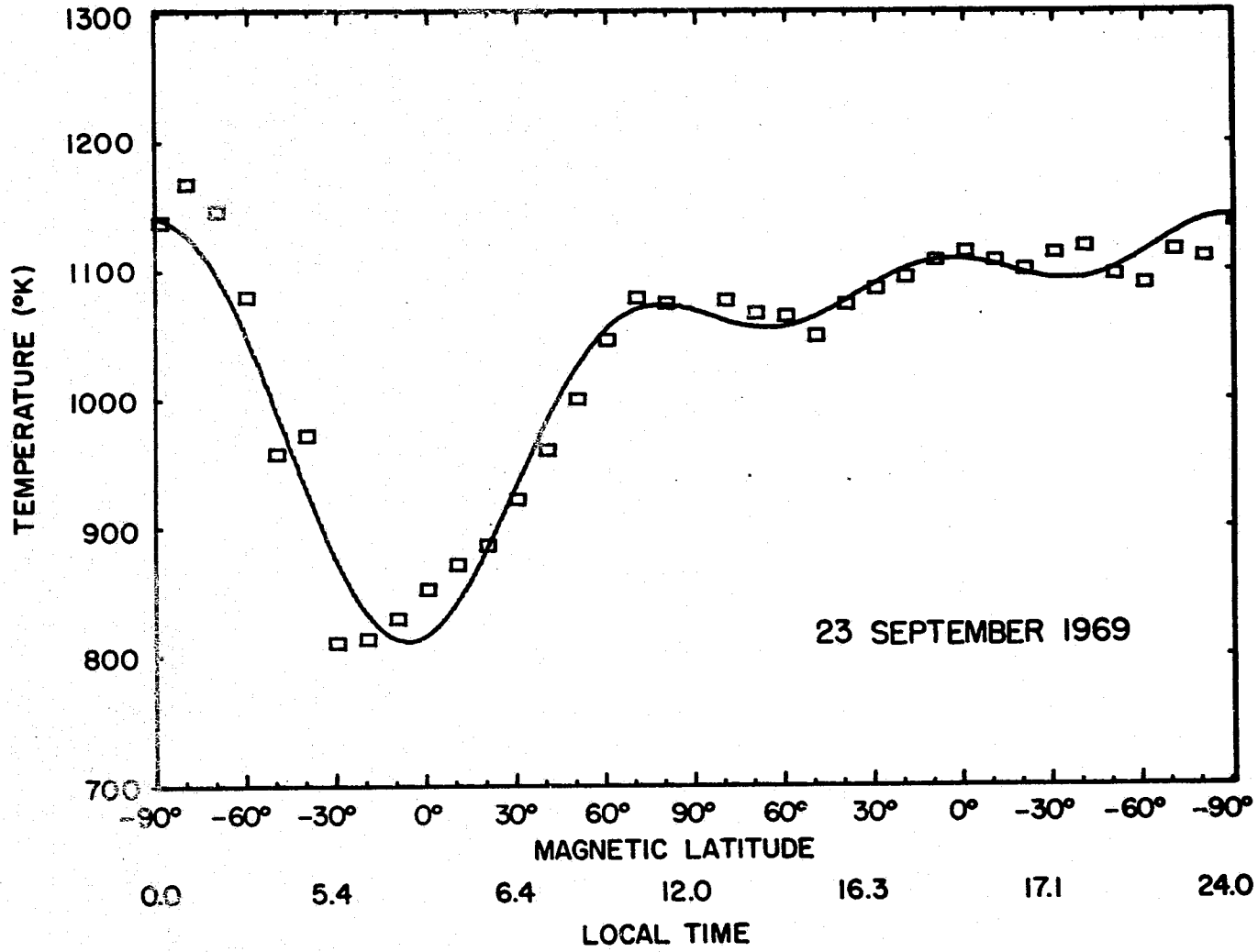

Figure 8 Orbital 6300 A temperature distribution with fourier series fit for September 69 equinox

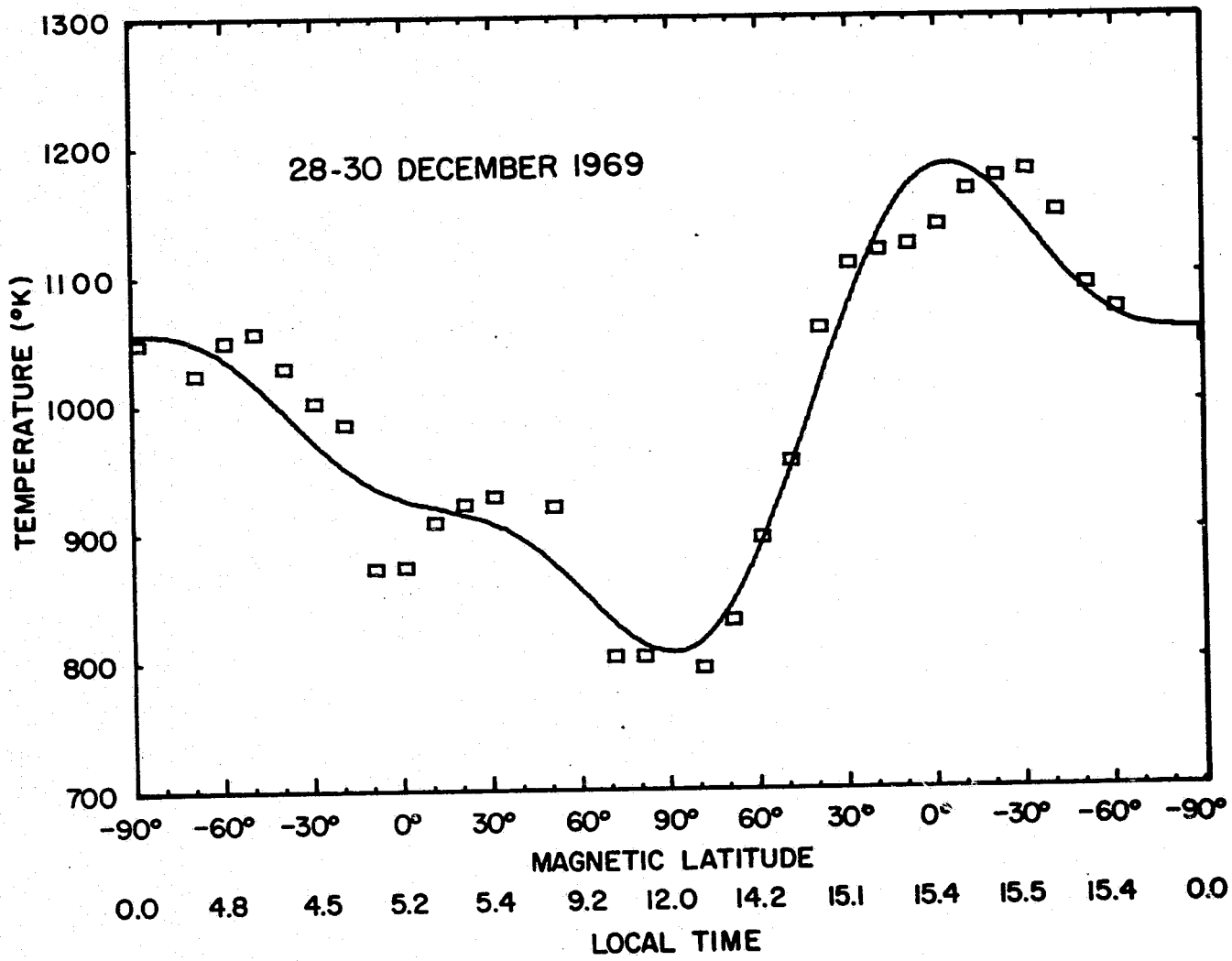

Figure 9 Orbital 6300 A temperature distribution with fourier series fit for December 69 solstice

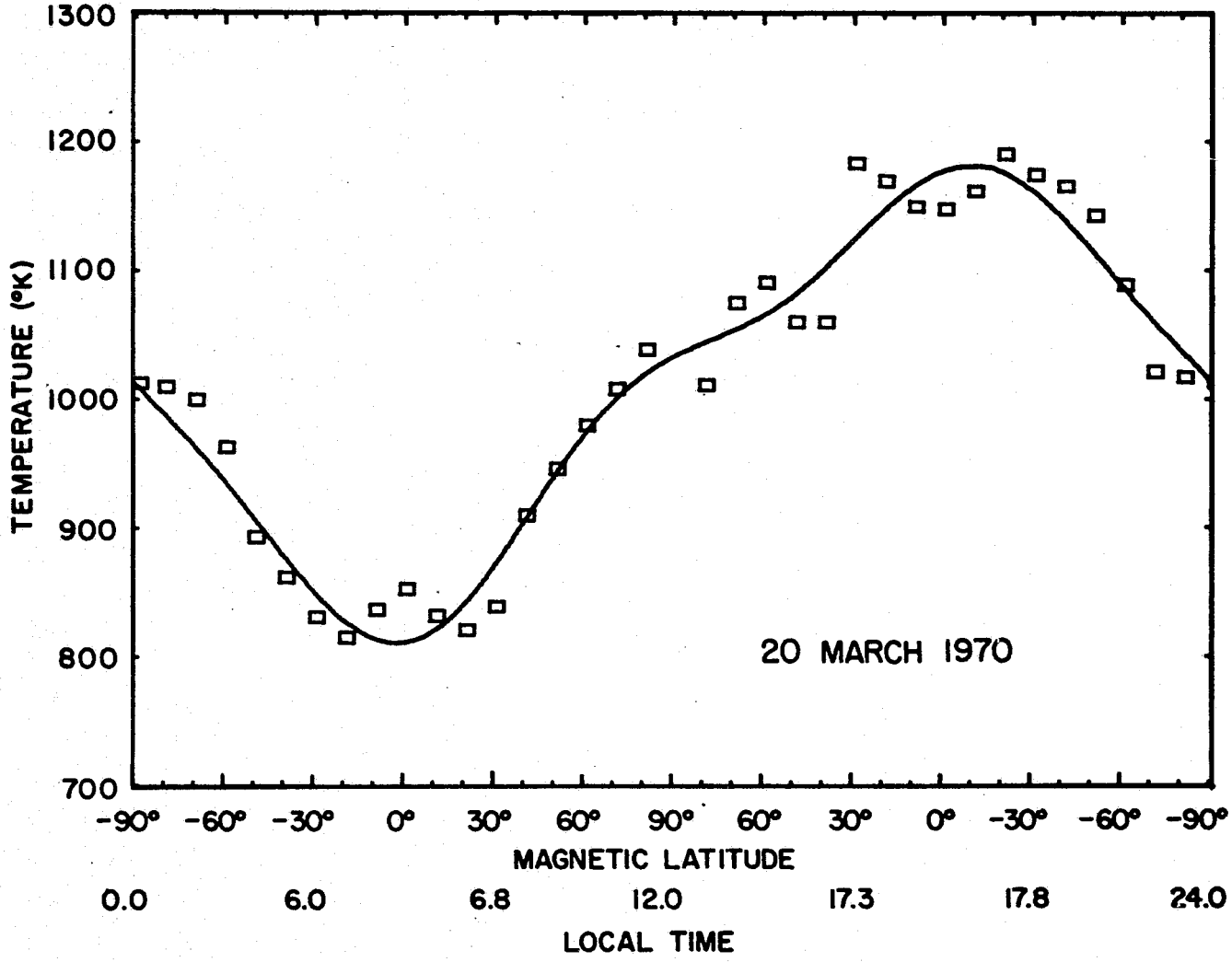

Figure 10 Orbital 6300 A temperature distribution with fourier series fit for March 70 equinox

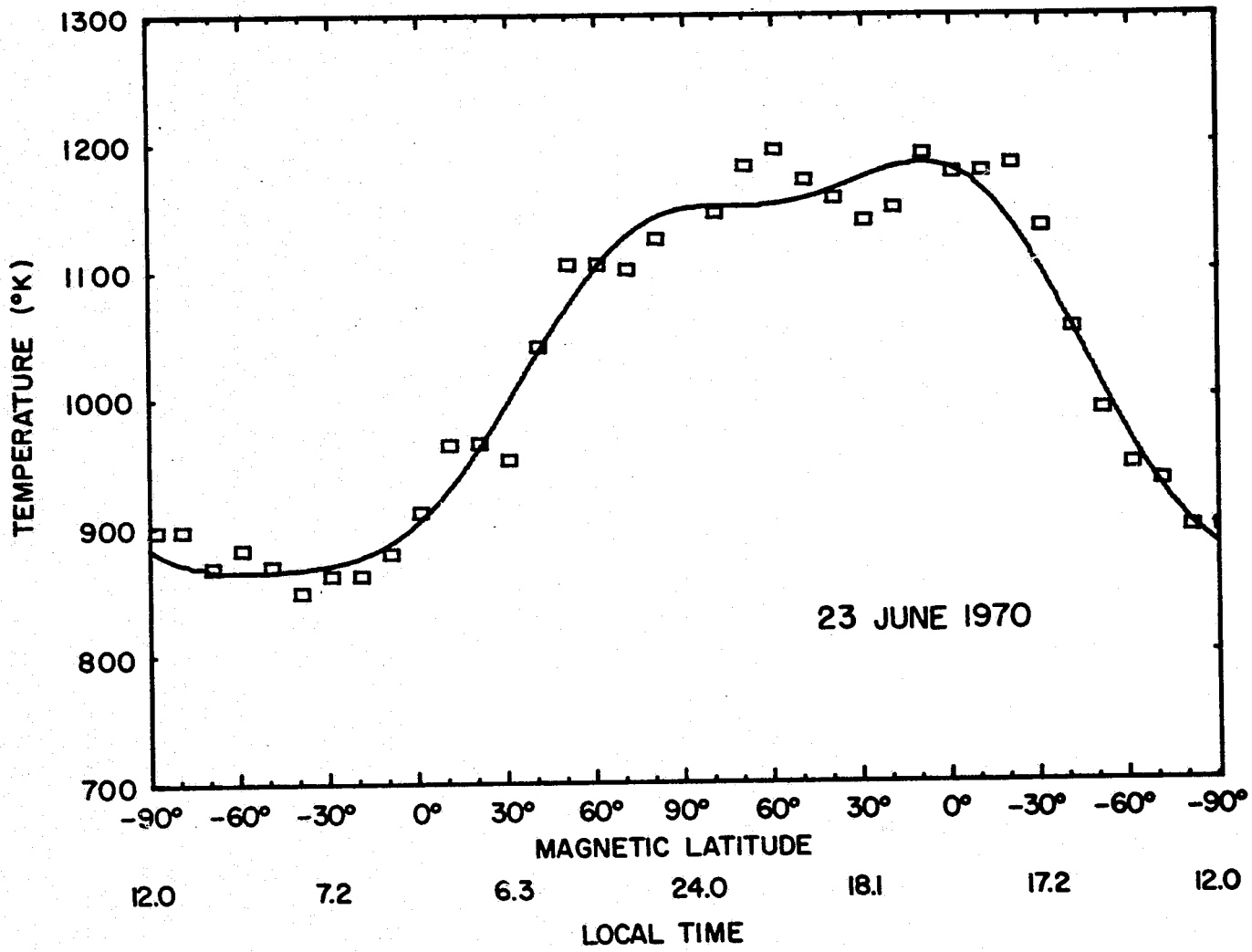

Figure 11 Orbital 6300 A temperature distribution with fourier series fit for June 70 solstice

Table 4: Coefficients of Fourier Series Fitted to Quiet Day Orbital Temperature Variations at Equinoxes and Solstices

$$T = A_0 + \theta_1 \sin\theta + A_1 \cos\theta + A_2 \cos 2\theta + B_2 \sin 2\theta + A_3 \cos 3\theta + B_2 \cos 3\theta$$

	A_0	A_1	B_1	A_2	B_2	A_3	B_3
$S_{10} = 127.4$ Summer 69	1019.48	103.92	115.79	12.56	31.82	-0.93	-37.93
$S_{10} = 144.5$ Fall 69	1036.86	-17.54	108.00	71.84	-14.87	-19.05	-38.93
$S_{10} = 158.7$ Winter 69	992.89	-105.77	95.55	-61.59	-87.09	-18.91	-32.64
$S_{10} = 142.2$ Spring 70	1005.39	2.41	162.55	14.58	-16.43	6.87	-20.21
$S_{10} = 139.1$ Summer 70	1028.9	119.71	119.29	-12.65	-16.20	12.83	-19.95

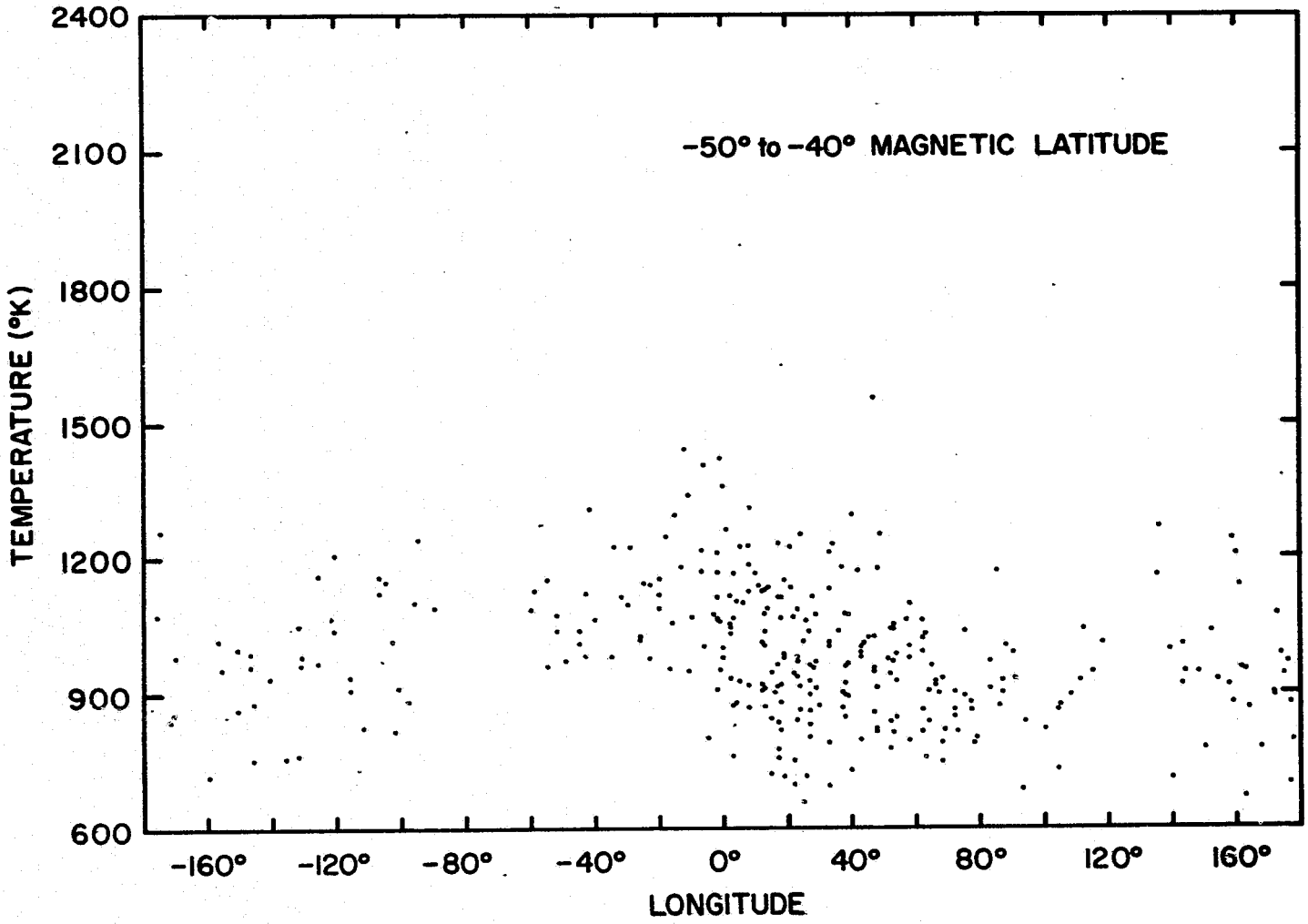

Figure 12 6300 A temperature data versus longitude for magnetic latitude between -50° and -40°

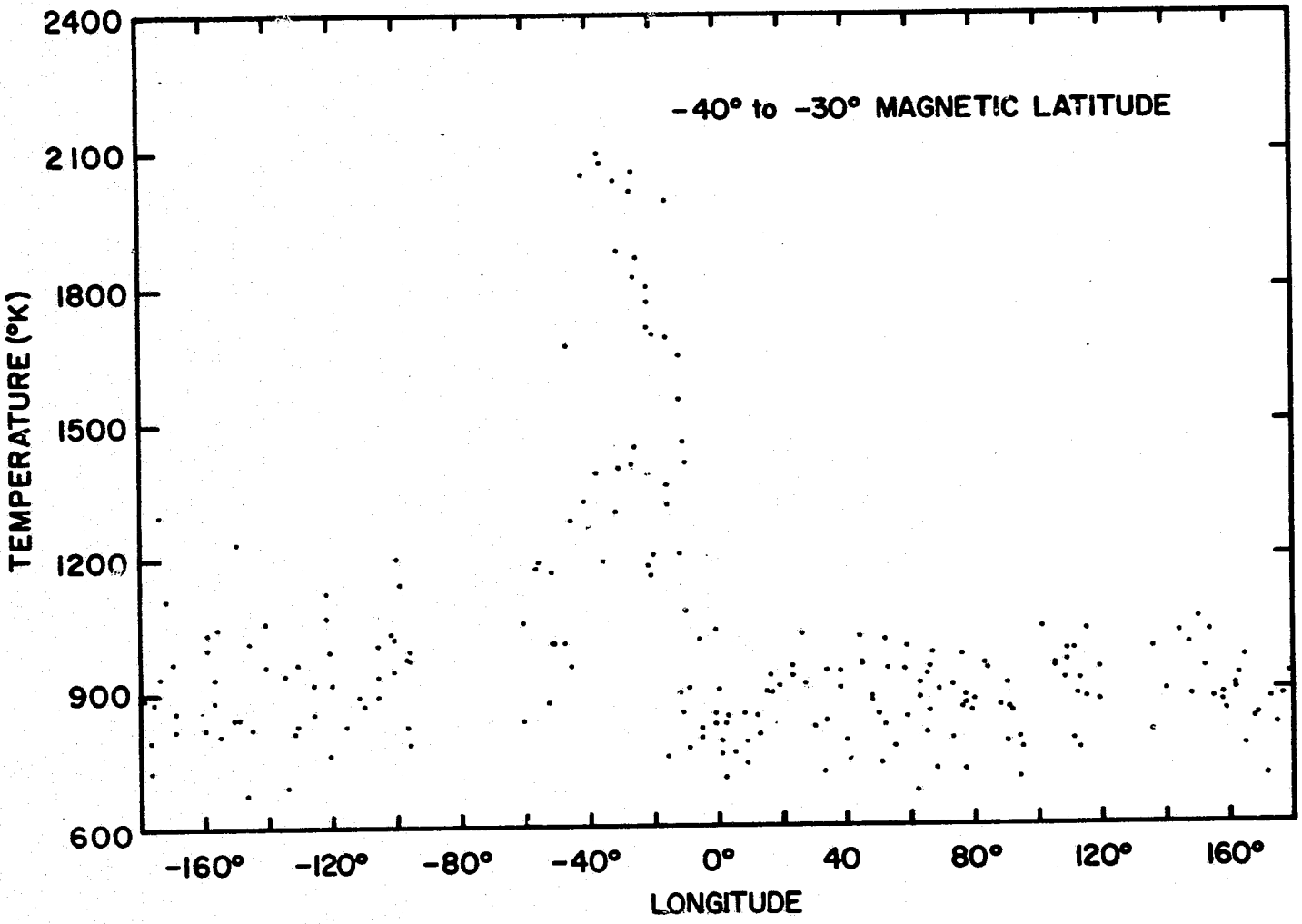

Figure 13 6300 A temperature data versus longitude for magnetic latitude between -40^{o} and -30^{o}

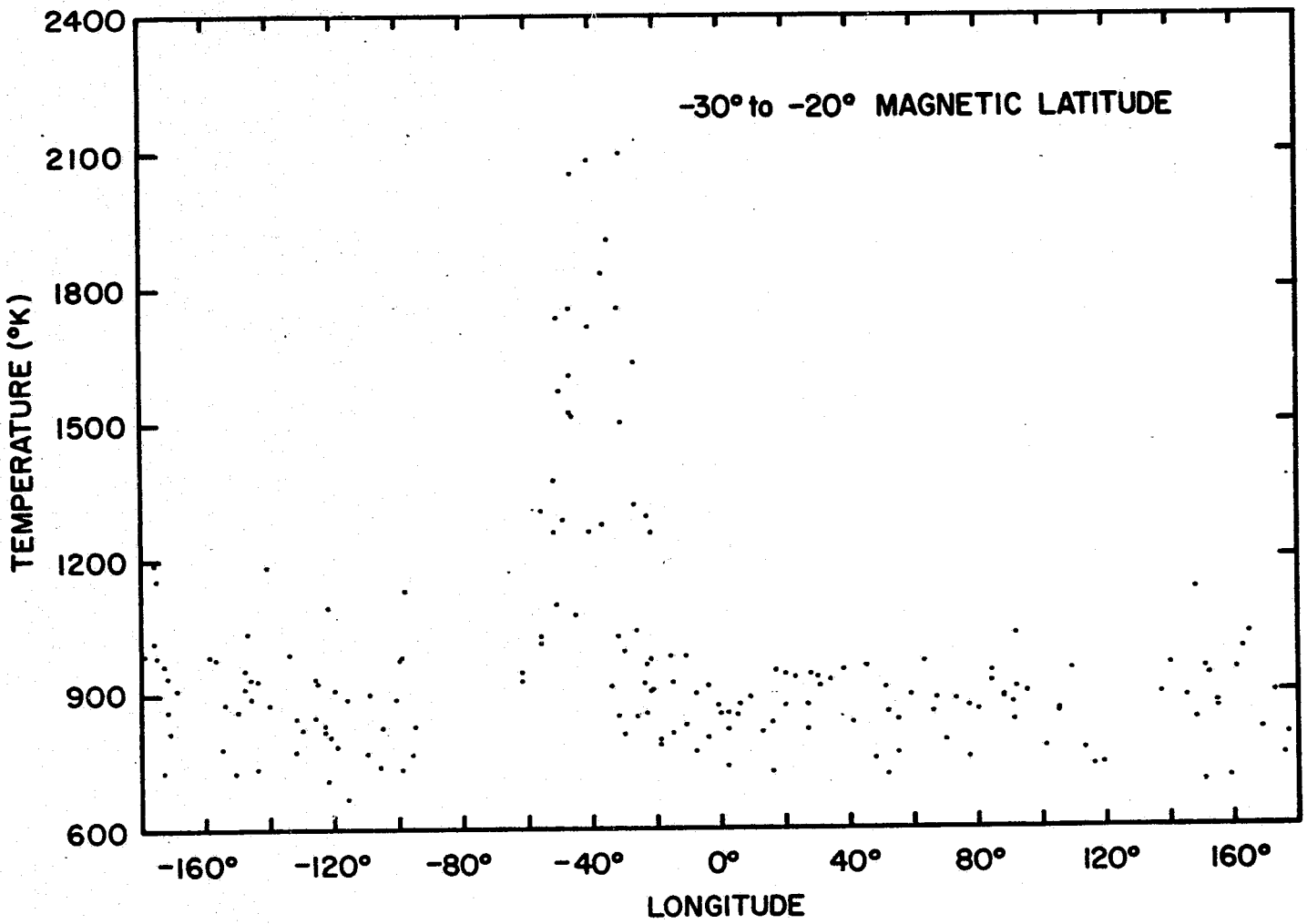

Figure 14 6300 A temperature data versus longitude for magnetic latitude between -30° and -20°

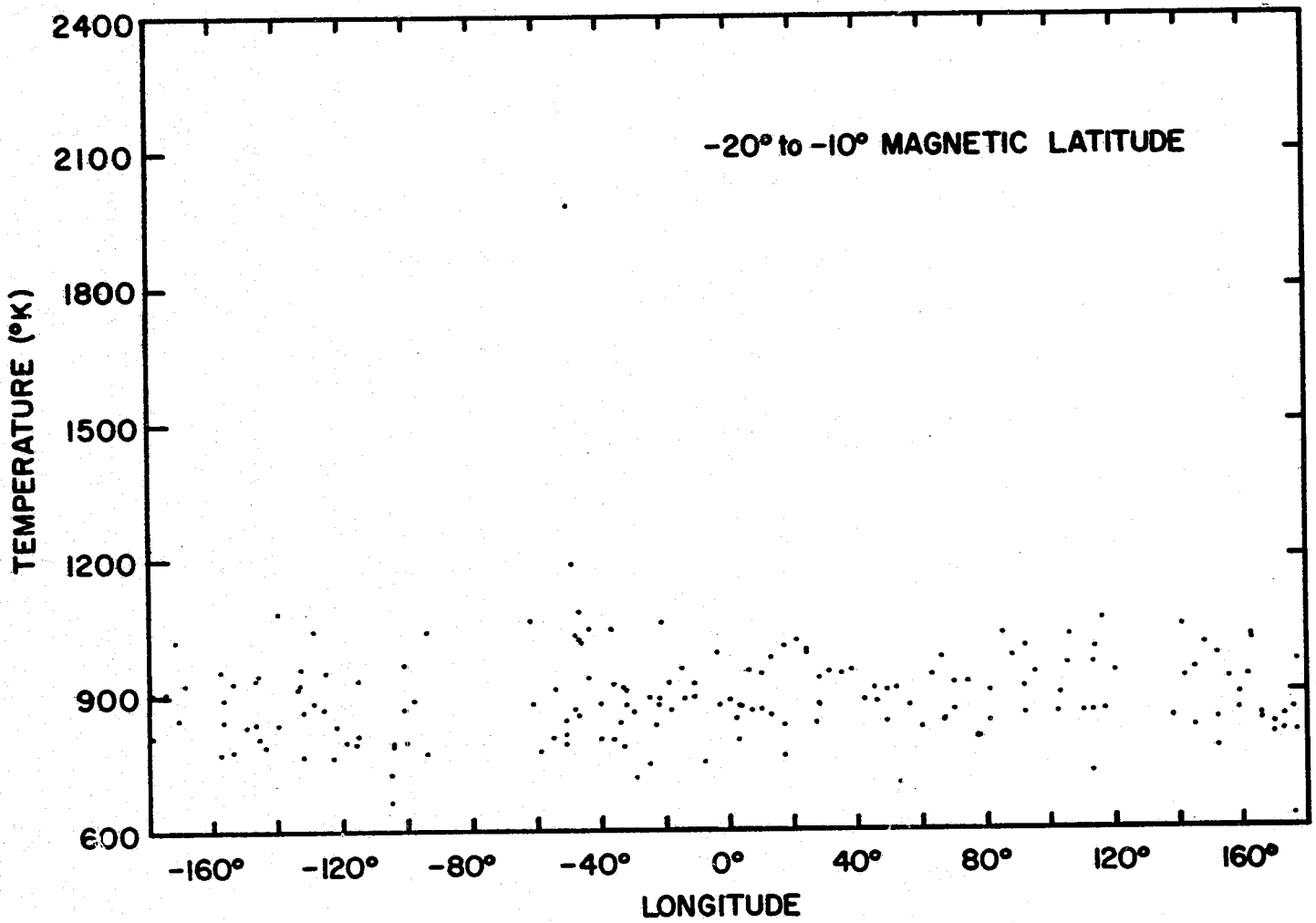

Figure 15 6300 A temperature data versus longitude for magnetic latitude between -20° and -10°

the observed temperatures do not correspond to the kinetic temperature of the ambient gas. Before the source of the emissions can be traced to its origin, a detailed examination of the spectra should be made. This project could be of great interest and further study appears to be warranted.

3.5 Temperatures at High Geomagnetic Latitudes

Blamont and Luton (1972) have discussed the evolution of the temperatures at high magnetic latitudes during the period from September 23, 1969 to October 7, 1969 which included two severe geomagnetic storms. In this section an attempt will be made to obtain some average characteristics of the polar thermosphere under different seasonal and magnetic conditions.

At high geomagnetic latitudes it has been shown that geophysical effects are represented most directly in a coordinate system based on geomagnetic latitude and geomagnetic time. In the present work the method of Agy (1965) was used as described in Appendix I of Matsushita and Campbell (1967) to calculate these parameters.

Temperatures at high magnetic latitudes are very variable and care must be taken in using satellite data to obtain time variations. The satellite precesses through 8 minutes in local time each day and storm conditions can cause an enhancement in temperature at the particular geomagnetic time when these measurements were made. To minimize, as far as possible, these fluctuations, it was decided to average the data over both hemispheres and quite extensive time periods.

The data was subdivided into ranges of geomagnetic latitude at 5^{o} intervals from 60^{o} to 90^{o} and in intervals of one hour in geomagnetic time, and in Kp ranges of 0 to 1.3, 1.3 to 4 and 4 to 6.9. The small number of data points above 85^{o} caused these temperatures to fluctuate greatly and thus measurements from 85^{o} to 90^{o} were averaged in 6 hour intervals.

The summer solstice data are shown in Figures 16, 17 and 18. The days used for the northern hemisphere were 6 June 1969 to 5 August 1969 and 7 May 1970 to 5 August 1970, and the days used to get the southern hemisphere summer were 5 November 1969 to 3 February 1970. The tabulated values are given in Tables 5, 6 and 7. The accuracies shown are the estimated accuracy of each measurement divided by the square root of the number of measurements.

The equinox data are shown in Figures 19, 20 and 21. The days used for these figures were 6 August 1969 to 4 November 1969, and days 4 February 1970 to 5 May 1970. The tabulated values are given in Tables 8, 9 and 10, and the accuracies are computed in the same way as the summer solstice.

The winter solstice data are shown in Figures 22, 23 and 24. The days used are the same as the summer solstice case with the appropriate polar region selected. The tabulated values are given in Tables 11, 12 and 13 with the accuracies computed in the same way as the summer solstice.

The seasonal effect at high geomagnetic latitudes appears to be greatest for low Kp values. The noon sector temperatures for 0 to 1.3 Kp during summer were about 100^{o}K hotter than winter, and during equinox were about 75^{o}K hotter than winter. The midnight sector

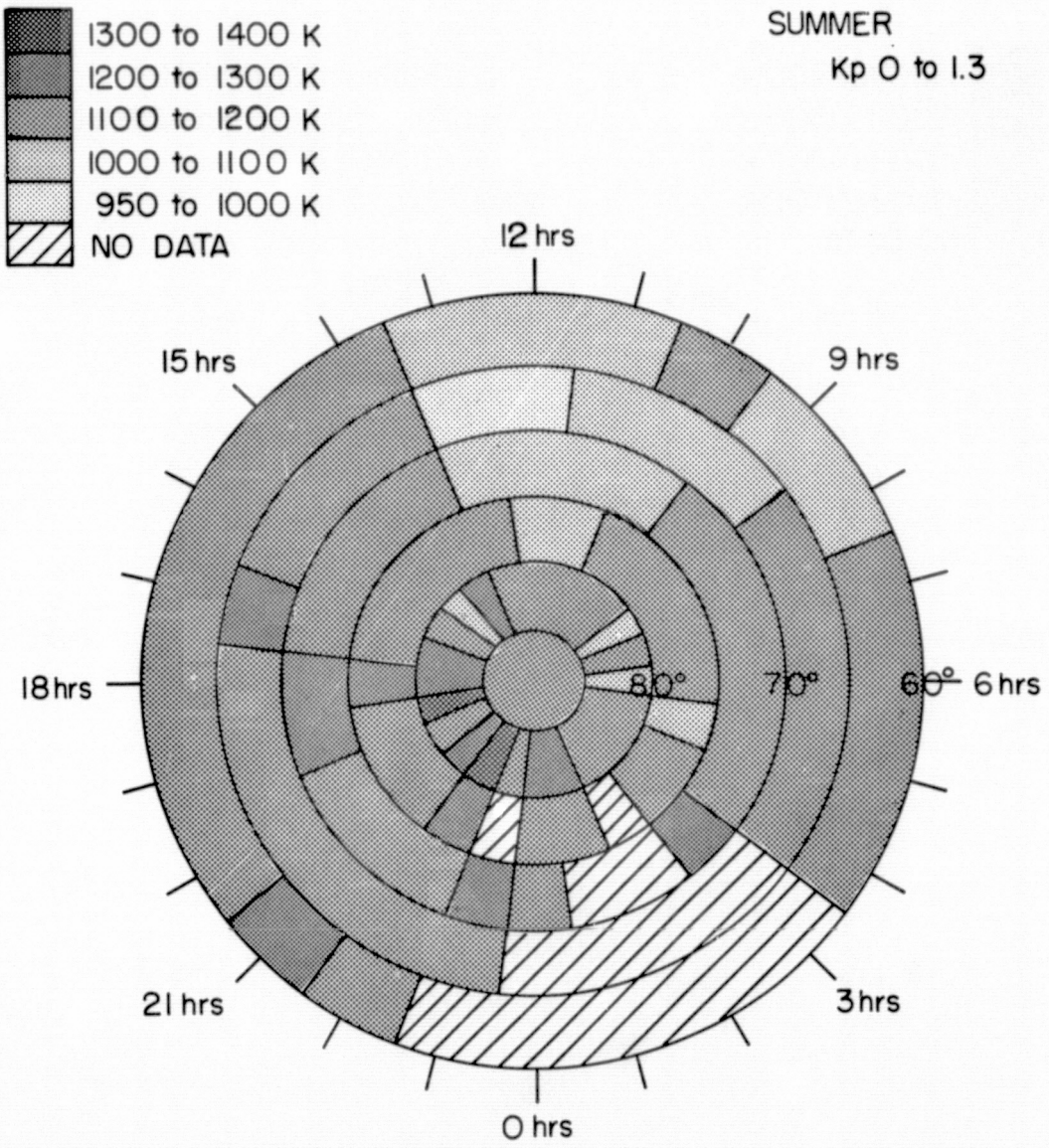

Figure 16 Exospheric temperature as a function of geomagnetic latitude and geomagnetic time for Kp range of 0 to 1.3 in Summer

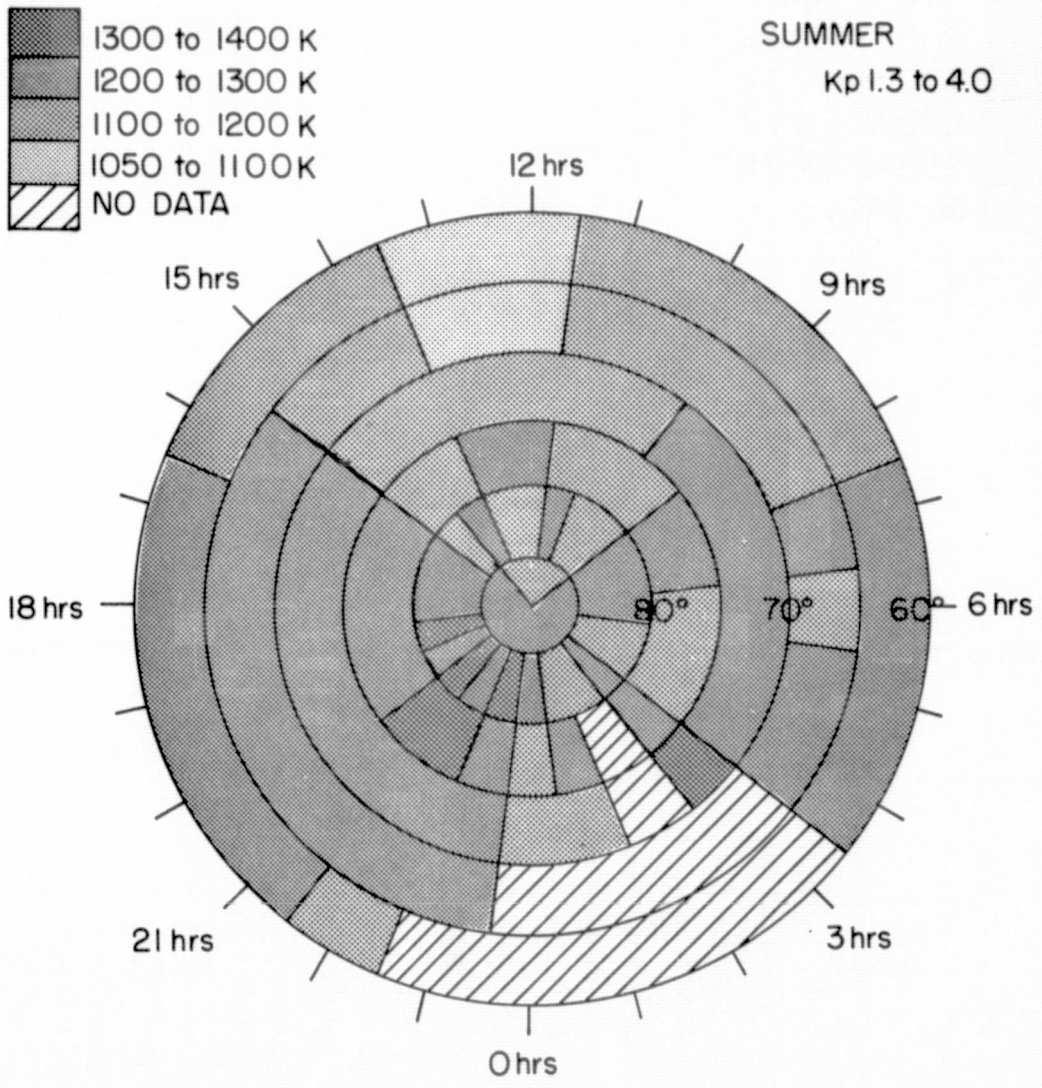

Figure 17 Exospheric temperature as a function of geomagnetic latitude and geomagnetic time for Kp range of 1.3 to 4.0 in Summer

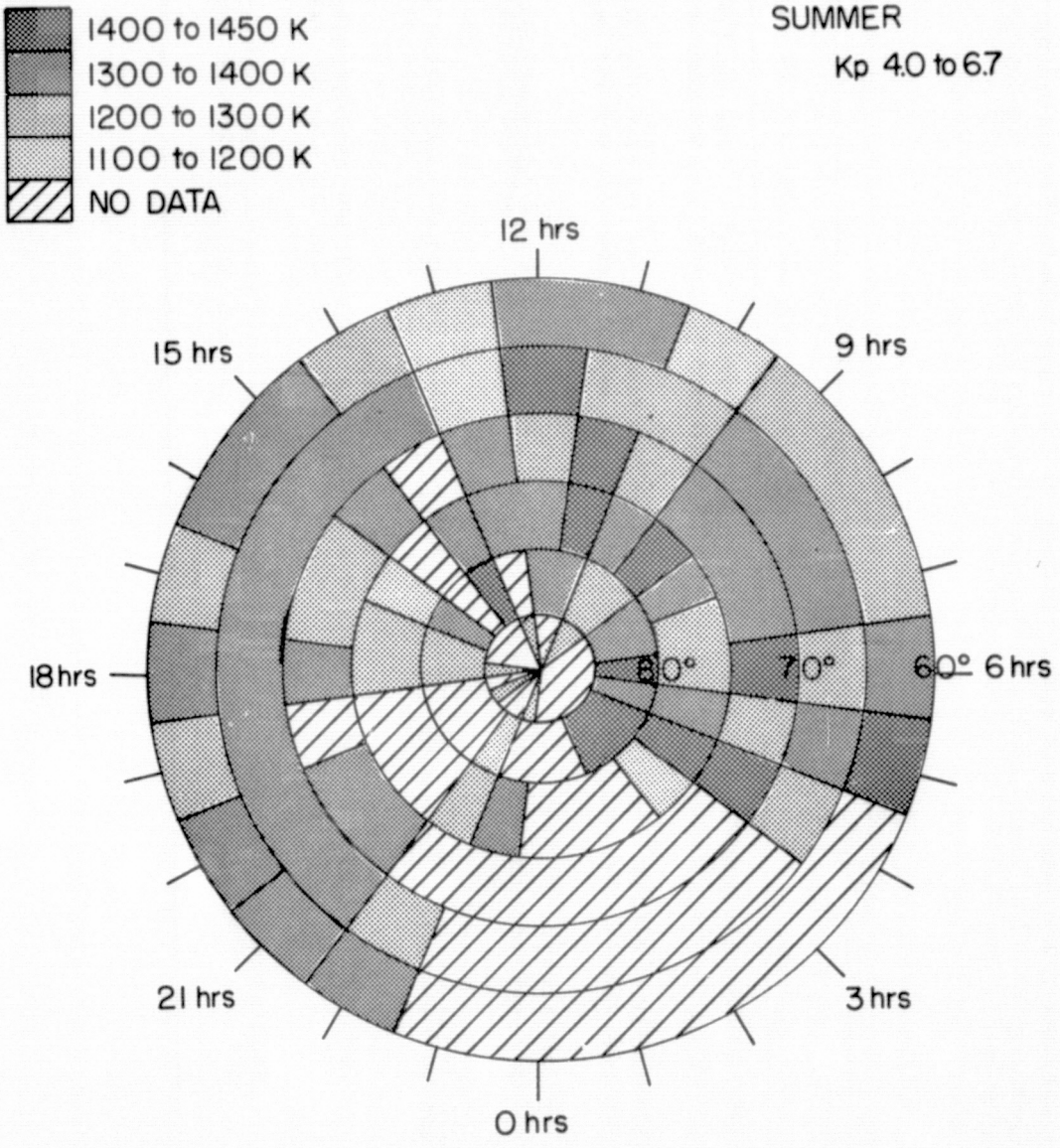

Figure 18 Exospheric temperature as a function of geomagnetic latitude and geomagnetic time for Kp range of 4.0 to 6.7 in Summer

Table 5: Exospheric Temperatures and Accuracy of Averaged Data Tabulated by Geomagnetic Latitude and Geomagnetic Time for Summer with Kp Range of 0 to 1.3

Geomagnetic Latitudes	Geomagnetic Time Hours																							
	1	2	3	4	5	6	7	8	9	10	11	12	13	14	15	16	17	18	19	20	21	22	23	24
85 - 90	1008 ±120	1095 ±69	1195 ±69	1087 ±60	1193 ±60	1244 ±69	1129 ±42	1206 ±54	1025 ±69	1369 ±120	1105 ±60	1216 ±45	1145 ±69	1153 ±54	1140 ±85		1149 ±69		994 ±85	1235 ±120	1320 ±69	1123 ±120	1203 ±120	
80 - 85	1208 ±54	1176 ±42	1139 ±32	1136 ±42	1139 ±29	1094 ±33	1147 ±28	1032 ±35	1127 ±33	1121 ±36	1127 ±31	1134 ±40	1184 ±35	1248 ±45	1076 ±42	1186 ±60	1204 ±49	1223 ±60	1340 ±85	1183 ±54	1256 ±69	1303 ±69	1138 ±85	1235 ±60
75 - 80	1368 ±120		1182 ±32	1126 ±27	1097 ±24	1119 ±29	1138 ±30	1152 ±28	1133 ±22	1130 ±24	1002 ±32	1048 ±35	1131 ±36	1115 ±35	1164 ±38	1148 ±33	1191 ±33	1277 ±69	1168 ±54	1107 ±120	1181 ±69	1205 ±69		1175 ±85
70 - 75			1236 ±60	1140 ±21	1100 ±24	1136 ±21	1114 ±21	1127 ±21	1139 ±29	1053 ±24	1076 ±24	1004 ±35	1039 ±35	1136 ±29	1126 ±28	1135 ±33	1166 ±25	1256 ±32	1267 ±36	1154 ±54	1171 ±49	1159 ±45	1276 ±69	1115 ±60
65 - 70				1196 ±30	1159 ±18	1155 ±20	1132 ±18	1108 ±18	1088 ±25	1083 ±24	1076 ±20	980 ±38	964 ±36	1132 ±23	1135 ±29	1177 ±32	1211 ±24	1192 ±26	1170 ±26	1141 ±40	1194 ±42	1188 ±49	1261 ±120	
60 - 65				1342 ±120	1162 ±20	1164 ±17	1129 ±15	1099 ±19	1086 ±26	1111 ±30	1045 ±22	1008 ±27	1063 ±36	1114 ±23	1161 ±28	1191 ±35	1162 ±26	1144 ±23	1184 ±24	1118 ±31	1282 ±36	1156 ±120		

Table 6: Exospheric Temperatures and Accuracy of Averaged Data Tabulated by Geomagnetic Latitude and Geomagnetic Time for Summer with Kp Range of 1.3 to 4.0

Geomagnetic Latitudes	Geomagnetic Time Hours																							
	1	2	3	4	5	6	7	8	9	10	11	12	13	14	15	16	17	18	19	20	21	22	23	24
85 - 90	1174 ±120	1189 ±85	1232 ±54	1171 ±60	1278 ±85	1315 ±54	1340 ±85	1202 ±42	1072 ±60	1369 ±120	1085 ±69	1126 ±49	1145 ±49	1319 ±85	1220 ±60	1256 ±60	1166 ±69	1212 ±54	1233 ±69	1318 ±60	1335 ±69	1299 ±60	1354 ±60	1314 ±85
80 - 85	1169 ±60	1196 ±42	1206 ±42	1171 ±28	1171 ±33	1208 ±26	1223 ±26	1216 ±29	1150 ±30	1182 ±42	1239 ±31	1156 ±40	1181 ±38	1232 ±28	1192 ±40	1226 ±40	1225 ±45	1254 ±42	1308 ±54	1280 ±35	1315 ±54	1297 ±45	1369 ±60	1284 ±49
75 - 80	1374 ±69	0	1228 ±25	1142 ±28	1196 ±24	1178 ±24	1225 ±29	1213 ±24	1198 ±20	1198 ±21	1182 ±25	1247 ±30	1247 ±31	1189 ±26	1191 ±26	1214 ±26	1264 ±38	1271 ±31	1267 ±36	1241 ±40	1317 ±30	1306 ±36	1286 ±45	1192 ±45
70 - 75	1195 ±120	0	1302 ±54	1224 ±21	1243 ±24	1205 ±21	1214 ±20	1226 ±17	1227 ±22	1150 ±21	1141 ±21	1118 ±30	1109 ±28	1134 ±26	1160 ±24	1226 ±23	1242 ±22	1239 ±24	1208 ±25	1290 ±24	1294 ±26	1254 ±26	1277 ±60	1191 ±85
65 - 70	0 0	0 0	0 0	1222 ±25	1272 ±16	1182 ±18	1203 ±13	1177 ±14	1155 ±23	1141 ±24	1115 ±20	1066 ±28	1064 ±29	1165 ±23	1167 ±29	1247 ±20	1271 ±23	1260 ±17	1251 ±19	1247 ±21	1259 ±24	1232 ±30	1259 ±60	0 0
60 - 65	0 0	0 0	0 0	1322 ±85	1269 ±15	1239 ±12	1211 ±12	1187 ±16	1175 ±22	1113 ±25	1101 ±24	1089 ±22	1071 ±24	1159 ±22	1189 ±24	1164 ±24	1222 ±18	1227 ±16	1217 ±14	1238 ±17	1273 ±19	1177 ±69	0 0	0 0

Table 7: Exospheric Temperatures and Accuracy of Averaged Data Tabulated by Geomagnetic Latitude and Geomagnetic Time for Summer with Kp Range of 4.0 to 6.7

Geomagnetic Latitudes	Geomagnetic Time Hours																							
	1	2	3	4	5	6	7	8	9	10	11	12	13	14	15	16	17	18	19	20	21	22	23	24
85 - 90	0	0	0	0	0	0	0	0	1178	1326	0	0	1364	0	0	0	0	1072	0	1427	0	0	1494	0
	0	0	0	0	0	0	0	0	±120	±120	0	0	±120	0	0	0	0	±120	0	±120	0	0	±120	0
80 - 85	0	1552	1648	1571	1336	1640	1325	1340	1250	1291	1332	1330	0	1459	0	1340	1252	1258	0	0	0	1163	0	0
	0	±120	±120	±85	±69	±85	±60	±60	±85	±120	±69	±69	0	±120	0	±120	±120	±85	0	0	0	±120	0	0
75 - 80	0	0	1173	1440	1394	1248	1295	1353	1414	1373	1456	1379	1362	1368	0	1186	1243	1292	0	0	0	1256	1368	0
	0	0	±85	±85	±42	±85	±54	±60	±54	±38	±69	±42	±54	±49	0	±120	±85	±69	0	0	0	±120	±120	0
70 - 75	0	0	0	1427	1297	1401	1337	1375	1322	1253	1446	1213	1315	0	1345	1203	1219	1346	0	1385	1315	0	0	0
	0	0	0	±54	±60	±54	±49	±38	±49	±45	±45	±85	±54	0	±38	±85	±60	±45	0	±120	±69	0	0	0
65 - 70	0	0	0	1254	1376	1299	1331	1342	1360	1259	1216	1476	1137	1383	1348	1341	1308	1344	1319	1340	1306	1273	0	0
	0	0	0	±120	±49	±49	±30	±40	±85	±45	±60	±69	±60	±69	±54	±54	±69	±35	±85	±69	±60	±85	0	0
60 - 65	0	0	0	0	1417	1340	1289	1259	1255	1195	1301	1325	1166	1274	1304	1356	1297	1354	1288	1305	1281	1308	0	0
	0	0	0	0	±38	±35	±30	±42	±69	±120	±54	±69	±69	±60	±69	±60	±60	±45	±85	±49	±54	±120	0	0

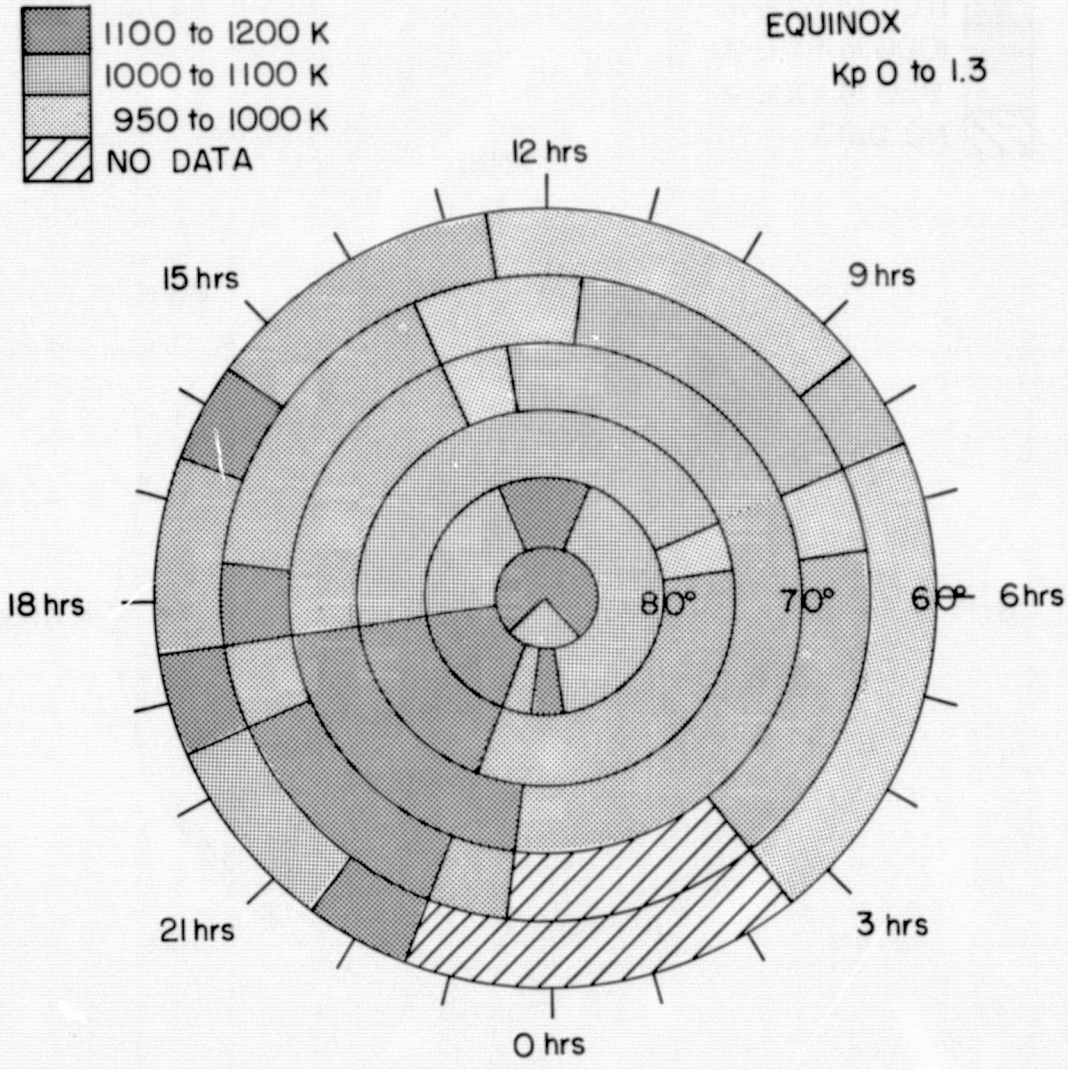

Figure 19 Exospheric temperature as a function of geomagnetic latitude and geomagnetic time for Kp range of 0 to 1.3 at equinox

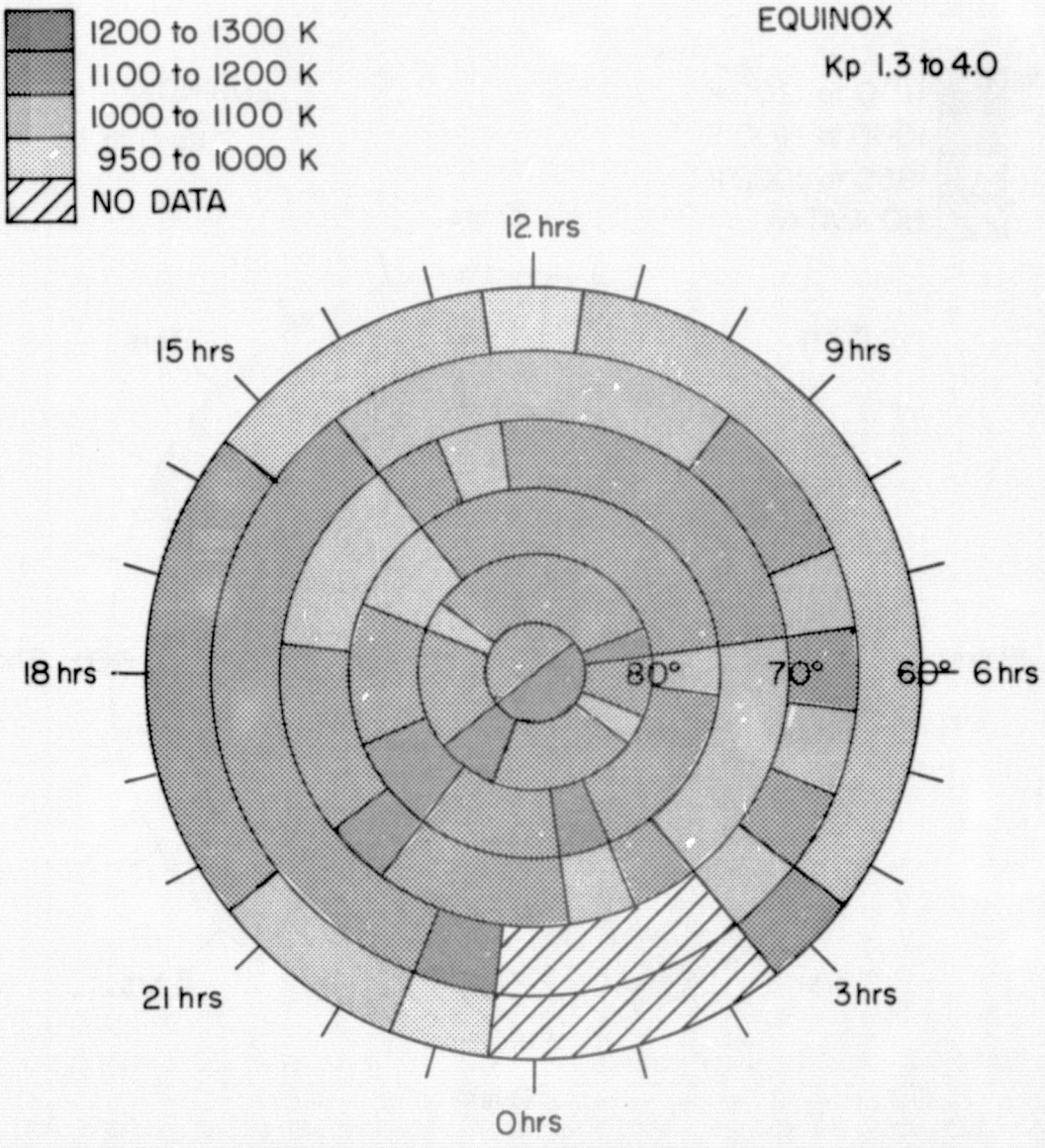

Figure 20 Exospheric temperature as a function of geomagnetic latitude and geomagnetic time for Kp range of 1.3 to 4.0 at equinox

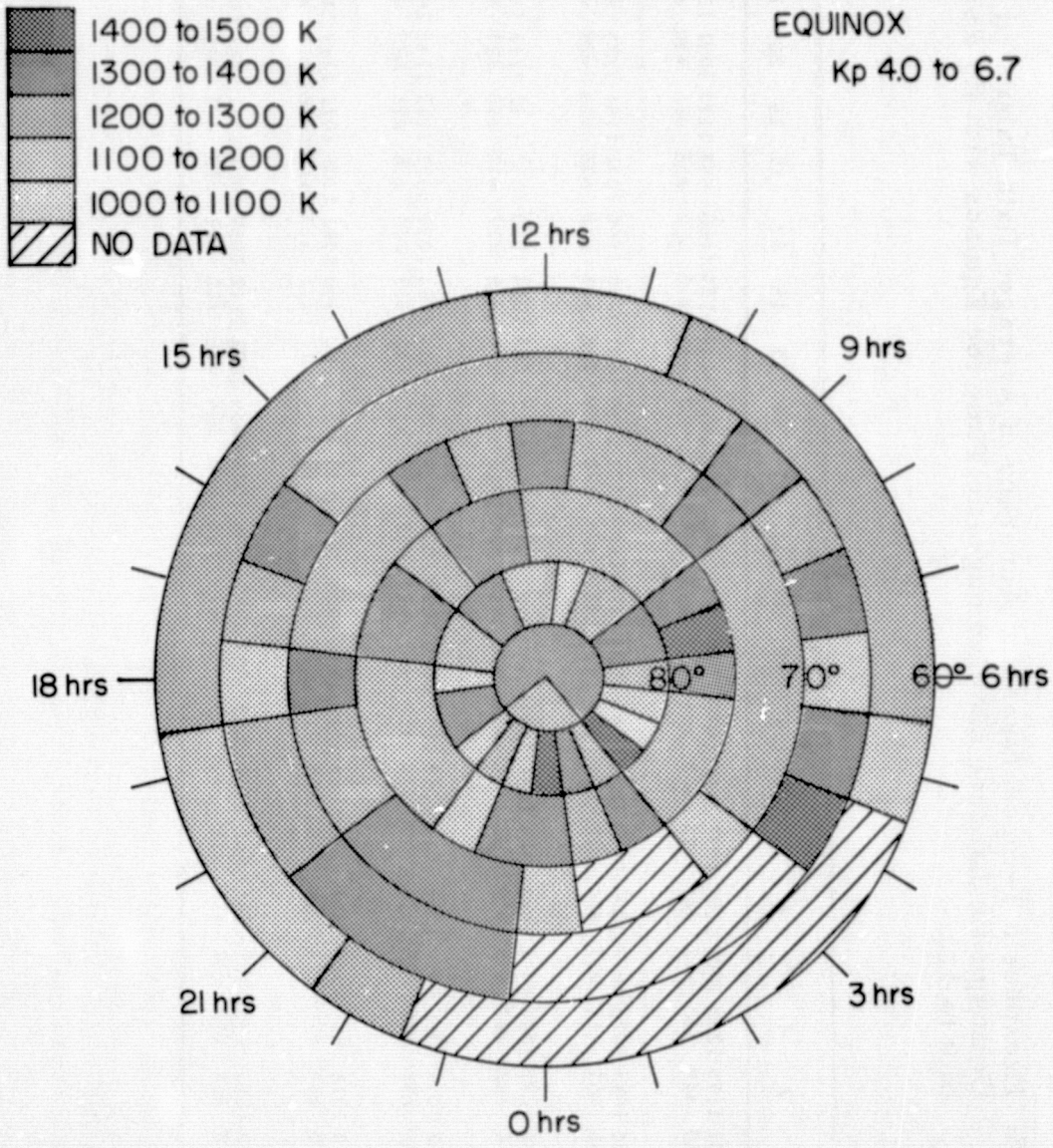

Figure 21 Exospheric temperature as a function of geomagnetic latitude and geomagnetic time for Kp range of 4.0 to 6.7 at equinox

Table 8: Exospheric Temperatures and Accuracy of Averaged Data Tabulated by Geomagnetic Latitude and Geomagnetic Time for Equinox with Kp Range of 0 to 1.3

Geomagnetic Latitudes	Geomagnetic Time Hours																							
	1	2	3	4	5	6	7	8	9	10	11	12	13	14	15	16	17	18	19	20	21	22	23	24
85 - 90	936 ±49	1151 ±40	1175 ±49	1202 ±40	1071 ±42	1180 ±45	1073 ±36	1138 ±60	1072 ±45	1018 ±49	1119 ±32	1145 ±40	1158 ±38	1097 ±32	1129 ±45	1159 ±30	1108 ±38	988 ±38	1113 ±36	1091 ±40	1079 ±38	1112 ±45	1091 ±54	1176 ±60
80 - 85	1093 ±27	1085 ±36	1083 ±31	1024 ±31	1073 ±27	1096 ±24	1093 ±19	1021 ±24	1043 ±21	1082 ±20	1110 ±21	1109 ±21	1122 ±20	1083 ±19	1041 ±18	1030 ±21	1100 ±22	1091 ±25	1156 ±28	1135 ±25	1145 ±24	1148 ±30	1068 ±29	1102 ±23
75 - 80	1065 ±31	1099 ±28	1071 ±32	1089 ±27	1072 ±27	1043 ±19	985 ±1	1026 ±12	1031 ±13	1080 ±13	1069 ±13	1072 ±14	1056 ±15	1021 ±14	1068 ±14	1044 ±16	1060 ±17	1092 ±17	1112 ±19	1113 ±21	1148 ±21	1143 ±22	1061 ±26	1064 ±26
70 - 75	889 ±120	1012 ±45	1014 ±42	1066 ±30	1010 ±26	1012 ±19	1036 ±15	1059 ±11	1013 ±11	1029 ±11	1025 ±12	1026 ±13	977 ±12	1030 ±17	1033 ±16	1082 ±13	1099 ±14	1097 ±16	1112 ±18	1142 ±20	1121 ±19	1122 ±20	1119 ±24	1097 ±45
65 - 70	0 0	0 0	1016 ±49	1022 ±33	1004 ±24	1012 ±18	978 ±15	1032 ±10	1010 ±10	1004 ±10	1033 ±10	988 ±11	986 ±15	1057 ±14	1088 ±17	1099 ±13	1081 ±15	1123 ±15	1072 ±16	1117 ±16	1130 ±17	1124 ±20	1039 ±45	0 0
60 - 65	0 0	0 0	1083 ±69	996 ±33	982 ±27	965 ±21	968 ±15	1027 ±9	985 ±9	983 ±8	987 ±10	995 ±13	1023 ±15	1039 ±14	1082 ±16	1112 ±12	1059 ±12	1061 ±13	1121 ±15	1086 ±15	1098 ±16	1179 ±33	896 ±85	0 0

Table 9: Exospheric Temperatures and Accuracy of Averaged Data Tabulated by Geomagnetic Latitude and Geomagnetic Time for Equinox with Kp Range of 1.3 to 4.0

Geomagnetic Latitudes	Geomagnetic Time Hours																						
	1	2	3	4	5	6	7	8	9	10	11	12	13	14	15	16	17	18	19	20	21	22	23	24
85 - 90	1178 ±40	1268 ±38	1218 ±31	1299 ±45	1152 ±54	1325 ±36	1261 ±30	1100 ±42	1105 ±38	1182 ±36	1158 ±29	1147 ±36	1247 ±40	1248 ±33	1113 ±49	1232 ±30	1069 ±40	1123 ±38	1242 ±36	1137 ±38	1135 ±35	1170 ±35	1268 ±42	1253 ±38
80 - 85	1168 ±26	1102 ±26	1148 ±32	1093 ±27	1156 ±24	1155 ±24	1222 ±18	1166 ±21	1159 ±20	1191 ±21	1175 ±22	1198 ±18	1190 ±21	1164 ±18	1125 ±17	1097 ±19	1141 ±18	1156 ±21	1149 ±19	1139 ±24	1213 ±22	1206 ±20	1174 ±24	1168 ±26
75 - 80	1230 ±24	1124 ±26	1163 ±24	1113 ±26	1153 ±22	1084 ±20	1149 ±16	1175 ±12	1152 ±12	1128 ±13	1159 ±12	1179 ±12	1170 ±15	1131 ±13	1091 ±12	1097 ±14	1160 ±16	1156 ±15	1151 ±18	1201 ±18	1206 ±19	1199 ±18	1129 ±22	1139 ±28
70 - 75	977 ±120	1190 ±69	1069 ±32	1071 ±24	1061 ±22	1074 ±17	1119 ±14	1145 ±10	1116 ±10	1113 ±9	1115 ±11	1102 ±11	1087 ±11	1107 ±12	1097 ±11	1093 ±10	1088 ±12	1176 ±14	1198 ±15	1193 ±16	1201 ±14	1147 ±15	1178 ±22	1140 ±38
65 - 70	0 0	0 0	1002 ±60	1120 ±33	1080 ±23	1110 ±13	1093 ±13	1131 ±8	1109 ±9	1048 ±8	1076 ±9	1047 ±10	1035 ±14	1097 ±12	1118 ±12	1160 ±11	1147 ±11	1102 ±12	1135 ±13	1148 ±14	1168 ±12	1107 ±15	1222	0 0
60 - 65	0 0	0 0	1113 ±120	1019 ±35	1060 ±23	1060 ±15	1086 ±11	1096 ±7	1063 ±7	1061 ±7	1012 ±9	999 ±11	1022 ±14	1014 ±12	1046 ±14	1128 ±11	1103 ±11	1113 ±11	1139 ±12	1112 ±12	1078 ±14	1088 ±26	923 ±60	0 0

Table 10: Exospheric Temperatures and Accuracy of Averaged Data Tabulated by Geomagnetic Latitude and Geomagnetic Time for Equinox with Kp Range of 4.0 to 6.7

Geomagnetic Latitudes	Geomagnetic Time Hours																							
	1	2	3	4	5	6	7	8	9	10	11	12	13	14	15	16	17	18	19	20	21	22	23	24
85 - 90	1438	1416	1392	0	1253	1352	1409	1263	1152	1427	1215	1216	1438	1373	0	1263	1282	1268	1341	1486	976	1199	1353	1274
	±120	±69	±120	0	±85	±85	±54	±69	±120	±60	±85	±120	±69	±54	0	±54	±60	±54	±85	±69	±120	±69	±69	±85
80 - 85	1388	1260	1529	1093	1189	1243	1303	1324	1240	1263	1166	1213	1289	1304	1321	1240	1228	1177	1312	1325	1197	1246	1197	1406
	±69	±60	±85	±60	±69	±54	±54	±38	±45	±42	±54	±54	±49	±36	±32	±38	±40	±49	±38	±49	±49	±49	±54	±60
75 - 80	1283	1216	1231	1212	1270	1342	1498	1341	1224	1247	1282	1294	1344	1306	1265	1315	1309	1285	1276	1265	1283	1193	1309	1310
	±60	±69	±69	±69	±60	±85	±60	±26	±31	±27	±28	±31	±42	±45	±28	±31	±38	±40	±40	±45	±49	±49	±60	±60
70 - 75	0	0	1108	1263	1283	1296	1250	1279	1340	1284	1249	1313	1275	1315	1209	1298	1245	1314	1288	1252	1315	1318	1332	1136
	0	0	±85	±85	±60	±54	±42	±21	±35	±24	±27	±49	±33	±35	±28	±26	±26	±35	±35	±38	±40	±45	±42	±69
65 - 70	0	0	0	1460	1353	1199	1313	1264	1326	1219	1273	1239	1272	1283	1255	1316	1275	1190	1284	1203	1335	1317	1370	0
	0	0	0	±120	±120	±45	±29	±20	±22	±24	±25	±31	±36	±40	±25	±26	±26	±26	±42	±31	±32	±45	±60	0
60 - 65	0	0	0	0	1194	1224	1271	1261	1277	1206	1116	1148	1240	1215	1213	1223	1226	1261	1177	1196	1192	1266	0	0
	0	0	0	0	±85	±45	±24	±17	±20	±19	±24	±30	±40	±33	±26	±26	±26	±32	±26	±24	±26	±69	0	0

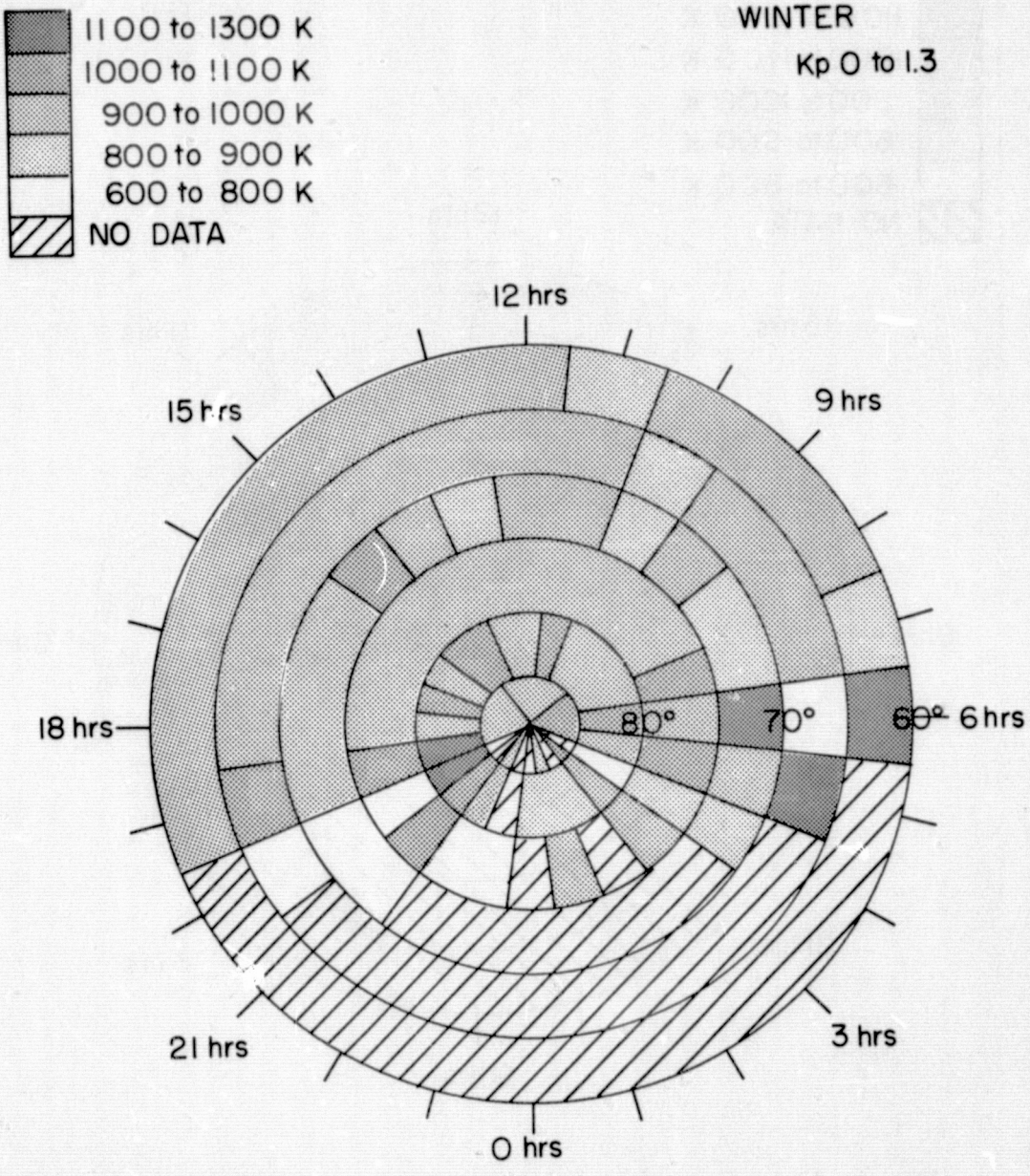

Figure 22 Exospheric temperature as a function of geomagnetic latitude and geomagnetic time for Kp range of 0 to 1.3 in Winter

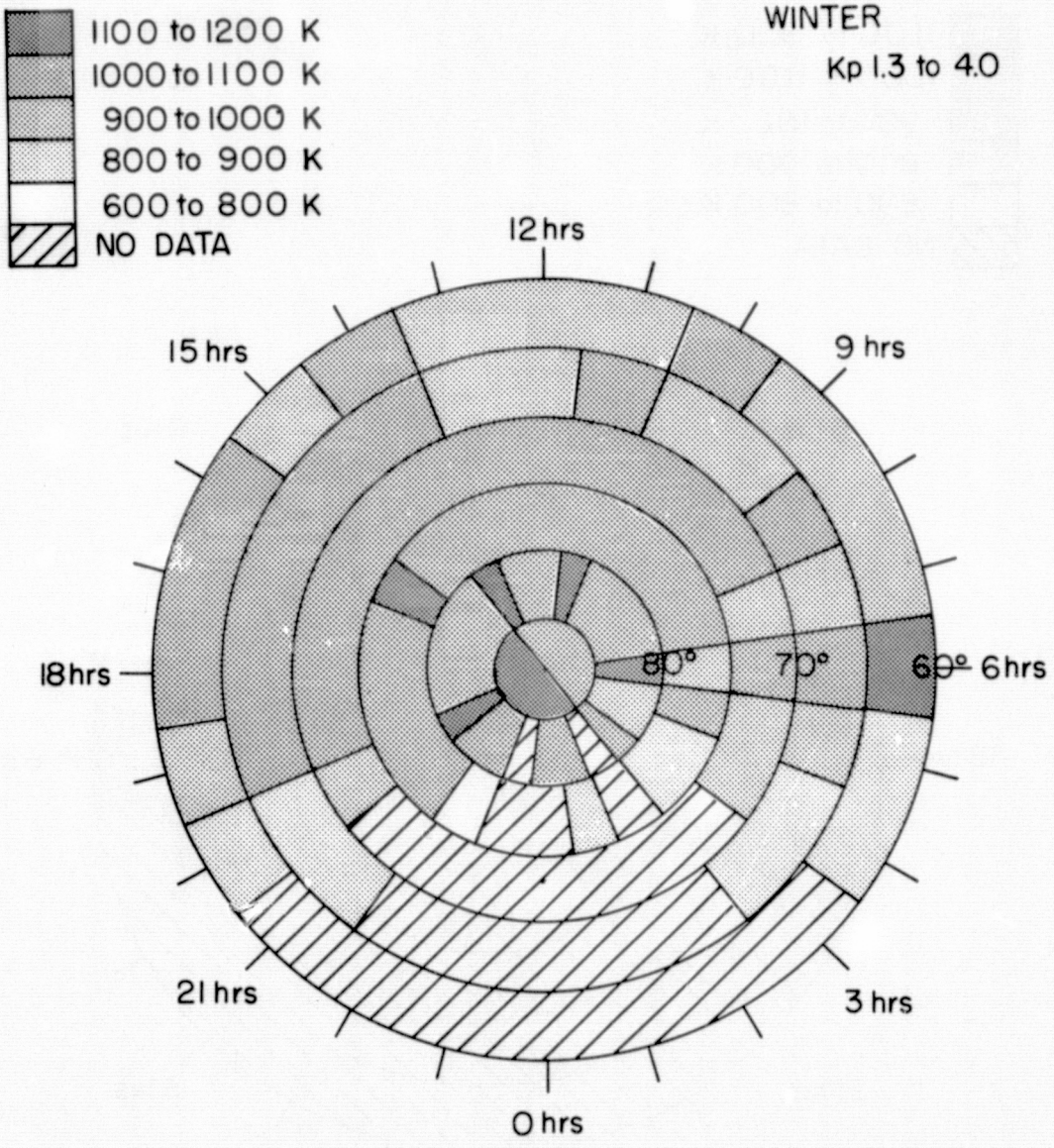

Figure 23 Exospheric temperature as a function of geomagnetic latitude and geomagnetic time for Kp range of 1.3 to 4.0 in Winter

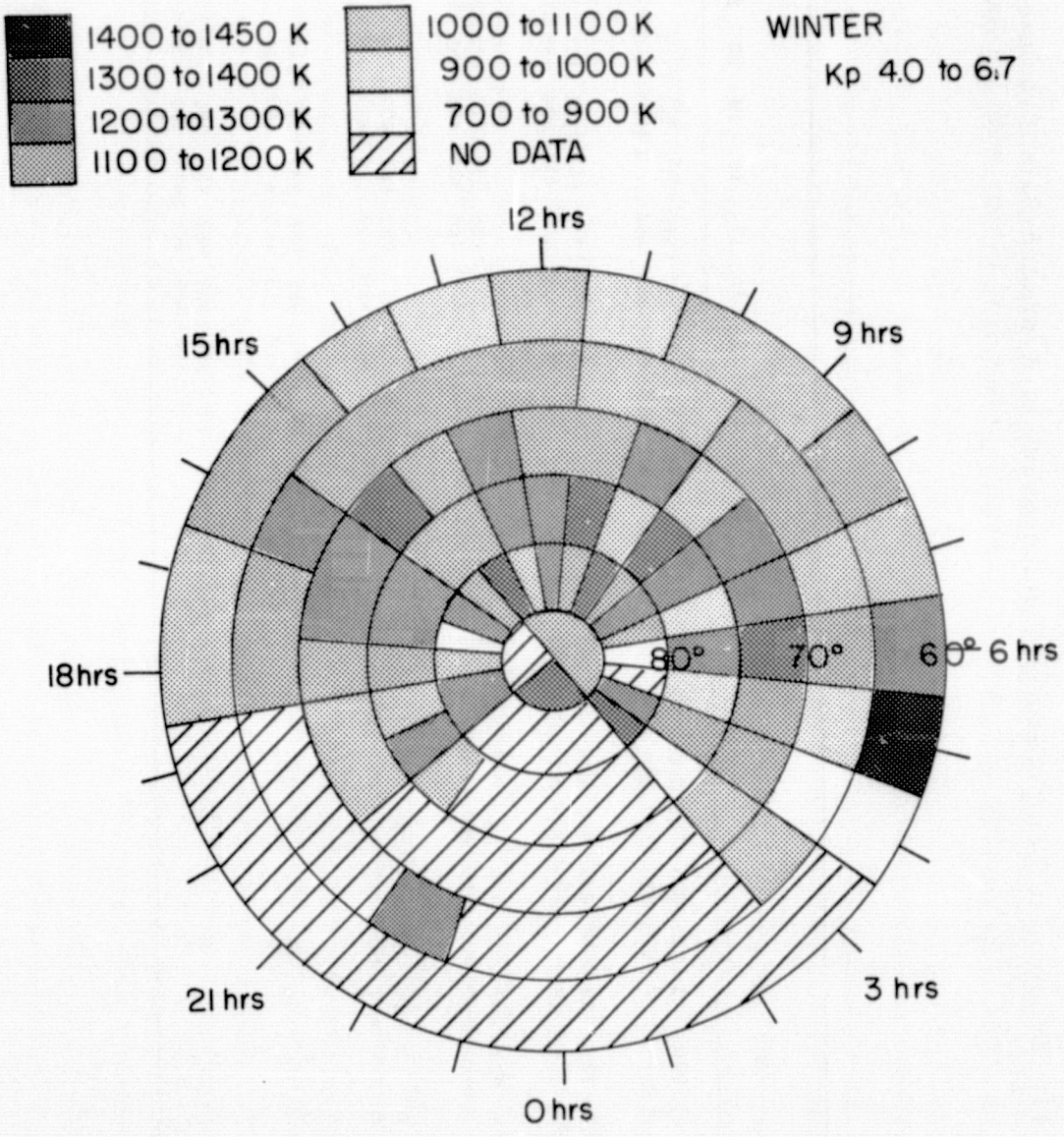

Figure 24 Exospheric temperature as a function of geomagnetic latitude and geomagnetic time for Kp range of 4.0 to 6.7 in Winter

Table 11: Exospheric Temperatures and Accuracy of Averaged Data Tabulated by Geomagnetic Latitude and Geomagnetic Time for Winter with Kp Range of 0 to 1.3

Geomagnetic Latitudes	Geomagnetic Time Hours																							
	1	2	3	4	5	6	7	8	9	10	11	12	13	14	15	16	17	18	19	20	21	22	23	24
85 - 90	795	0	970	0	830	1023	865	1282	792	854	936	928	798	1034	901	921	1030	972	741	1114	0	937	0	0
	±120	0	±120	0	±120	±69	±120	±60	±120	±85	±120	±120	±85	±69	±85	±85	±54	±69	±120	±60	0	±85	0	0
80 - 85	1277	897	929	730	946	1024	932	974	974	961	1024	921	935	1002	1015	867	1003	965	1100	1151	1021	901	0	892
	±85	±69	±85	±120	±45	±54	±38	±45	±40	±42	±32	±29	±42	±36	±60	±38	±33	±38	±54	±85	±120	±120	0	±120
75 - 80	976	0	903	897	1072	976	1054	983	968	922	975	957	931	999	987	999	946	978	1013	982	1010	693	706	0
	±120	0	±120	±120	±85	±36	±54	±[illegible]	±29	±28	±28	±23	±18	±31	±28	±26	±28	±26	±54	±85	±120	±120	±120	0
70 - 75	0	0	0	884	991	1105	844	862	916	878	927	924	876	976	1058	952	998	967	901	704	771	0	0	0
	0	0	0	±60	±45	±45	±60	±33	±35	±25	±27	±22	±19	±19	±21	±20	±19	±22	±40	±85	±120	0	0	0
65 - 70	0	0	0	0	1123	600	922	952	910	868	982	910	914	928	941	963	950	957	1071	642	0	0	0	0
	0	0	0	0	±120	±120	±45	±38	±35	±21	±19	±17	±15	±15	±19	±18	±21	±18	±69	±120	0	0	0	0
60 - 65	0	0	0	0	0	1311	898	971	916	944	867	944	910	955	921	969	982	966	996	0	0	0	0	0
	0	0	0	0	0	±120	±54	±33	±38	±31	±21	±17	±12	±13	±14	±19	±20	±19	±60	0	0	0	0	0

Table 12: Exospheric Temperatures and Accuracy of Averaged Data Tabulated by Geomagnetic Latitude and Geomagnetic Time for Winter with Kp Range of 1.3 to 4.0

Geomagnetic Latitudes	Geomagnetic Time Hours																						
	1	2	3	4	5	6	7	8	9	10	11	12	13	14	15	16	17	18	19	20	21	22	23	24
85 - 90	1532	1369	0	0	879	0	1254	1149	1040	947	983	1257	1068	1008	1598	1157	1100	1036	876	1088	882	850	1056	1116
	±120	±85	0	0	±60	0	±69	±60	±49	±85	±60	±120	±54	±85	±120	±49	±49	±60	±85	±42	±85	±120	±120	±120
80 - 85	1085	0	1006	924	936	1170	1052	1026	1052	1046	1116	1043	1070	1127	1073	1043	1034	1037	1051	1117	1081	1006	0	732
	±85	0	±85	±85	±49	±54	±42	±35	±31	±40	±26	±23	±30	±26	±33	±28	±38	±33	±49	±60	±85	±69	0	±120
75 - 80	857	0	851	889	1044	995	1072	1068	1087	1093	1093	1093	1025	1081	1096	1113	1037	1023	1056	1036	1010	693	0	0
	±85	0	±60	±54	±42	±29	±30	±25	±22	±20	±22	±20	±17	±20	±21	±22	±20	±26	±42	±54	±120	±120	0	0
70 - 75	0	0	0	942	921	1010	961	1008	1036	1029	1036	1041	1018	1070	1090	1091	1034	1010	1001	956	0	0	0	0
	0	0	0	±85	±49	±36	±33	±18	±22	±17	±18	±16	±15	±15	±16	±17	±14	±16	±31	±69	0	0	0	0
65 - 70	0	0	853	800	934	1091	992	1016	993	984	1011	938	988	1042	1053	1048	1027	1020	1011	879	807	0	0	0
	0	0	±120	±85	±45	±69	±32	±19	±18	±18	±16	±14	±13	±14	±15	±15	±15	±12	±35	±45	±120	0	0	0
60 - 65	0	0	0	812	882	1131	934	981	950	1027	948	977	935	1007	965	1007	1016	1022	941	833	0	0	0	0
	0	0	0	±69	±120	±85	±42	±22	±24	±18	±15	±13	±10	±12	±12	±15	±16	±14	±40	±85	0	0	0	0

Table 13: Exospheric Temperatures and Accuracy of Averaged Data Tabulated by Geomagnetic Latitude and Geomagnetic Time for Winter with Kp Range of 4.0 to 6.7

Geomagnetic Latitudes	Geomagnetic Time Hours																							
	1	2	3	4	5	6	7	8	9	10	11	12	13	14	15	16	17	18	19	20	21	22	23	24
85 - 90	1719	0	0	0	0	0	1393	1006	1115	1021	0	0	1236	1417	0	0	0	0	0	0	1290	0	0	1559
	±120	0	0	0	0	0	±120	±85	±120	±85	0	0	±120	±120	0	0	0	0	0	0	±120	0	0	±120
80 - 85	0	0	1530	1202	0	796	1156	1299	1185	1371	1166	1269	1072	1310	1198	1215	860	1044	1248	1210	0	0	0	0
	0	0	±120	±85	0	±85	±69	±120	±54	±69	±69	±85	±60	±69	±69	±60	±120	±120	±85	±120	0	0	0	0
75 - 80	0	0	863	1192	942	1254	911	1235	1374	1021	1305	1245	1232	1182	1188	1220	1256	1162	1003	1240	1014	0	0	0
	0	0	±120	±54	±85	±120	±60	±54	±69	±85	±60	±85	±54	±49	±54	±54	±45	±120	±69	±69	±120	0	0	0
70 - 75	0	0	1053	1190	1193	1358	1270	1220	1072	1241	1154	1187	1264	1125	1306	1267	1232	1155	1054	1040	0	0	0	0
	0	0	±85	±85	±85	±120	±85	±36	±69	±42	±40	±40	±42	±60	±49	±38	±49	±40	±69	±120	0	0	0	0
			105																					
65 - 70	0	0	1058	833	916	1158	1064	1151	1141	1051	1071	1127	1134	1151	1128	1222	1114	1148	0	0	0	1270	0	0
	0	0	±120	±120	±85	±60	±49	±54	±60	±60	±45	±38	±42	±45	±38	±40	±40	±40	0	0	0	±120	0	0
60 - 65	0	0	0	867	1448	1224	1035	1194	1020	1062	986	1082	984	1098	1150	1105	1054	1079	0	0	0	0	0	0
	0	0	0	±120	±85	±42	±60	±69	±69	±85	±69	±31	±31	±35	±30	±38	±49	±31	0	0	0	0	0	0

temperatures for Kp from 0 to 1.3 during summer were about 325°K hotter than winter, and during equinox were about 225°K hotter than winter. The summer and equinox seasonal variation for the 5 to 6.7 range of Kp were about one-third as large as for the 0 to 1.3 Kp range.

The effect of magnetic activity on the temperatures during summer showed an increase of 80°K for the 1.3 to 4 Kp range from the 0 to 1.3 Kp range temperatures, and an increase of 200°K for the 4 to 6.7 Kp range from the 0 to 1.3 Kp range temperatures. The equinox temperatures showed increases of 75°K for the 1.3 to 4 Kp range and 250°K for the 4 to 6.7 Kp range from the 0 to 1.3 Kp range temperatures. The winter temperatures showed increases of 100°K for the 1.3 to 4 Kp range and 350°K for the 4 to 6.7 Kp range from the 0 to 1.3 Kp range temperatures.

The geomagnetic local time effect is evident from the large maximum of temperature around 1900 to 2100 hours and a small maximum around 700 to 1000 hours. The noon sector is generally the minimum temperature area. The absolute maximum temperature area can not be denoted as there is little data available in the geomagnetic local times near 100 hours, however, there are indications that the maximum is in the pre-midnight sector. Caution is necessary regarding the geomagnetic local time effects as the separation of temporal and magnetic activity effects is difficult. The 2100 hour maximum and the noon minimum temperatures appear consistently throughout the data. The 900 hour maximum temperature appears often, but as the variation is smaller, it is not as apparent as the 2100 hour maximum.

Figure 25 shows the incidence of auroral forms in 1964 and 1965 and modified to give a resolution similar to the temperature data. This can be used to compare with the polar maps already presented. The outstanding feature of Figure 25 is that the incidence of auroral forms is highest near 2100 hours and 800 hours geomagnetic local time which correspond to the aforementioned geomagnetic local time temperature maxima. The behavior in general is, however, very different. The exospheric temperatures do not decrease within the auroral oval and show much less spatial structure. In almost all the graphs it can be seen that the magnetic pole is at a temperature close to the maximum in the region above 60°. It would appear that the effects of convection and conductivity are important enough to redistribute the energy deposited throughout the polar region and particularly, within the auroral oval. The gradients are quite large, however, compared with those found elsewhere. Even under quiet conditions with Kp $<$ 1.3 they are as large as 200 K in 1500 km in the noon sector.

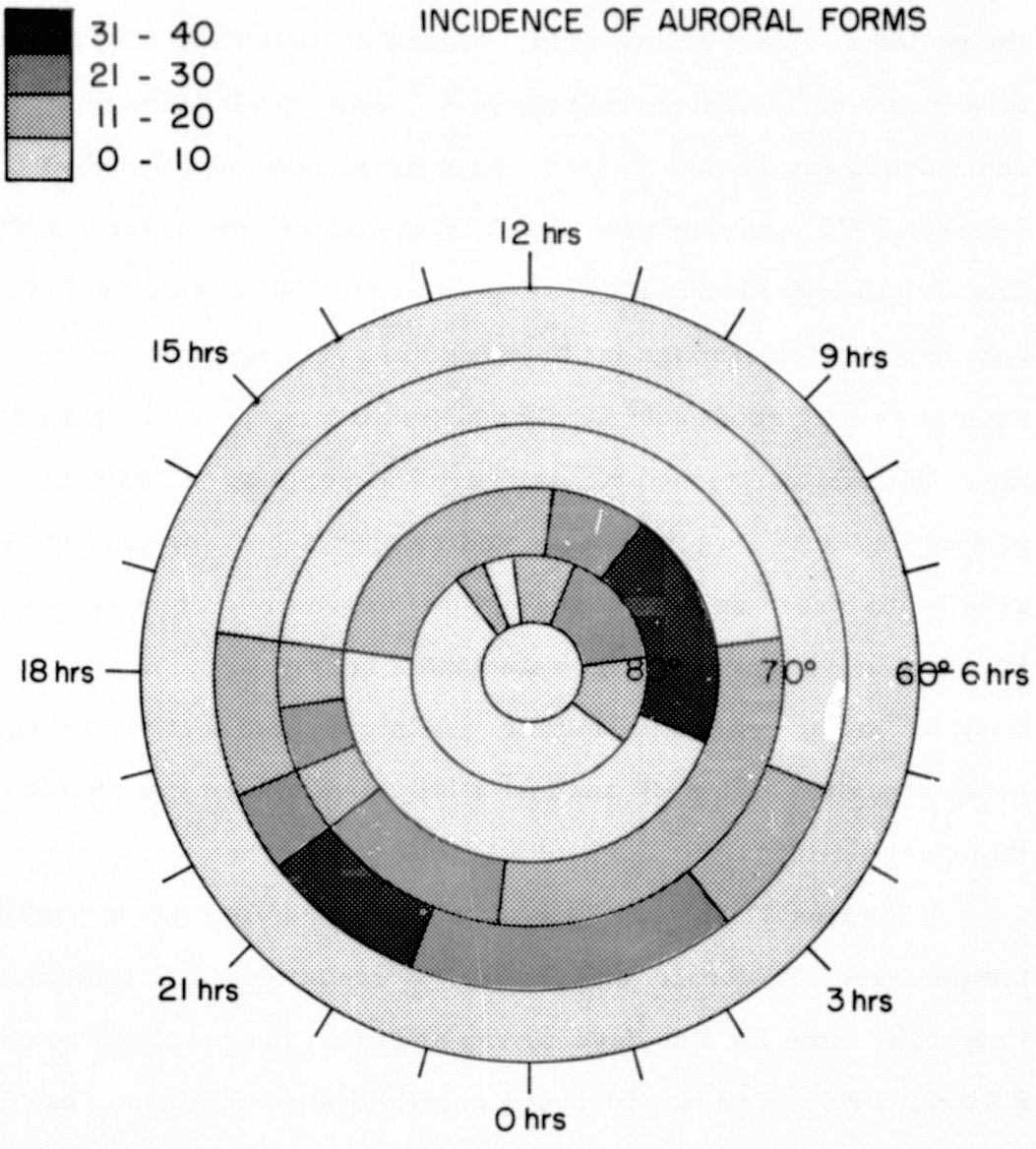

Figure 25 Incidence of auroral forms during 1964 and 1965 after Stringer and Belon (1966)

3.6 Description of the Temperature, N_2 Density, O Density, Pressure and Boundary Oxygen Density Variation During the Great Storm of 8 March 1970

Figures 1, 2 and 3 in Section 3.1 have already given an indication of the variation of the temperature in the northern hemisphere for the period around 8 March 1970. Figure 26 shows the 6300A temperature from -60° magnetic latitude to 90° magnetic latitude for the undisturbed day 11 March 1970, the moderately disturbed days 6 and 7 March 1970, and during the peak temperatures on 8 March 1970. The large temperature increase of 600°K to 700°K is evident at both north and south high latitude regions. The increase at the equator is only about 200°K. The latitudinal temperature gradient for the moderately disturbed day is about 7°K per degree latitude to the pole and slightly larger than the undisturbed day. The gradient for greatly disturbed day is about 11°K per degree latitude from 10° to 50° magnetic latitude and then fluctuates near 0°K per degree latitude from 50° to 90° magnetic latitude. This indicates that the energy is being deposited above 50° magnetic latitude and then transported to the lower latitudes.

Figures 27, 28 and 29 show a contoured view of the 6300A temperature, N_2 density and O density versus magnetic latitude and Universal Time for five days during and after the great storm of 8 March 1970. Day No. 67 is the greatly disturbed day and day No. 71 is an undisturbed day which may be used for comparison. Unfortunately, the density data was lost for day No. 67 until U.T. of 1900 hours. The Kp and AE indices for the interval are shown in Figure 30.

The 6300A temperatures in Figure 27 illustrate the rapid response of the thermosphere to a large heat source. The time of

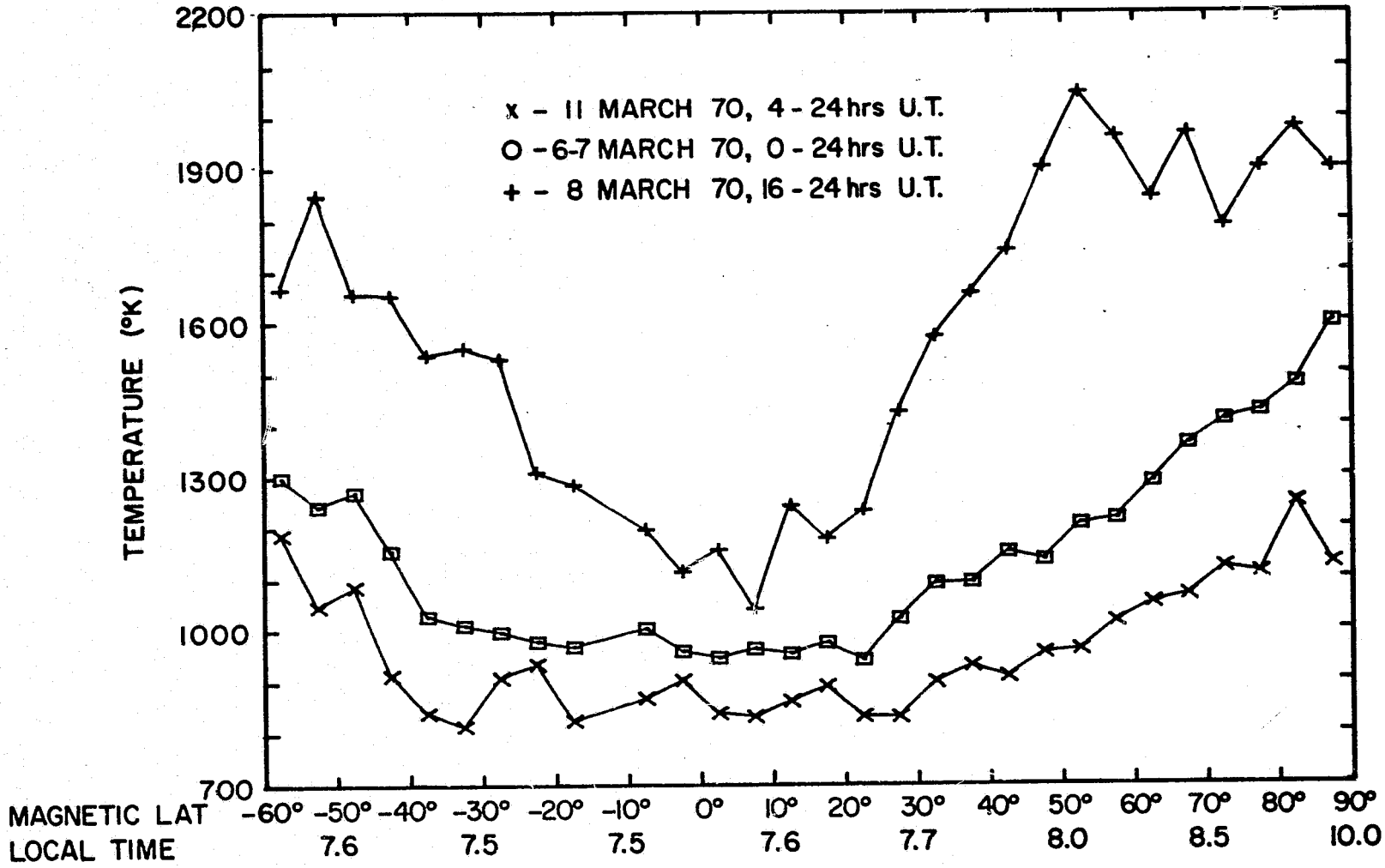

Figure 26 6300 A temperature versus magnetic latitude for undisturbed, moderately disturbed and greatly disturbed periods in March 1970

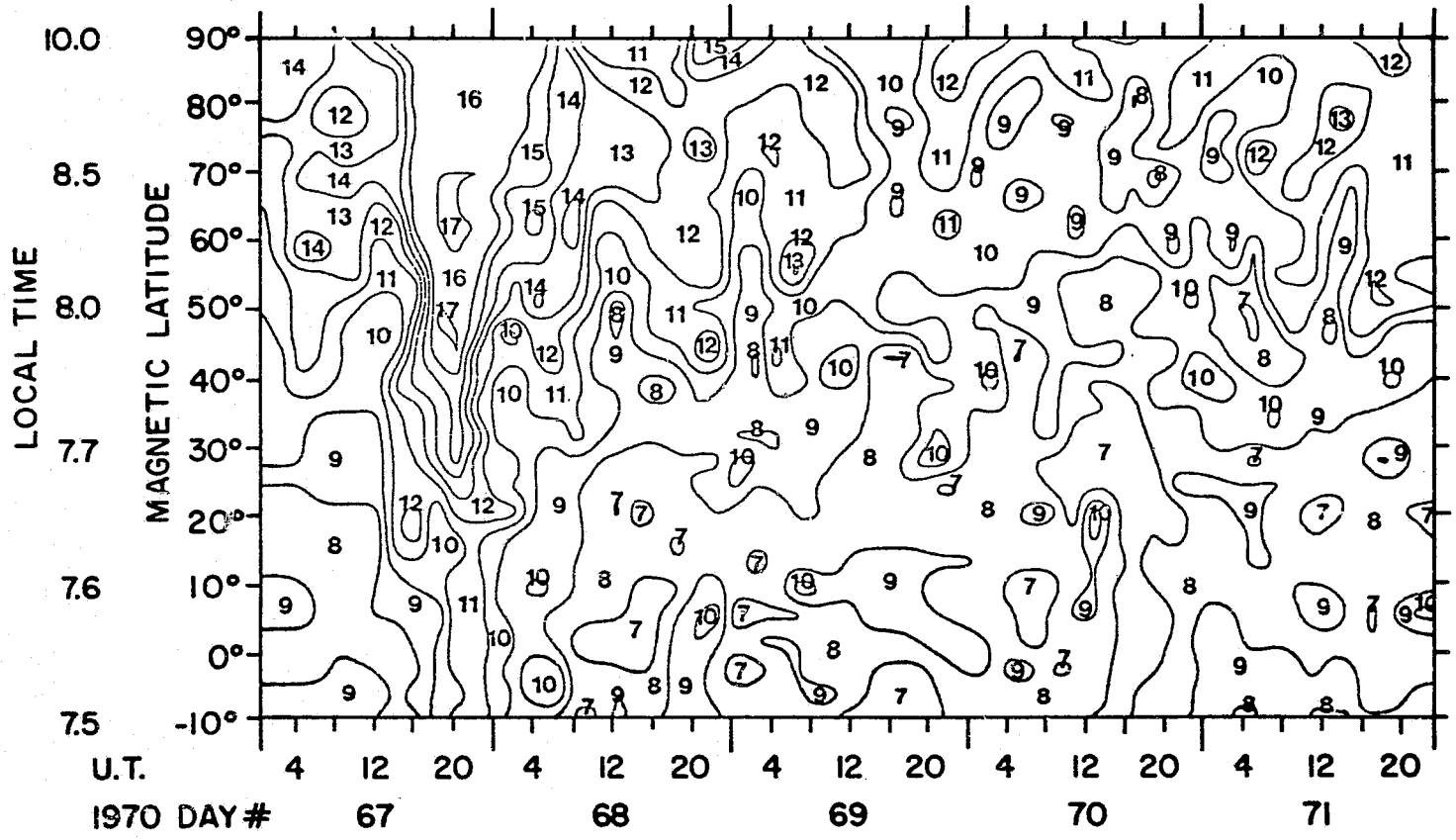

Figure 27 6300 A temperature (in hundreds of ^{o}K) contour map representing the 300 km variations with magnetic latitude and universal time for five days in March 1970

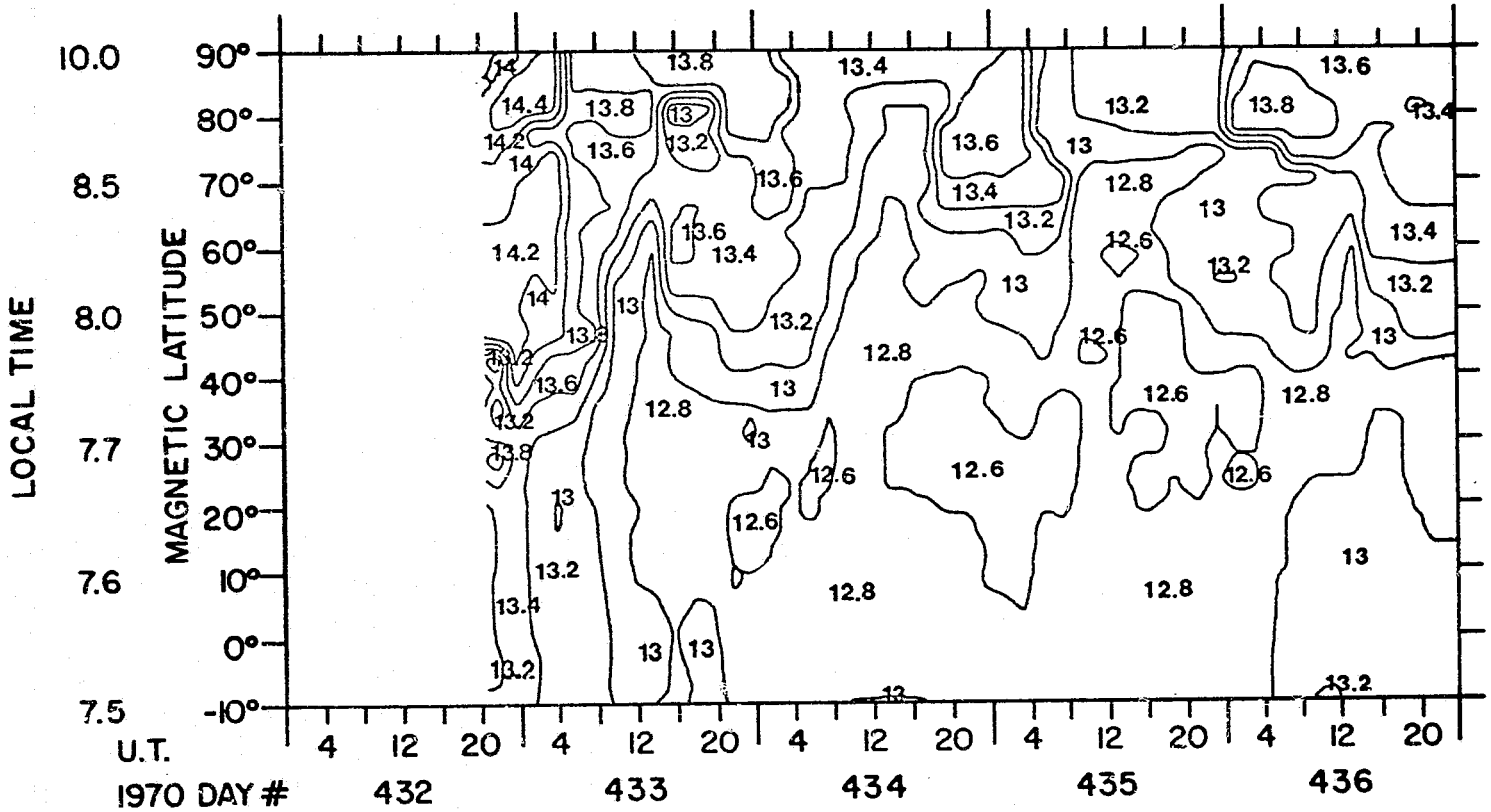

Figure 28 Log_{10} (N_2 number density (m^{-3})) contour map representing the 400 km variations with magnetic latitude and universal time for five days in March 1970

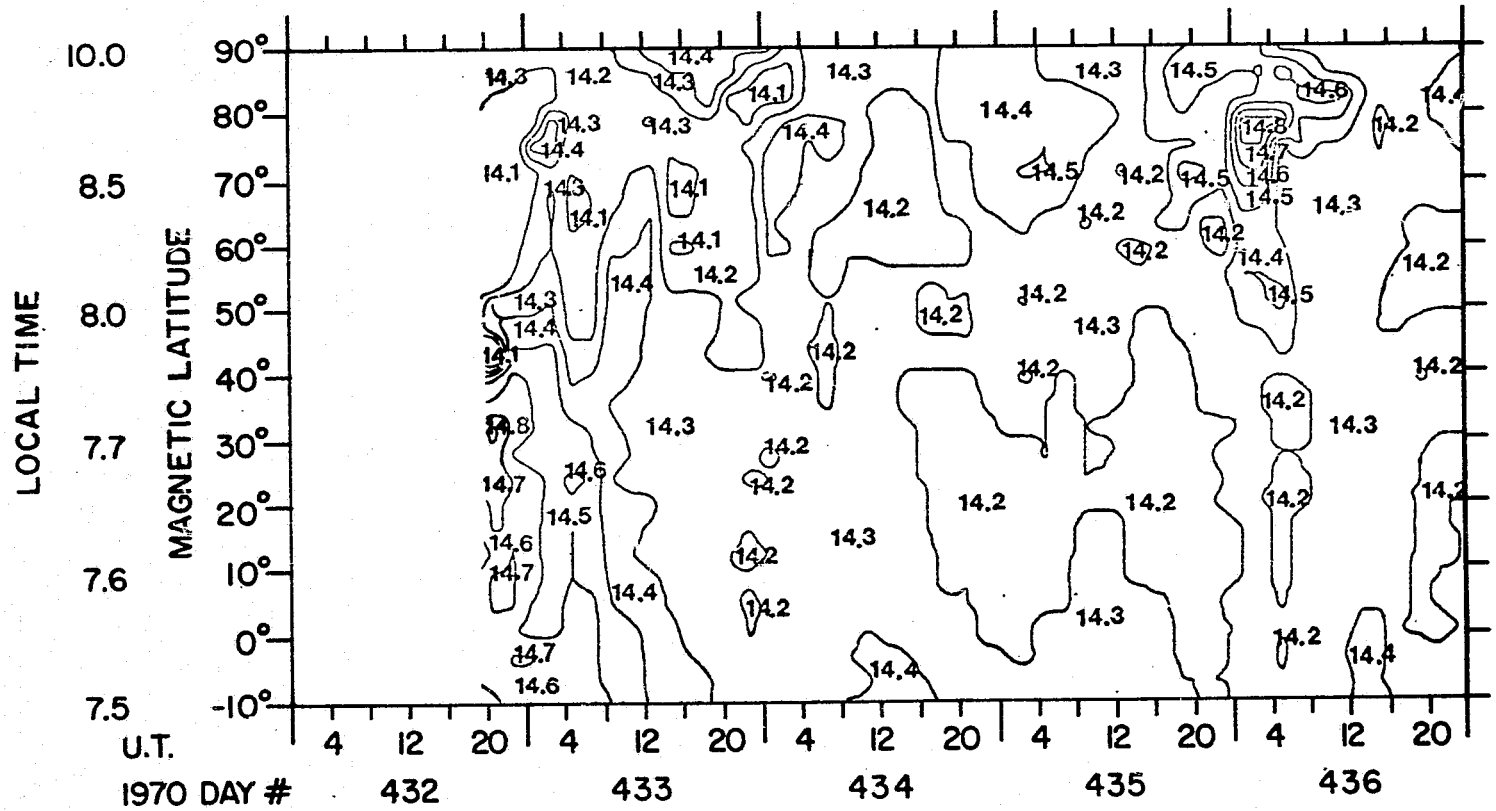

Figure 29 Log_{10} (0 number density (m^{-3})) contour map representing the 400 km variations with magnetic latitude and universal time for five days in March 1970

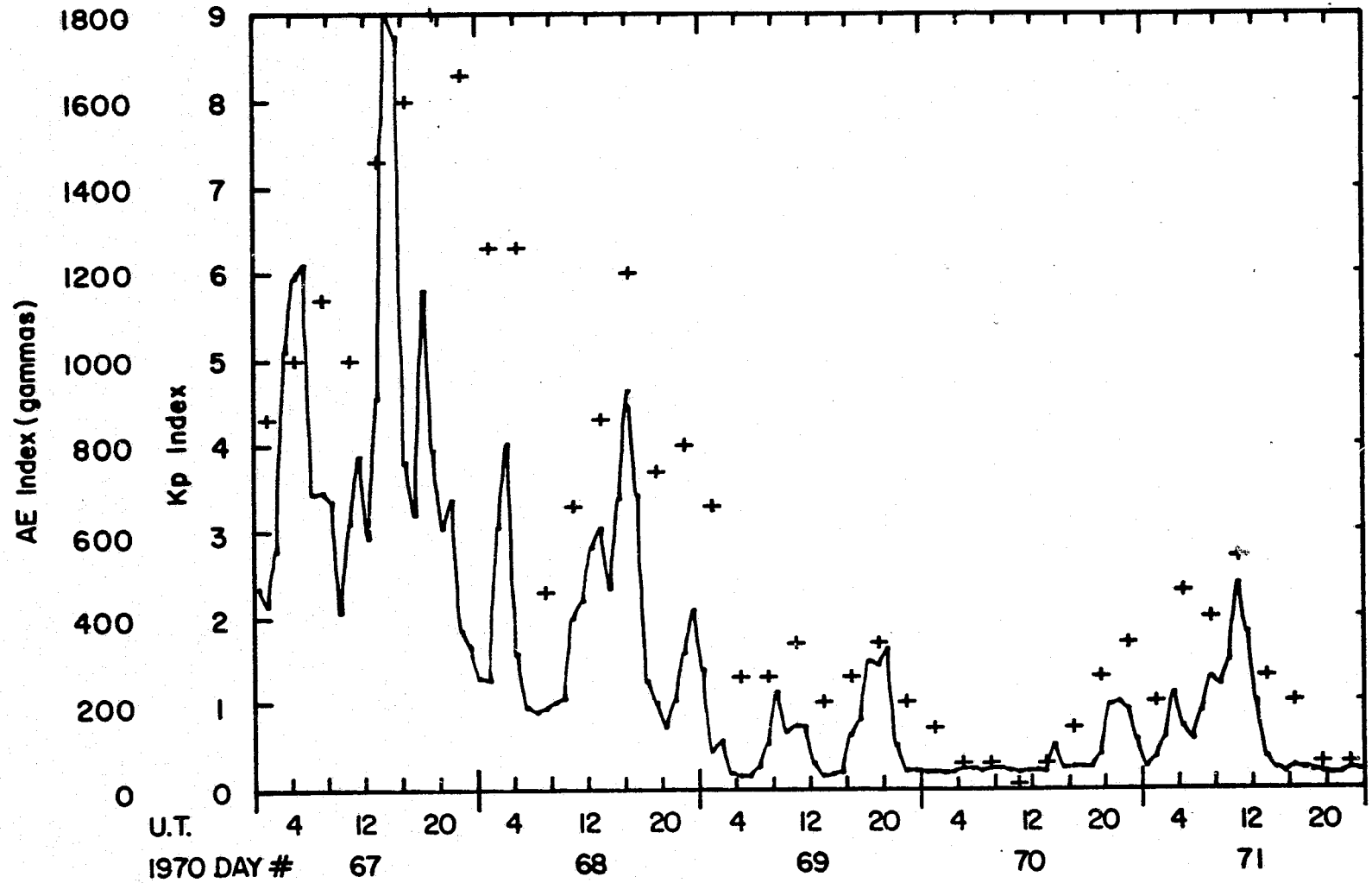

Figure 30 AE and Kp indices for the period of March 8 to 12, 1970

response at the high latitudes is less than one hour while the response time at the equator is around three or four hours. These reduced time responses from previously published results (Roemer, 1972 and Alcayde, et al., 1974) are certainly a result of the expansion of the auroral oval and the equatorward movement of the heat source, as was mentioned previously and can be seen in Figure 27.

The 400 km N_2 density contours of Figure 28 also show an order of magnitude difference between the densities at the pole and the equator. The latitude variation on day No. 71 is very much smaller. The general variation of the N_2 density contours can be seen to be quite similar to the 6300A temperature contours, though there are disagreements at several locations as had been previously pointed out in Sections 3.1 and 3.2 when the N_2 density derived temperatures were compared to the 6300A temperatures.

The atomic oxygen 400 km density contours are presented in Figure 29 and can be seen to have variations which are strikingly different from the N_2 density and 6300A temperature contours. The most important feature of Figure 29 is the moderate increase of atomic oxygen below 35° magnetic latitude and the large decrease of atomic oxygen above 35° magnetic latitude. Thus, the variation of atomic oxygen with moderate or large magnetic activity can be increasing or decreasing depending on the magnetic latitude which is being investigated. This behavior of the atomic oxygen explains the variations of the total density derived temperatures discussed in Sections 3.1 and 3.2 and also affects the pressure variations.

The pressure during undisturbed, moderately disturbed and greatly disturbed March 70 morning periods is shown in Figure 31.

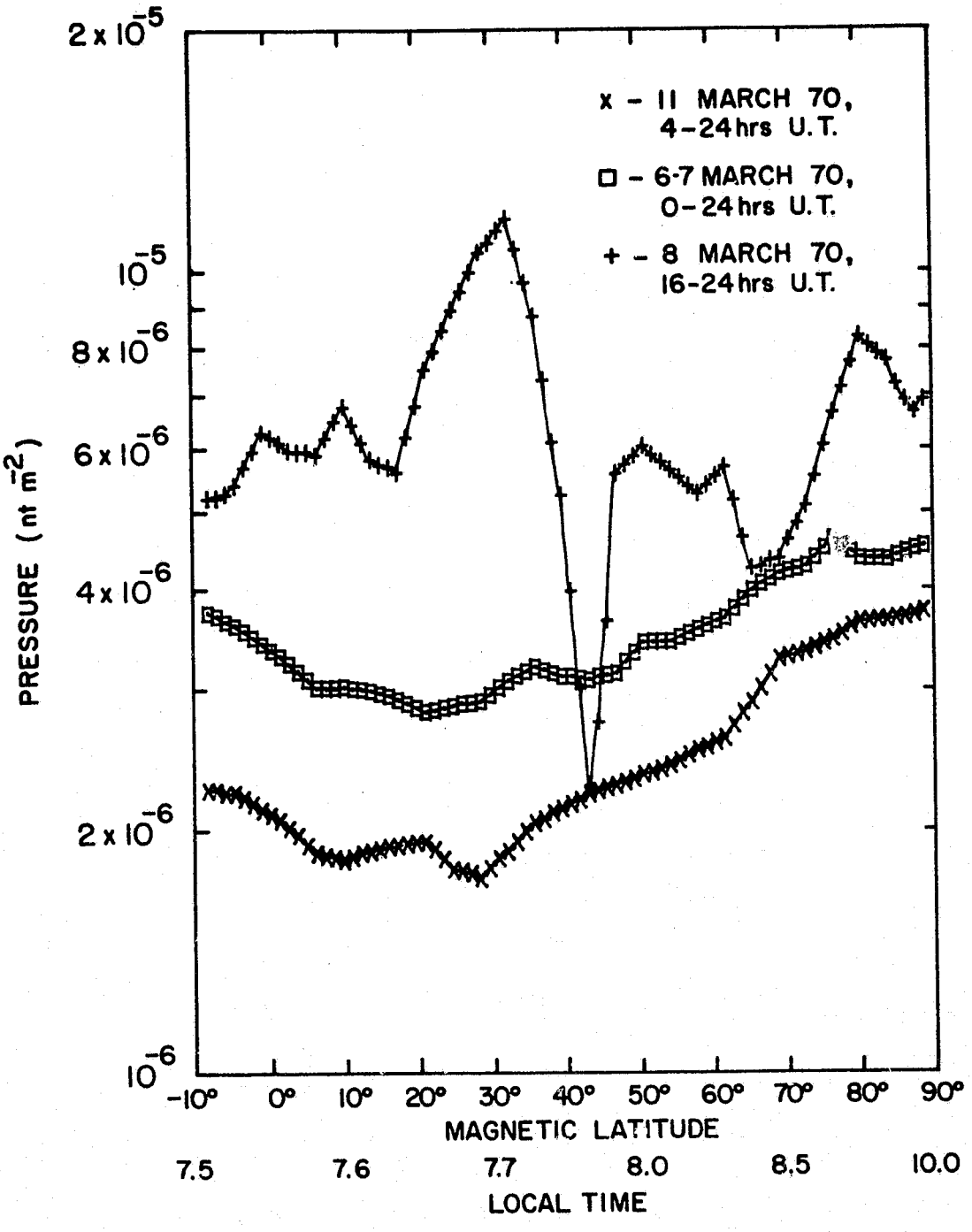

Figure 31 Variation of pressure at 400 km versus magnetic latitude for undisturbed, moderately disturbed and greatly disturbed period in March 1970

The undisturbed and moderately disturbed periods indicate a low pressure region around 20° to 30° magnetic latitude and higher pressures towards the poles. The greatly disturbed pressure variation is generally flatter with large gradients at several locations. The pressure appears to equalize very quickly during large disturbances which would indicate large but short-lived winds are generated and the atomic oxygen quickly transported to low pressure areas to equalize the global pressure.

Figure 32 shows the undisturbed, moderately disturbed and greatly disturbed magnetic latitude variations of the atomic oxygen near 120 km. The boundary atomic oxygen density was calculated using the following equation

$$n(O_0) = n(O)\ (T/T_0)\ \exp\left(\int_{Z_0}^{Z} m_0 g/kT\ dZ\right) \qquad (6)$$

where

$n(O_0)$ and T_0 are the boundary density and temperature

$n(O)$ and T are the 400 km density and temperature

and the exponential term is evaluated using the N_2 density and 6300 A temperatures. Figure 32 shows a moderate increase in the boundary oxygen density at magnetic latitudes below 40° and a great depletion above 40° magnetic latitude. This would indicate winds up and away from the high magnetic latitudes down and into the low magnetic latitudes during magnetic disturbances.

Figure 33 shows the 400 km atomic oxygen variations corresponding to the same intervals as Figure 22. It must be noted that the depletion at the high latitudes is smaller at 400 km and that the

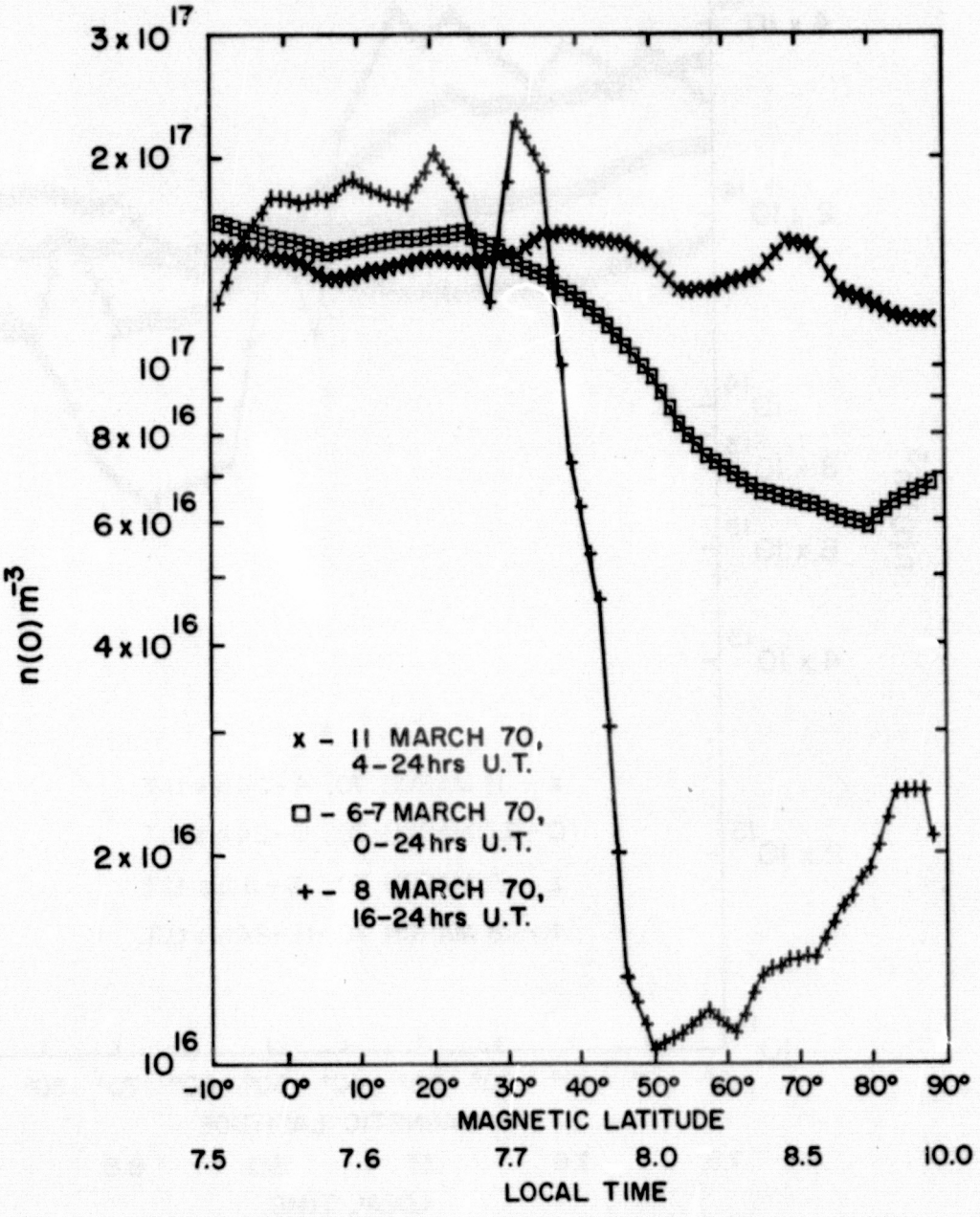

Figure 32 Variation of lower boundary atomic oxygen versus magnetic latitude for undisturbed, moderately disturbed, and greatly disturbed periods in March 1970

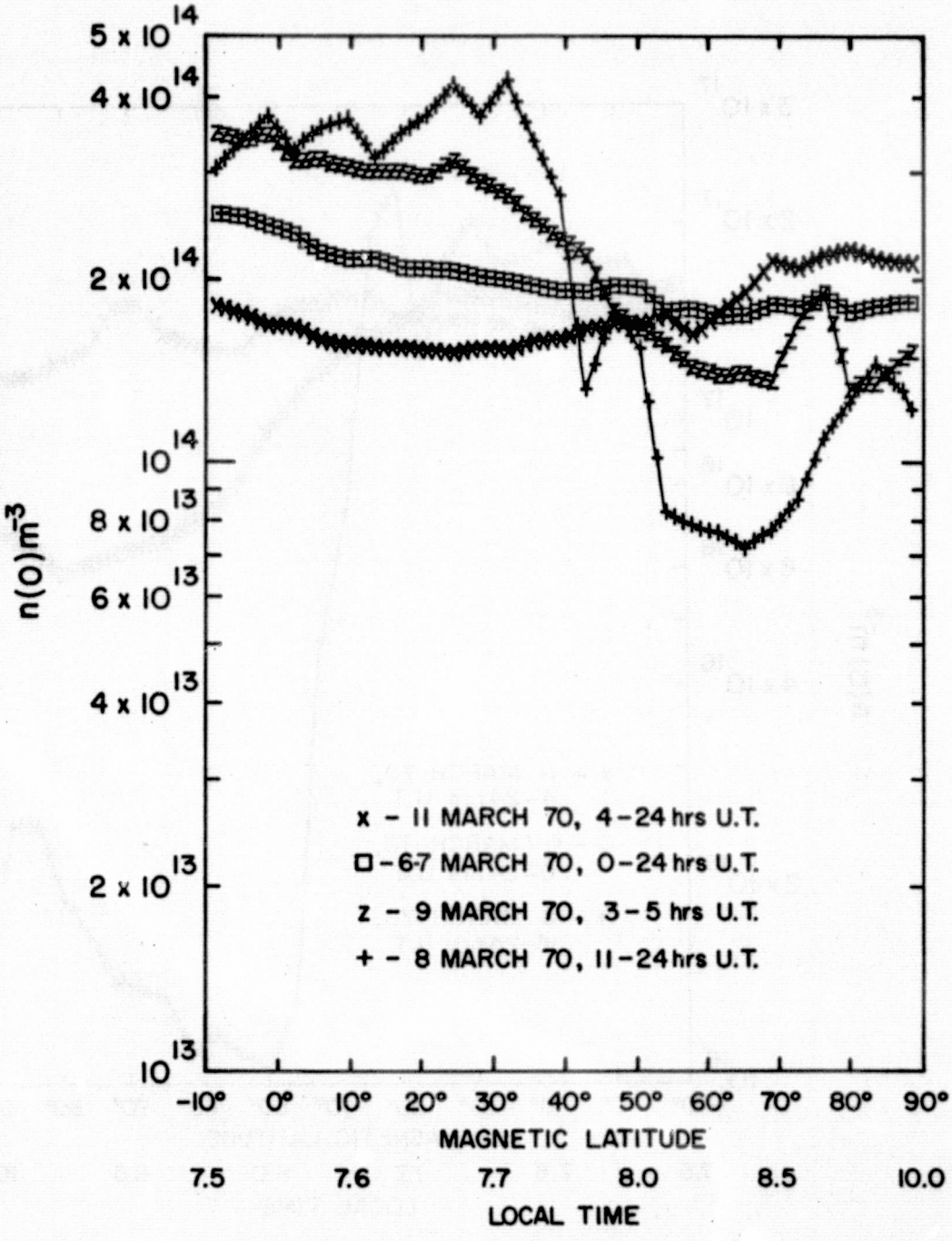

Figure 33 Atomic oxygen at 400 km versus magnetic latitude for undisturbed, moderately disturbed and greatly disturbed periods, and 3 hours after the greatly disturbed period in March 1970

enhancement at the low latitudes is larger than the atomic oxygen near 120 km. This is consistent with a transport of atomic oxygen up and away from the high latitudes and a subsidence at the low latitudes.

3.7 Time Constants of Thermospheric Effects Due to Magnetic Activity

In a magnetic storm, energy deposition occurs in the high latitude regions. While the AE and Kp indices provide a measure of the geomagnetic activity, it must be presumed that the effects will demonstrate both time delay and energy storage phenomena. Time delays result from the time necessary to transport the energy to lower latitudes by winds and gravity waves, and the storage effects will be associated with the time required to change the temperature gradients at lower altitudes.

If it is assumed that the thermosphere has an integrating effect with regard to the magnetic activity, then the thermosphere would be responsive to the magnetic activity over some preceeding time interval, and after an impulse of magnetic activity heating would relax to its original condition with some relaxation time. To test this hypothesis and attempt to determine the time constant which would relate the thermospheric response to magnetic activity, three different periods of activity were selected. The three intervals were: (1) Fall 69, 1 to 11 September 1969, (2) Spring 70, 1 to 11 March 1970 and (3) Summer 70, 14 to 24 June 1970.

It has been shown in Section 3.4 that the initial response to a magnetic disturbance can be very rapid and that the increase in temperature can be related to the magnetic indices using delays ranging from less than an hour at 60° magnetic latitude to about

10 hours at the equator. If the period after the storm is observed, it is apparent that the temperatures do not return to the quiet values as quickly as the magnetic indices because of the energy storage in the thermosphere. This is the cause of two common errors in dealing with the thermospheric temperatures. First, the model temperatures based on a one-to-one relation to Kp will underestimate the temperatures following a storm. Second, experimenters may use quiet day data to construct models of the thermosphere from periods where the Kp was low, but with temperatures that were enhanced due to the relaxation time constant effect of a preceeding storm period.

It is apparent from the data that what is needed is a method of using the magnetic indices so that the beginning of the storm is well defined and the period after influenced by the relaxation time effect. With this in mind, a new index has been employed to analyze the 6300A temperatures. A factor W was introduced to account for the magnetic variation where W is evaluated by

$$W(t, t_d, \tau) = \sum_{i=0}^{n} Kp\,(t-t_d-3i)\exp(-3i/\tau) \Big/ \sum_{i=0}^{n} \exp(-3i/\tau) \qquad (7)$$

where

t = time (U.T.), t_d = time delay (hrs), τ = relaxation time constant (hrs), and $Kp\,(t-t_d-3i)$ is the appropriate magnetic index weighted by $\exp(-3i/\tau)$ and $\sum_{i=0}^{n} \exp(-3i/\tau)$ is a normalizing factor so that W values for different τ's are of comparable magnitude.

Figure 34 shows the error of the fit for the different periods already specified as a function of the relaxation time constant τ. $\tau = 0$ is just the variation with Kp. A linear function of W was used in this study. The best fit for Spring and Fall corresponds to $\tau = 6$ hrs, while the best fit for Summer was $\tau = 12$ hrs. There appears to be a definite seasonal variation in the relaxation time constant although there doesn't seem to be a local time variation.

Figure 35 shows the magnetic latitude variation of the $\Delta T/\Delta W$ coefficient for Summer 70 AM and PM. As expected, the coefficients for 700 hrs local time are significantly larger than those for 1800 hrs and the high latitude coefficient larger than the low latitudes.

Figure 36 shows the magnetic latitude variation of the 6300 A temperature with W = 0 for the Summer 70 period using the fitting function. A comparison of Figure 36 with Figure 11 shows an excellent agreement between the quiet day 23 June 70 temperature data and the results of the fit with W = 0. This indicates a good representation of the magnetic activity by the W factor.

Some important conclusions can be drawn about the relaxation time of the thermosphere for magnetic activity. It does not appear that these times are longer than 12 hours and there does not seem to be a large latitudinal gradient in the relaxation time.

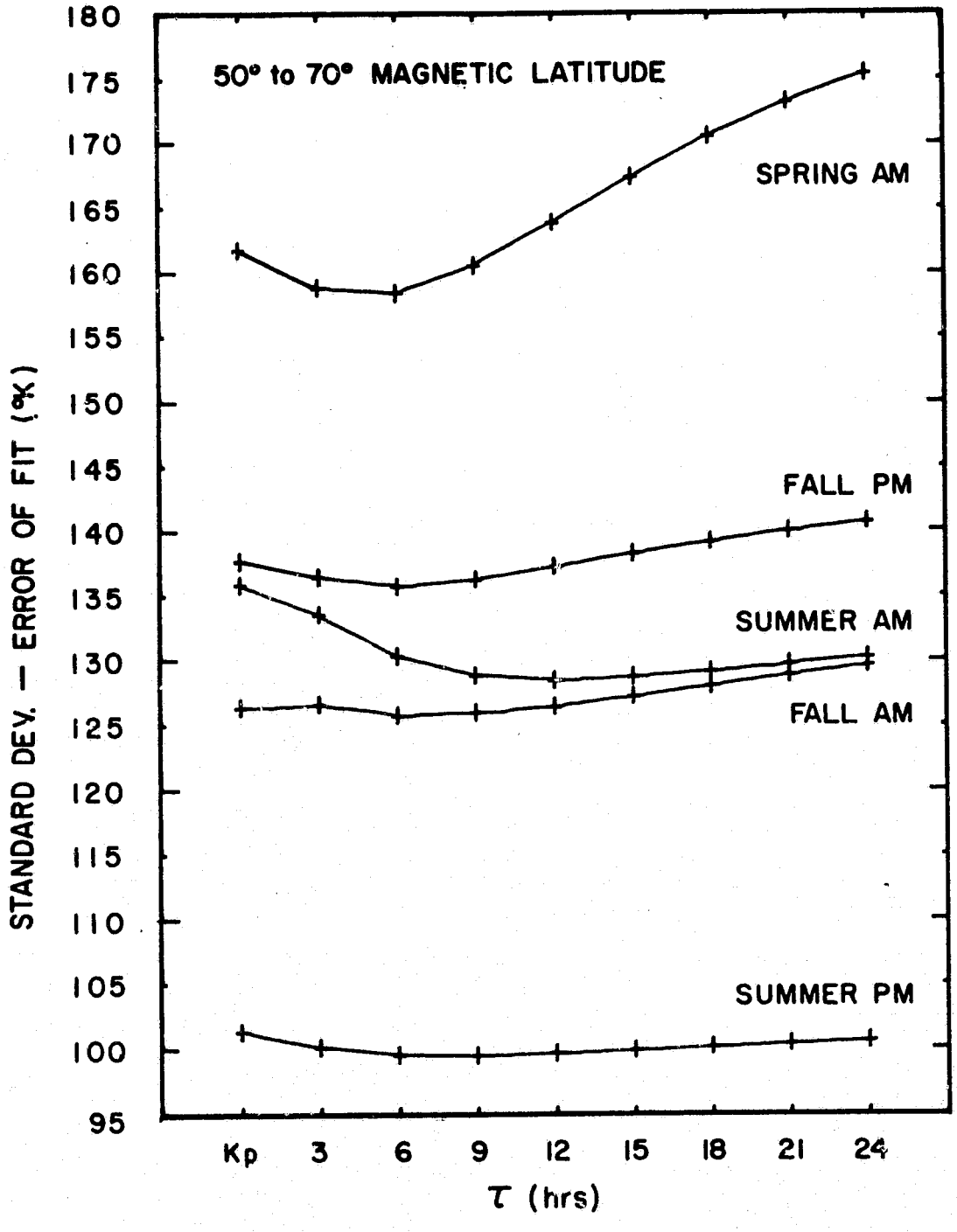

Figure 34 Standard deviation of least squares fit of 6300 A temperature data versus relaxation time constant τ for Fall 69, Spring 70 and Summer 70 for AM and PM local times

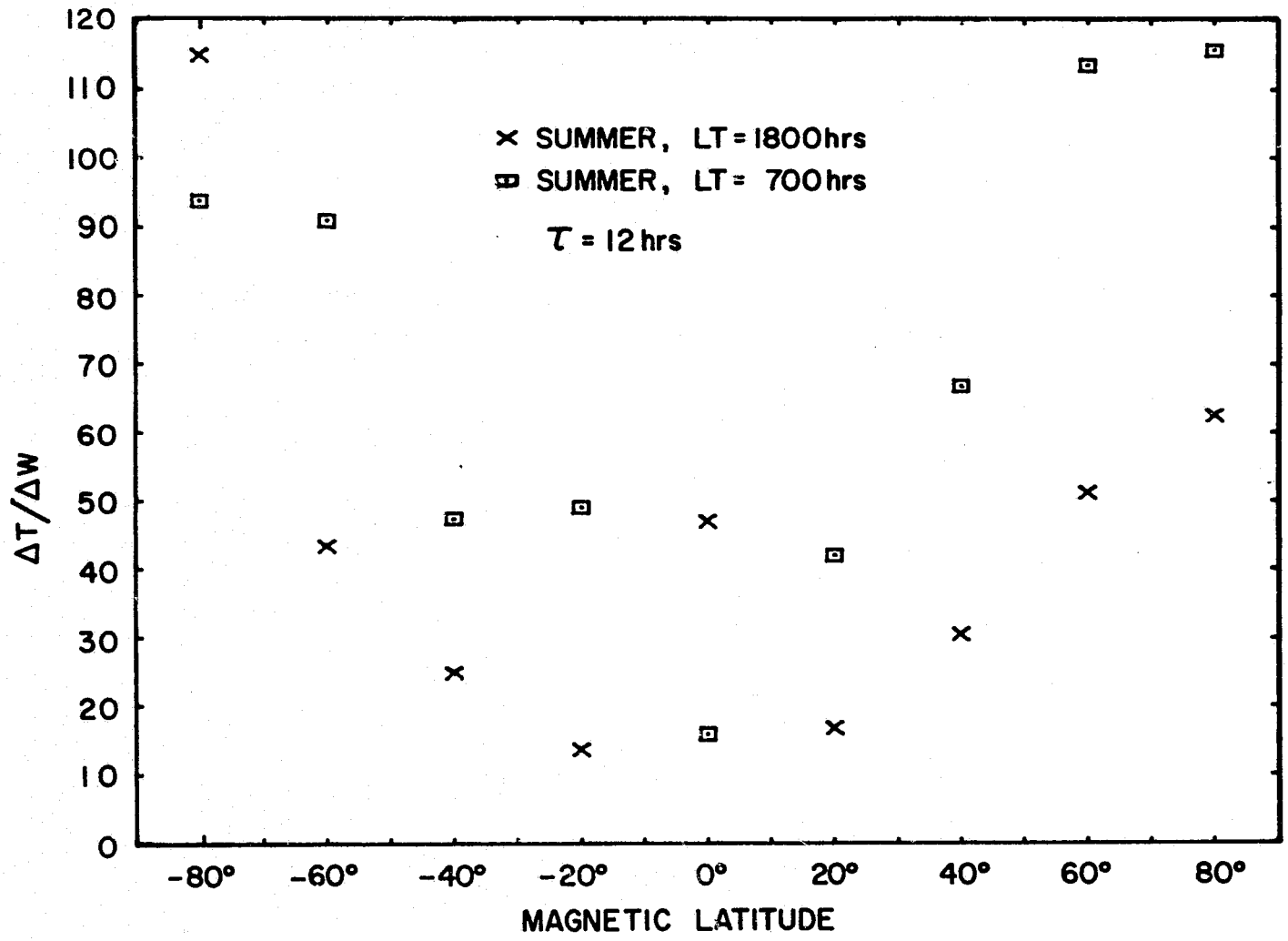

Figure 35 Δ T/Δ W versus magnetic latitude for Summer AM and PM local times

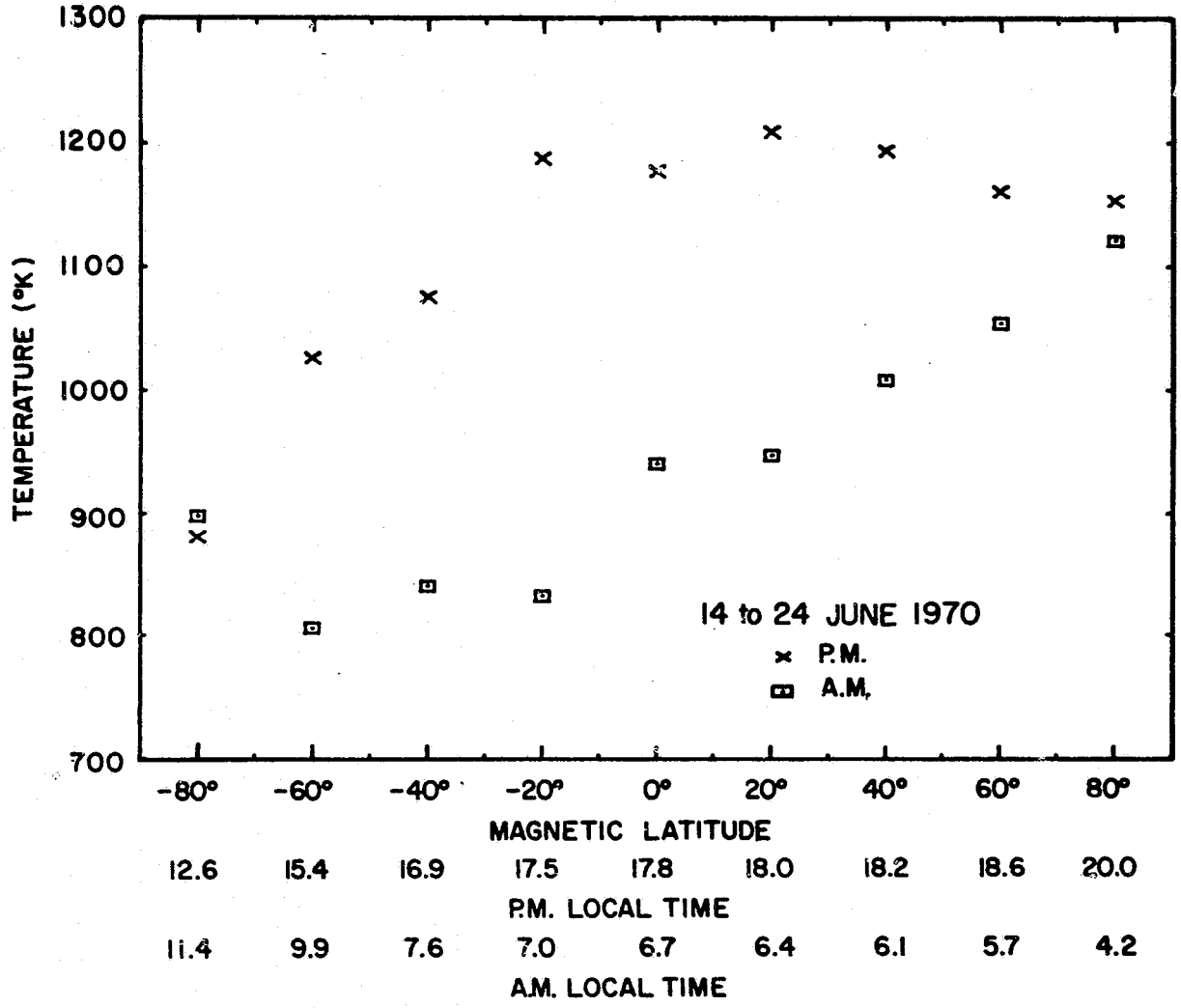

Figure 36 Exospheric temperature versus magnetic latitude for W = 0 and 10.7 cm solar flux = 150 for Summer AM and PM local times

CHAPTER IV

CONCLUSIONS

4.1 Comparison of the 6300 A Temperature with Temperatures Derived from Total Density and from N_2 Density

It has been shown that the total density when used with static diffusion models with constant boundary conditions and shape parameters gives an exceedingly poor measurement of the global variation of the neutral temperature under both quiet and disturbed conditions. Under quiet conditions the temperatures derived from total density show a variation from equator to pole of about 80°K compared with the equator pole variation of 300°K for the 6300 A temperatures and 150°K for the temperatures derived from N_2 density. Under disturbed conditions the temperatures derived from total density fail to describe the global variation of temperature. The depletion of atomic oxygen in the high latitudes causes the temperatures derived from the total densities to be quite different from the kinetic temperatures as shown in Figure 3.

The agreement between the 6300 A temperatures and the temperatures derived from N_2 densities was much closer than the total density derived temperature, but there were still major discrepancies. In agreement with incoherent scatter measurements at mid-latitudes, the N_2 derived temperature was found to be 100°K to 200°K too high under quiet conditions. During disturbed conditions, the temperatures derived from the N_2 densities agreed quite well with the 6300 A temperatures, but the latitudinal temperature gradient in the N_2 derived temperature gradient was much greater in the region

below the auroral zone and the N_2 derived temperature poleward of the auroral zone decreased rather than increased as the 6300 A temperatures indicated. The reason for these discrepancies are probably more closely associated with the temperature gradient in the lower thermosphere rather than with transport effects. It is known that large changes in the temperature profile and total density occur in the region of 120 km due to the semi-diurnal tide. Large changes also appear to occur during conditions of high magnetic activity so that it is not surprising that there is not a one-to-one correspondence between exospheric temperature and 400 km density. The temperature derived from the N_2 densities would be expected to give a closer measurement of the temperature than any other gas because it is the major constituent in the region where eddy diffusion and transport are important, and because its mass density is close to that of the mean molecular mass in this region.

4.2 Temperature Variations as a Function of Kp Magnetic Index

The results of the analysis of 6300 A temperatures and temperatures derived from N_2 density and total mass density are summarized in Tables 1, 2 and 3.

The results shown in Table 3 clearly indicate a strong local time variation of the global K_0 and latitudinal K_1 coefficients of $\Delta T / \Delta Kp$ for both Fall 69 and Summer 70 storm periods. There is a moderate seasonal variation in the global K_0 coefficient but no clear seasonal variation in the latitudinal K_1 coefficient.

Tables 1 and 2 show that the latitude gradient in the 6300 A temperature enhancement is an order of magnitude larger than

C-2

indicated by the method used to derive the coefficients for Jacchia (1971). There was general agreement between the total density measurements and the total densities of Jacchia (1971), however, several important departures in detail were noticed. At the peak of the storm the total density decreased rapidly with increasing latitude in the region of the midlatitude trough. The reasons for these discrepancies were studied. It is apparent from Figure 32 that the changes are due to changes in the lower boundary conditions of atomic oxygen and represent the effects of transport.

The 6300 A temperature $\Delta T/\Delta Kp$ coefficients showed good agreement with the variations calculated using the temperatures derived from the N_2 density except that the N_2 density derived temperature variations underestimated the effects at low latitudes and overestimated the effects at high latitudes.

4.3 Equinox and Solstice Global Variations for Quiet Magnetic and Solar Conditions

The Fourier series analysis of the quiet day global temperature distribution allows an easy means of comparing the 6300 A temperatures measured during solstice and equinox conditions with model temperatures or other experimental temperature data. The coefficients are presented in Table 4.

4.4 Anomalous Southern Hemisphere Temperature Longitude Variation

A large enhancement of the 6300 A temperature measurements in the area of the South Atlantic magnetic field anomally was demonstrated by Figures 12, 13, 14 and 15. The enhancement was of the

order of 1000°K. No evidence of a corresponding variation of the O or N_2 densities was seen. Further investigation into the cause of this temperature effect is needed.

4.5 Temperature Variation as a Function of Geomagnetic Time and Geomagnetic Latitude

The results of the analysis of the 6300 A airglow temperatures as a function of geomagnetic time and geomagnetic latitude are shown in Section 3.4. The local time variation should be regarded with caution because of difficulties in separating the temporal and magnetic activity effects. The enhanced temperatures in the pre-midnight sector and the low temperatures in the noon sector seem to be real geophysical effects and are clearly seen in the summer and equinox data. Latitudinal gradients are not large and high temperatures are maintained up to the magnetic pole. Season variations are larger under low magnetic activity than for high magnetic activity.

4.6 Temperature, Density, Pressure and Boundary Oxygen Behavior Before, During and After a Large Magnetic Storm

The great storm of 8 March 1970 was analyzed in detail in Section 3.6. Figures 27, 28 and 29 showed the Universal Time and magnetic latitude variations of the temperature, N_2 density and O density at 400 km corresponding to the magnetic activity indicated in the magnetic indices shown in Figure 30. A fast response at all magnetic latitudes was shown to be on the order of one hour at 60° magnetic latitude to about three hours at the equator. The cause of the short response time may be the expansion of the auroral oval to midlatitudes which would advance the source of heating closer to the equator.

The 6300 A temperatures and N_2 densities demonstrated similar variations during the interval investigated. The N_2 densities exhibited several sharp latitude gradients which were not present in the temperatures.

The atomic oxygen variation was strikingly different from either the N_2 density or the 6300 A temperatures. Figures 32 and 33 showed the boundary oxygen and 400 km oxygen density variations to be indicative of a transport mechanism which moves the atomic oxygen up and away from the high latitudes towards the equator where the movement subsides.

The cause of the atomic oxygen behavior appears to be connected with the pressure. With the OGO-6 satellite, independent measurements of the neutral temperature and density could be combined to obtain an excellent measure of the pressure. As seen in Figure 31 the north-south pressure gradient was generally small except for several large localized gradients at the height of the storm. It appears that the thermospheric pressure induces winds of such magnitude that the pressure gradients are minimized.

4.7 Temperature Relaxation Time Constant

A new magnetic activity index W was introduced to allow the response of the thermosphere to magnetic storms to be modeled better. This index is defined in equation 7. It is based on the Kp index and it includes both a delay time and an exponential time delay. It was found that this index provided significantly better fits between temperatures and the index than did the Kp value itself. It was found that the relaxation time constant was of the order of 3 to 12 hours and

not strongly latitude or local time dependent. The time delays varied from less than one hour at high latitudes to 10 hours at the magnetic equator.

REFERENCES

Agy, V., Geomagnetic coordinates and geomagnetic time, NBS Rept., No. 8789, 1965.

Allen, R. R. and G. E. Cook, Thermospheric densities during an intense magnetic storm, from the LOGACS experiment, J. Atmos. Terr. Phys., 36, 1739-1752, 1974.

Amayenc, P. and G. Vasseur, Neutral winds deduced from incoherent scatter observations and their theoretical interpretation, J. Atmos. Terr. Phys., 34, 351-364, 1972.

Anderson, A. D., The relation between low-latitude neutral density variations near 400 km and magnetic activity indices, Planetary Space Sci., 21, 2049-2060, 1973.

Bates, D. R., Some problems concerning the terrestrial atmosphere above about the 100 km level, Proc. Roy. Soc. London, A, 253, 451-462, 1959.

Bauer, P., P. Waldteufel and D. Alcayde, Diurnal variations of the atomic oxygen density and temperature determined from incoherent scatter measurements in the ionospheric F-region, J. Geophys. Res., 75, 4825-4832, 1970.

Blamont, J. E. and J. M. Luton, Geomagnetic effect on the neutral temperature of the F-region during the magnetic storm of September 1969, J. Geophys. Res., 77, 3534-3556, 1972.

Blum, P. W. and I. Harris, The global wind system in the thermosphere, in: Rycroft, M. J. and Runcorn, S. K. (Eds.), Space Research XIII, Proceedings of the Fifteenth Plenary Meeting of COSPAR, Madrid, 1972, Volume 1, Adademie-Verlag, Berlin, pp. 369-377, 1973.

Brekke, A., J. R. Doupnik and P. M. Banks, A preliminary study of the neutral wind in the auroral E-region, J. Geophys. Res., 78, 8235-8250, 1973.

Brekke, A., J. R. Doupnik and P. M. Banks, Observations of neutral winds in the auroral E-region during the magnetospheric storm of August 3-9, 1972, J. Geophys. Res., 79, 2448-2456, 1974.

Burge, J. D., D. Eccles, J. W. King and R. Ruster, The effects of thermospheric winds on the ionosphere at low and middle latitudes during magnetic disturbances, J. Atmos. Terr. Phys., 35, 617-623, 1973.

Carignan, G. R. and W. H. Pinkus, OGO-FØ4 experiment description, Technical Note 08041-31T, University of Michigan, Ann Arbor, Michigan, 1968.

Carpenter, L. A. and V. W. J. H. Kirchhoff, Daytime three-dimensional drifts at Millstone Hill Observatory, Radio Science, 9, 217-222, 1974.

Chang, S. C., S. T. Wu and R. E. Smith, Joule heating and winds due to geomagnetic disturbances, J. Atmos. Terr. Phys., 36, 889-896, 1974.

Champion, K. S. W., The properties of the neutral atmosphere, in: Bowhill, S. A., Jaffee, L. D. and Rycroft, M. J. (Eds.), Space Research XII, Proceedings of the Fourteenth Plenary Meeting of COSPAR, Seattle, Washington, USA, 1971, Volume 1, Akademie-Verlag, Berlin, pp. 529-563, 1972.

Champion, K. S. W., Review of the properties of the lower thermosphere, in: Champion, K. S. W., Smith, P. A. and Smith-Rose, R. L. (Eds.), Space Research IX, Proceedings of the Eleventh Plenary Meeting of COSPAR, Tokyo, 1968, North-Holland Publishing Company, Amsterdam, pp. 459-477, 1969.

Chandra, S. and J. R. Herman, F-region ionization and heating during magnetic storms, Planetary Space Sci., 17, 841-851, 1969.

Chandra, S., E. J. Maier and P. Stubbe, The upper atmosphere as a regulator of subauroral red arcs, Planetary Space Sci., 20, 461-472, 1972.

CIRA 1965, COSPAR International Reference Atmosphere, North-Holland Publishing Company, Amsterdam, 1965.

CIRA 1972, COSPAR International Reference Atmosphere, Adademie-Verlag, Berlin, 1972.

Cole, K. D., Thermospheric winds induced by auroral electrojet heating, Planetary Space Sci., 19, 1010-1012, 1971.

DeVries, L. L., Analysis and interpretation of density data from the low-G accelerometer calibration system (LOGACS), in: Bowhill, S. A., Jaffee, L. D. and Rycroft, M. J. (Eds.), Space Research XII, Proceedings of the Fourteenth Plenary Meeting of COSPAR, Seattle, Washington, USA, 1971, Volume 1, Akademie-Verlag, Berlin, pp. 776-789, 1972a.

DeVries, L. L., Structure and motion of the thermosphere shown by density data from the low-G accelerometer calibration system (LOGACS), in: Bowhill, S. A., Jaffee, L. D. and Rycroft, M. J. (Eds.), Space Research XII, Proceedings of the Fourteenth Plenary Meeting of COSPAR, Seattle, Washington, USA, 1971, Volume 2, Akademie-Verlag, Berlin, pp. 867-879, 1972b.

Evans, J. V., Midlatitude ionospheric temperature on magnetically quiet and disturbed days, J. Geophys. Res., 70, 2726-2731, 1965.

Evans, J. V., Midlatitude ionospheric temperatures during three magnetic storms in 1965, J. Geophys. Res., 75, 4803-4813, 1970.

Evans, J. V., Incoherent scatter observations of an overhead aurora, in: Data on Solar-Geophysical Activity Associated with the Major Geomagnetic Storm of 8 March 1970, World Data Center A Upper Atmosphere Geophysics Report UAG-12, part II, pp. 191-193, 1971.

Evans, J. V., The causes of storm-time increases in the F-layer at mid-latitudes, J. Atmos. Terr. Phys., 35, 593-616, 1973.

Forbes, J. M. and F. A. Marcos, Thermospheric density variations associated with auroral electrojet activity, J. Geophys. Res., 78, 3841-3847, 1973.

Hedin, A. E., H. G. Mayr, C. A. Reber, N. W. Spencer and G. R. Carignan, Empirical model of global thermospheric temperature and composition based on data from the OGO-6 quadrupole mass spectrometer, NASA-GSFC Report X-621-73-37, 1972.

Hedin, A. E., B. B. Hinton and G. A. Schmidt, Role of gas surface interactions in the reduction of OGO-6 neutral gas particle mass spectrometer data, NASA Technical Note D-7239, 1973.

Hedin, A. E., H. G. Mayr, C. A. Reber, N. W. Spencer and G. R. Carignan, Empirical model of global thermospheric temperature and composition based on data from the OGO-6 quadrupole mass spectrometer, J. Geophys. Res., 79, 215-225, 1974.

Hays, P. B., R. A. Jones and M. H. Rees, Auroral heating and the composition of the neutral atmosphere, Planetary Space Sci., 21, 559-573, 1973.

Hays, P. B. and R. G. Roble, Direct observations of thermospheric winds during geomagnetic storms, J. Geophys. Res., 76, 5316-5321, 1971.

Jacchia, L. G., Two atmospheric effects in the orbital acceleration of artificial satellites, Nature, 183, 526-527, 1959a.

Jacchia, L. G., Corpuscular radiation and the acceleration of artificial satellites, Nature, 183, 1662, 1959b.

Jacchia, L. G., Static diffusion models of the upper atmosphere with empirical temperature profiles, Smithsonian Astrophysical Observatory Special Report No. 170, 1964.

Jacchia, L. G., Static diffusion models of the upper atmosphere with empirical temperature profiles, Smithsonian Contrib. Astrophysical, 8, 215, 1965.

Jacchia, L. G., New static models of the thermosphere and exosphere with empirical temperature profiles, Smithsonian Astrophysical Observatory Special Report No. 313, 1970.

Jacchia, L. G., Revised static models of the thermosphere and exosphere with empirical temperature profiles, Smithsonian Astrophysical Observatory Special Report No. 332, 1971.

Jacchia, L. G., Variations in thermospheric composition: A model based on mass spectrometer and satellite drag data, J. Geophys. Res., 13, 1923-1927, 1974.

Johnson, F. S. and B. Gottlieb, Atomic oxygen transport in the thermosphere, Planetary Space Sci., 21, 1001-1009, 1973.

Johnson, F. S., Energy input to the lower thermosphere, J. Atmos. Terr. Phys., 36, 1707-1713, 1974.

Knight, D. E., R. Uribe and B. E. Woodgate, Low latitude density variations in the earth's neutral atmosphere between 200 and 400 km, from August 1969 to May 1970, Planetary Space Sci., 21, 253-271, 1973.

Kohl, H. and J. W. King, Atmospheric winds between 100 and 700 km and their effects on the ionosphere, J. Atmos. Terr. Phys., 29, 1045-1062, 1967.

Lew, S. K., On the dynamic response of the thermosphere at low latitudes to geomagnetic disturbances, J. Geophys. Res., 74, 5093-5098, 1969.

Matsushita, S. and W. H. Campbell, eds., Physics of Geomagnetic Phenomena, Volume 2, Academic Press, New York, 1967.

May, B. R. and D. E. Miller, The correlation between air density and magnetic disturbance deduced from changes of satellite spin-rate, Planetary Space Sci., 19, 39-48, 1971.

Mayr, H. G. and H. Volland, Magnetic storm effects in the neutral composition, Planetary Space Sci., 20, 379-393, 1972.

Mayr, H. G. and H. Volland, Magnetic storm characteristics of the thermosphere, J. Geophys. Res., 78, 2251-2264, 1973.

Mayr, H. G. and H. Volland, Magnetic storm dynamics of the thermosphere, J. Atmos. Terr. Phys., 36, 2025-2036, 1974.

Newton, G. P., Latitudinal dependence of the diurnal density variation, J. Geophys. Res., 75, 5510-5516, 1970.

Nicolet, M., Structure of the thermosphere, Planetary Space Sci., 5, 1-32, 1961.

Nisbet, J. S., On the construction and use of a simple ionospheric model, Radio Sci., 6, 437-464, 1971.

Nisbet, J. S., Neutral atmospheric temperatures from incoherent scatter observations, J. Atmos. Sci., 24, 586, 1967.

Philbrick, C. R., Satellite measurements of neutral atmospheric composition in the altitude range 150 to 450 km, Space Research XIV, 1974.

Prolss, G. W. and U. Von Zahn, ESRO-4 gas analyzer results to direct measurements of changes in the neutral composition during an ionospheric storm, J. Geophys. Res., 79, 2535-2539, 1974a.

Prolss, G. W. and U. Von Zahn, Magnetic storm associated changes in neutral composition of the atmosphere at midlatitudes observed by the ESRO-4 gas analyzer, Space Research XIV, 1974b.

Reber, C. A., A. E. Hedin and S. Chandra, Equatorial phenomena in neutral thermospheric composition, J. Atmos. Terr. Phys., 35, 1223-1228, 1973.

Reber, C. A. and A. E. Hedin, Heating of the high-latitude thermosphere during magnetically quiet periods, J. Geophys. Res., 79, 2457-2461, 1974.

Rees, D., Upper atmosphere neutral temperature profiles in the auroral zone 1968-1970, Planetary Space Sci., 19, 233-241, 1971.

Roemer, M., Recent observational results on the neutral upper atmosphere, in: Kondratyev, K. Ya., Rycroft, M. J. and Sagan, C. (Eds.), Space Research XI, Proceedings of the Thirteenth Plenary Meeting of COSPAR, Leningrad, 1970, Volume 2, Adademie-Verlag, Berlin, pp. 761-778, 1971a.

Roemer, M., Geomagnetic activity effect on atmospheric density in the 250 to 800 km altitude region, in: Kondratyev, K. Ya., Rycroft, M. J. and Sagan C. (Eds.), Space Research XI, Proceedings of the Thirteenth Plenary Meeting of COSPAR, Leningrad, 1970, Volume 2, Akademie-Verlag, Berlin, pp. 965-974, 1971b.

Roemer, M. and Lay, G., Characteristics of the geomagnetic activity effect in the thermosphere, in: Bowhill, S. A., Jaffe, L. D. and Rycroft, M. J. (Eds.), Space Research XII, Proceedings of the Fourteenth Plenary Meeting of COSPAR, Seattle, Washington, USA, 1971, Volume 1, Akademie-Verlag, Berlin, pp. 797-802, 1972.

Romanovsky, Y. A. and V. V. Katyushina, On thermospheric composition and temperature variations during geomagnetic disturbances, Space Research XIV, 1974.

Rostoker, G., Geomagnetic indices, Rev. Geophys. Space Phys., 4, 935-950, 1972.

Salah, J. E. and J. V. Evans, Measurements of thermospheric temperatures by incoherent scatter radar, in: Rycroft, M. J. and Runcorn (Eds.), Space Research XIII, Proceedings of the Fifteenth Plenary Meeting of COSPAR, Madrid, 1972, Volume 1, Akademie-Verlag, Berlin, pp. 267-286, 1973.

Salah, J. E. and J. M. Holt, Mid-latitude thermospheric winds from incoherent scatter radar and theory, Radio Science, 9, 301-313, 1974.

Stein, J. A. and J. C. G. Walker, Models of the upper atmosphere for a wide range of boundary conditions, J. Atmos. Sci., 22, 11, 1965.

Stringer, W. T. and A. E. Belon, The statistical auroral zone during IQSY and its relationship to magnetic activity, J. Geophys. Res., 72, 245-250, 1967.

Swartz, W. E. and J. S. Nisbet, Diurnal variation of the neutral temperature profile at Arecibo from incoherent scatter measurements and its relevance to the 1400-hour density maximum, J. Geophys. Res., 76, 185, 1971.

Taeusch, D. R., G. R. Carignan and C. A. Reber, Neutral composition variation above 400 kilometers during a magnetic storm, J. Geophys. Res., 76, 8318-8325, 1971a.

Taeusch, D. R., G. R. Carignan and C. A. Reber, Response of the neutral atmosphere to geomagnetic disturbances, in: Kondratyev, K. Ya., Rycroft, M. J. and Sagan, C. (Eds.), Space Research XI, Proceedings of the Thirteenth Plenary Meeting of COSPAR, Leningrad, 1970, Volume 2, Akademie-Verlag, Berlin, pp. 995-1002, 1971b.

Thomas, G. E. and B. K. Ching, Upper atmospheric response to transient heating, J. Geophys. Res., 74, 1796-1811, 1969.

Truttse, Yu. L., Upper atmosphere during geomagnetic disturbances. III. Some regularities in density variations, Planetary Space Sci., 17, 181-187, 1969.

Truttse, Yu. L. and O. T. Yurchenko, Temperature of the upper atmosphere from the 6300 A emission data. Planetary Space Sci., 19, 545-546, 1971.

Vasseur, G., Dynamics of the F-region observed with Thomson-scatter - I Atmospheric circulation and meutral winds, J. Atmos. Terr. Phys., 31, 397-420, 1969.

Volland, H. and H. G. Mayr, Response of the thermospheric density to auroral heating during geomagnetic disturbances, J. Geophys. Res., 76, 3764-3776, 1971.

Von Zahn, U., Neutral air density and composition at 150 kilometers, J. Geophys. Res., 75, 5517-5527, 1970.

Waldteufel, P. and L. Cogger, Measurements of the neutral temperature at Arecibo, J. Geophys. Res., 76, 5322-5336, 1971.

Watkins, B. S. and P. M. Banks, A preliminary study of high-latitude thermospheric temperatures from incoherent scatter radar observations, J. Geophys. Res., 79, 5307-5310, 1974.

Zimmerman, S. P. and N. W. Rosenberg, Wind energy deposition in the upper atmosphere, in: Bowhill, S. A., Jaffe, L. D. and Rycroft, M. J. (Eds.), Space Research XII, Proceedings of the Fourteenth Plenary Meeting of COSPAR, Seattle, Washington, USA, 1971, Volume 1, Akademie-Verlag, Berlin, pp. 623-628, 1972.